STUDIES OF SOME PHYSICAL AND CHEMICAL PROPERTIES OF UNIMOLECULAR FILMS

by

J.M. Ramaradhya, M.Sc.

Thesis submitted to the Faculty of
Graduate Studies and Research of
McGill University in partial fulfillment
of the requirements for the Degree of
Doctor of Philosophy.

McGill University
Montreal
Canada

September 1958.

ACKNOWLEDGEMENTS

The author is extremely grateful to his Research Director Dr. R.F. Robertson for his kindly and helpful advice during this research.

For the help given on many occasions, the author expresses his gratitude to Dr. S.G. Mason and Dr. L. Yaffe.

For friendly help rendered during the course of these investigations, the author wishes to acknowledge his sincere thanks to Dr. W. Rabinovitch and Mr. Frank Kavcic.

Sincere gratitude is expressed to Mrs. A. Ramaradhya for the various forms of assistance rendered during the preparation of this thesis.

Acknowledgement is made to the Defence Research Board for financial assistance (1956 - 1958) and to the National Research Council for a summer grant (1958).

....

TABLE OF CONTENTS

I. INTRODUCTION

Page

TABLE OF CONTENTS (cont.)

TABLE OF CONTENTS (cont.)

III RESULTS

TABLE OF CONTENTS (cont.)

....

I INTRODUCTION

(1) General: Present work.

The experimental work of this thesis can be divided into two distinct parts. The first part is a continuation of the investigation of the isotopic exchange reaction between α- iodostearic acid monolayers and substrate iodide ions. The second part is a study of the effect of various substituents in the hydrocarbon chain of stearic acid on the mechanical properties of the respective monolayers.

Because of the large volume of literature which has been published on unimolecular films and the wide scope of this investigation, the introduction has been divided into the following five distinct sections. Each section is a review of the available literature deemed pertinent to the present investigation but from one particular aspect of the overall problem. The first section is an historical survey of the development of the surface film technique for the study of substances spread at the air/water interface. In the second section the modern methods for the measurement of the physical and chemical properties of these films is discussed, together with the significance of the properties determined. The classification of the various monolayer films at the air/water interface on the basis of the mechanical properties of the films is considered in the third section of the introduction. A brief review of surface potentials of monolayers constitutes the fourth part. A review of the experimental investigations on the chemical reactivity of monolayers with particular reference to isotopic exchange reactions is given in the final section of the introduction.

(2) Monomolecular Films

(a) History of Surface Films

It is a characteristic property of certain organic liquids that when a drop of the liquid is placed on water, the liquid spreads. This spreading has been observed to have a great effect on the apparent surface tension of the water. Rayleigh (1) in 1890, measured the amount of olive oil necessary to check the motion of camphor on a water surface and he determined the depression of the surface tension accompanying the presence of the mininum quantity of oil on water required to stop the camphor movements (2,3). The diminution of surface tension at this point, on the basis of a monolayer, was calculated to be about 16 dynes per cm. The area per molecule of the oil at this point calculated on the basis of triolein was 100 Sq. Å. U. This value is in excellent agreement with recent measurements for triolein which give 97 Sq. Å. U. per molecule for an equivalent surface tension depression.

Miss Agnes Pockels (4) reported that very small amounts of oil on a sufficiently large surface of water have no appreciable effect on the surface tension, but that the surface tension begins to decrease suddenly when the amount of oil per unit area is increased beyond a certain characteristic limit.

The development of experimental methods for the study of surface films at the air/water interface began with Pockels' observation that the surface of water could be freed from contamination, even of molecular dimension, by sweeping with a solid barrier. She employed a long rectangular tin trough, filled to the brim with water, with a transverse strip of tin resting on the edges of the trough as the barrier. The barrier was used to confine the oil to known regions of the trough and to sweep the water surface clean. The surface tension of both the clean and film covered water was obtained by measuring, with an ordinary balance, the force necessary to pull from the surface either a small disc or a larger ring,

In 1899, Lord Rayleigh (5) confirmed Pockels' observation regarding the manner of variation of surface tension with the relative area of the film and concluded that at the point where the surface tension first began to fall, the films were one molecule thick.

Devaux (6,7,8) and Marcelin (9) have used the barrier technique in their study of oil films. The barriers were either glass or paper strips. However barriers of the type employed by these early workers were not an efficient means of keeping the film confined within a given area of the surface, since leakage occurred slowly around the barriers, thus vitiating their results.

Langmuir (10) was the first tc measure directly the force which acts on the film in the plane of the surface. Later Adam (11) and Harkins (12) and their coworkers made monumental contributions to the development of the methodolgy of surface films. Modern techniques of measurements will be dealt with elsewhere in the thesis.

(b) Concept of Spreading and Surface Pressure

The spreading of one liquid over another can be explained in terms of surface tension. The first attempt to relate spreading and surface tension is the work of Duprè(13). When a drop of an organic liquid is placed on the surface of water, it is subjected to three forces, the surface tension of water (Υ_1), the surface tension of the organic liquid (Υ_2) and the interfacial tension of the water-organic liquid (γ_{12}). When the sum of the surface tension of the organic liquid and the tension of the water-organic liquid interface is less than the surface tension of water, the organic liquid tends to spread. The equation derived by Duprè for the condition of spreading based on this concept

$$\gamma_1 + \gamma_2 = \gamma_{12} + (-\Delta\gamma_{12}) \qquad \text{--(1)}$$

was found to be of only limited use in describing the spreading of one liquid on the surface of another. In the above equation, $(-\Delta\gamma_{12})$ represents the decrease in surface tension which occurs when the two liquids approach each other.

There are three other views of the criterion of spreading cited in the literature. These are:

(a) All liquids spread on the surface of clean water. To prevent spreading, it is necessary to have a foreign substance on the surface: Rayleigh's theory (14)

(b) On the basis of experiments on a number of organic acids, alcohols and esters, Langmuir (10,15,16) came to the conclusion that for spreading to occur on water, an "Active" or "Polar" group such as the carboxyl group was necessary. The active groups in the organic compound would be in contact with and possibly hydrogen bonded to the water, while the rest of the molecule (the hydrocarbon chain) would be arranged vertically perhaps side by side on the water surface. Thus the idea of orientation of molecules in surface films was introduced. According to this view, liquids whose molecules contained polar groups would spread on water, while non-polar liquids such as the hydrocarbons would not.

(c) The thermodynamic theory of Harkins et al (17,18,19,20) is not limited to the spreading of liquids on liquids but applies to the spreading of solids on liquids and to the spreading of mobile films on solids as well and hence may be considered a generalized treatment. The theory may be briefly outlined as follows:

If a drop of an insoluble oil (b) is placed on a clean water surface (a), it may or may not spread. The condition which determines whether or not the oil spreads is exceedingly simple. If the oil"likes"itself (W_C) better than water (W_A), it will not spread. In order to use this in a quantitative sense however, it is necessary to express the term "likes" as a thermodynamic quantity. This is done in the following equation:

$$C_{b/a} = -\left(\frac{\partial F}{\partial \sigma}\right) = W_A - W_C \qquad \text{--(2)}$$

in this equation, $-\left(\frac{\partial F}{\partial \sigma}\right)$ is the rate of decrease of the free energy (F) of the system with increase of area (σ) of the duplex film and the concomitant decrease in the area of the clean surface of the water. W_A is the work of adhesion, the work required to pull the oil and water apart from an interface 1 sq. cm. in area and W_C is the work of cohesion, the work required to rupture a bar of oil with a sq. cm. cross-section. A consideration of these work terms gives the following values for W_A and W_C in terms of the surface energy of pure water γ_a, pure oil γ_b, and the surface energy of the oil-water interface γ_{ab}:

$$W_A = \gamma_a + \gamma_b - \gamma_{ab} \qquad \text{--(3)}$$

$$W_C = 2\gamma_b \qquad \text{--(4)}$$

The difference $W_A - W_C$ is called the spreading coefficient

$$C_{b/a} = \gamma_a - (\gamma_b + \gamma_{ab}) \qquad \text{--(5)}$$

where the subscript b/a indicates that the oil b is spread on the water a. It is obvious that a positive value of the spreading coefficient corresponds to spreading, a negative value to non-spreading. From the above equation, it does not follow that a should spread on b. The co-efficient for a to spread on b is given by

$$C_{a/b} = \gamma_b - (\gamma_a + \gamma_{ab}) \geqslant 0 \qquad \text{--(6)}$$

One of the principal effects of the presence of a polar group is to increase the work of adhesion (W_A). When a very polar group, for example, -OH, -COOH, -CONH, -CHO, -CN, -$CONH_2$, is present in the molecule, the value of W_A is very high and the term W_C in the equation,

$$C = W_A - W_C \qquad \text{--(7)}$$

is never large enough to give a negative value of the spreading coefficient and hence spreading occurs. However when the work of adhesion toward water is small, the liquid may still spread for sufficiently small values of W_C. Thus hexane for which the value of W_A is small (40.23 ergs) spreads, since W_C is even smaller (36.86 ergs) and the value of C is 3.37, a positive quantity. The work of cohesion W_C in octyl alcohol is almost 20 ergs greater than that for hexane, but this alcohol is able to spread on water since W_A is still greater (51.71 ergs). This demonstrates the important effect of the presence of a polar group in producing spreading by increasing the work of adhesion to a greater extent than the work of cohesion.

It is customary, in the case of surface films to measure a quantity called the "Surface Pressure". The surface pressure is expressed in terms of the diminution of the surface tension of water by the presence of the film. Surface tension is defined as the free energy per unit area of the surface. If a monolayer of an insoluble substance is spread on the surface of a liquid of surface energy γ_o ergs cms $^{-2}$, the surface energy falls to γ ergs cms $^{-2}$. The surface energies being numerically equal to the surface tensions, it is easily established that the surface pressure, π , is related to the surface tension by

$$\pi = \gamma_0 - \gamma \qquad \text{--(8)}$$

This surface pressure is analogous to the three dimensional osmotic pressure. The comparison between surface pressure and osmotic pressure has been made by Adam (11).

(3) Techniques and Results

(a) Experimental Methods for the Study of Surface Films

Quantitative measurements in the investigation of surface films are made with a surface film balance. The first practical surface film balance was devised by Langmuir (10). Since then, Langmuir's balance has undergone numerous modifications and other types of surface film balances have been developed.

Rayleigh (5) using the Wilhelmy slide (21) first measured the surface tensions by using an ordinary laboratory balance. The surface tensions were measured in terms of the force exerted on the perimeter of a vertical microscope slide partially immersed in water. Then γ , the surface tension for zero contact angle was given by

$$\gamma = \frac{(G - W + \rho ltw)}{2\ (t + w)} \qquad \text{--(9)}$$

where,

G = apparent weight of the partially immersed slide
W = weight of free dry slide
ρ = density of the liquid
l = depth of immersion of the slide
t = thickness of the slide
w = width of the slide

It was soon discovered that after some time the glass slides became greasy and the angle of contact could not be considered zero.

Langmuir (10) devised the first horizontal film balance. It consisted of an enamelled trough 60 cm x 15 cm which could be filled with water to the brim. Two strips of paraffined paper were used as barriers to confine the film. One of the strips, the movable barrier, was laid across the trough to rest on the edges. The other strip, about 5 mm less than the width of the tray, called the immovable barrier, was floated on the water at the other end of the trough. Two glass rods fixed to the immovable barrier were connected to the main knife edges of a chemical balance. When the movable barrier was moved so as to alter the area of the film, a force acting in the plane of the surface was exerted on the other barrier resulting in a lateral displacement of this barrier. The displacement in turn altered the position of equilibrium of the chemical balance. The weight necessary to restore the equilibrium of the chemical balance was a measure of the force acting on the film.

Starting from the immovable float, the movable barrier was moved to the other end of the tray, thus sweeping clean the surface of the water. Then a predetermined volume of a film forming substance in a benzene solution of known concentration was dropped on the surface of water. The benzene evaporated leaving behind the film. A suitable weight was applied to the pan and the movable barrier was moved along until equilibrium was reached. A meter stick attached to the tray gave the distance between the movable barrier and the float and hence the area occupied by the film. By varying the weights on the pan, the film could be had, subjected to various degrees of compression. Since the concentration of the acid was known and the area of the film could be calculated from the dimensions of the trough, the area per molecule could be determined.

Tiny jets of compressed air were used at the gap between the immovable barrier and the trough to prevent leakage. This technique suffered from some major disadvantages including the effect of the air jet on the balance sensitivity. In 1922, Adam (22) reduced the gap from 5mm to 1 mm and used a special gravity bob to adjust the sensitivity of the balance. This balance too had its disadvantages when film pressures below 0.5 dynes/cm were to be measured. Adam and Jessop (23) finally designed a new balance abandoning the air jet and using a torsion wire and an optical lever arrangement for measuring surface pressure.

Various other instruments for measuring film pressures have been constructed, particularly those of Marcelin (24) and Lyons and Rideal (25). Marcelin's aneroid type of balance was very ingenious. The main feature of this film balance was that the movable float was eliminated. Puddington (26) constructed a surface film balance on the principal of a two dimensional Bourdon gauge. Harkins and Myers (27) and Harkins and Fischer (28) have designed surface film balances to work at thermostated temperature ranging from - 30°C to +70°C.

Another considerable advance was made when Harkins and Anderson (29) designed the vertical pull film balance. This balance employed quartz or pyrex glass troughs and barriers, a thermostated air-bath and a dipping plate suspended from one arm of an analytical balance. A fine aluminium wire was attached at the bottom of one pan and passed through the thermostat. The end of this wire carried a microscope slide partially immersed in the substrate solution. Any deflection in the beam of the balance, arising from the development of surface pressure during compression of the film was magnified and read on a scale by an optical lever. The surface pressure π, was given by the equation

$$\pi = \frac{k \; \Delta s}{2 \; (t+w)} \qquad \text{--(10)}$$

Here Δs = shift of the beam of light, t = thickness and w = width of slide. The value of k was obtained from values of Δs corresponding to different weights on the balance pan with the slide immersed in a clean water surface according to the equation

$$k = \frac{g \; \Delta M}{\Delta s} \qquad \text{--(11)}$$

where ΔM was the added weights and g the gravitational constant.

This type of balance was easily constructed and operated. Since it avoided the use of metals in its construction, it facilitated the study of the effect of metallic ions on films. Bull (30) and Abribat et al (31) have successfully used this apparatus to study monolayers of various proteins and long chain polymers. This instrument suffered from the disadvantage of inaccuracy when working with low film pressures. A proper choice of dipping slide material had to be made to assure that the contact angle, assumed to be zero in calibrating the balance, could actually be considered to satisfy this assumption.

The vertical pull method was used in another way for measuring surface pressure by R. Matsuura (32). Here the change in length of a quartz spring carrying the dipping slide was used to measure the surface pressure π. The equation developed for this balance had the form

$$\pi = (tw\rho g + k) /2 (t + w) (\alpha - \alpha_0) \qquad \text{--(12)}$$

where t and w are thickness and width of the slides respectively, k = spring constant, ρ = density of water, g = gravitational constant, α and α_0 are cathetometer readings of the extension on the quartz spring.

Various investigators (33 to 36) have designed different modifications and improvements of surface film balances embodying the principles of the Langmuir technique.

(b) Molecular dimensions and Molecular orientation from Mololayer studies at the Air/Water interface

The monolayer technique has served to elucidate the physical dimensions of film forming substances giving molecular dimensions closely comparable to those obtained by other independent physical measurements. This technique has further served to demonstrate experimentally the high degree of orientation present in unimolecular films. A brief review will now be given of the techniques used and the results obtained in the investigation of these two properties in monolayers.

From the weight of the film forming substance used, its molecular weight and Avogadro number, it is possible to calculate the number of molecules in a film. Knowing the total area available between the barriers, the area covered by each molecule can be obtained. This can be assumed to be proportional to the cross-section of the molecules. Assuming the density in bulk and the density in the film to be the same, the length of the molecules can also be calculated. The volume of each molecule is found by dividing the molecular volume (M/ρ), where M = molecular weight and ρ = bulk density of the substance, by the Avogadro number (N). By dividing this volume by the apparent cross-sectional area of each molecule, the length of the molecules can be obtained.

Langmuir (10) investigated a wide variety of saturated alcohols, acids and esters on the film balance. An examination of his results shows that the cross-section of the molecules varies over a wide range from 21 to 126 x 10^{-16} sq. cm. By a study of pressure-area diagrams, Langmuir showed that for any saturated fatty acid the cross-sectional area per molecule is essentially constant, about 21 x 10^{-16} sq. cm. By a systematic study of these compounds, he concluded that each homologous series would give rise to same area per molecule at a sufficiently high compression and this area would remain constant even when the length of the hydrocarbon chain was changed.

These measurements led Langmuir to postulate that the molecules are oriented in a definite manner on the surface of a liquid with the functional group anchored in the surface of the water and the hydrocarbon chains packed side by side vertically above the surface. The distance between carbon atoms according to Langmuir was 1.5 Å.U.

On decreasing the area per molecule in the film by compression, it was found that the orientation of the molecules to the surface was altered. As the film was compressed, a definite change in the state of the monolayer was observed apparently due to a change in orientation. Surface-pressure area diagrams in conjunction with surface-potential measurements have proved of great value in establishing these changes of state in a monolayer, which accompany the changes in orientation and molecular association.

(c) Types of films

Adam (11), on the basis of an experimental survey of the film properties of a large number of organic compounds, came to the conclusion that there are three general classes of films, the condensed, the expanded and the gaseous film. A brief survey of the properties of these films according to Adam will now be given since they are considered pertinent to the work of this thesis.

(i) Condensed films

Films of this type were studied by Adam (22,37,38,39) and Adam and Dyer (40). In these condensed films, the molecules possess strong lateral adhesion and the form of the pressure-area curves for condensed films reflects the marked influence of these lateral forces in a steep rise in the surface pressure as the area is reduced to that at which the molecules are closely packed.

There are two main types of condensed films, solid condensed and liquid condensed. In a solid condensed film, the molecules are firmly bound and hence the area per molecule in the condensed phase should be closely related to the cross-sectional area of the individual molecules. This is usually true, but in some cases as with stearic acid, the area 20.5 $Å^2$ per molecule obtained from surface film studies is not in agreement with the cross-sectional area 18.4 $Å^2$ per molecule obtained from x-ray data (41,42). To explain this disagreement, Lyons and Rideal (25) suggested that the oriented molecules were tilted at a definite angle and that the zig-zag chains packed themselves by interlocking, resulting in a stable film. Müller's (41) x-ray analysis of crystals of fatty acids has supported this view.

Adam (43) has disagreed with the interlocking theory. His work (44) on the flexibility of long chain hydrocarbons has shown that the interlocking of zig-zag chains is doubtful. Adam is of the opinion that the condensed film structure is a close-packed one, with close-packed heads or close-packed chains. Alexander (45) in a study of the general structure of condensed films and Eda and Masuda (46) working on the pressure-area relationships of α-amino-lauric acid monolayers have supported this close-packed structure of Adam. No experimental study has as yet contradicted the close-packed nature of condensed films and Adam's view still prevails.

In several cases, one substance can form two different condensed films with a temperature of transition (11). In the case of acetamide derivatives possessing the NH. CO. CH_3 end group, a transition occurs from a solid film at low temperatures to a liquid film at higher temperatures. In the solid condensed film, according to Adam, the molecules may not be able to rotate freely about their long axis but at the temperature of transition and above, the power of free rotation may suddenly become possible because of the increased kinetic energy of the molecules. The transition between the two forms of condensed films, found with substituted ureas, appears to be similar to that between two allotropic modifications of the solid substances (39).

Rosenheim and Adam (47) investigated the condensed films of complex cholesterol structures. Cholesterol spreads into a highly incompressible condensed film with an area of 48 $Å^2$ per molecule. But ψ-cholesterol with the

-CHOH group on carbon atom seven has twice the area and is more compressible. This change in behaviour is probably due to a shift in the water attracting group -CHOH, causing a change in the angle of tilt of the molecule with the surface.

Dervichian (48) states that the packing of long chain molecules, whose limiting areas are between 19.5 $Å^2$ and 25.26 $Å^2$ is similar to the molecular areas found in the crystal lattices of solid fatty acids. He assumes that the links in the chains form a helical spiral in the condensed layer. Since these links have no fixed position in the chain and since each CH_2 group undergoes rotation, the whole chain appears to rotate.

Müller (49) and Bernal (50) have also suggested on the basis of x-ray studies that molecules in the fluid condensed state rotate about their vertical axis. Vold (51), while studying molecular cross-sectional areas of liquid and solid films suggested that the liquid state may correspond to the free-rotation of the molecules, while the solid condensed film may correspond to the close packed arrangement with hindered or little rotation.

(ii) Expanded Film

Labrouste (52) in 1920 found that a surface film expanded as the temperature was raised. The temperature at which this change begins to occur is designated the "Temperature of Expansion" and the resulting film is called the expanded film. The temperature of expansion depends upon the chain length, molecular weight and the substrate composition. For each additional $-CH_2$ group in any homologous series, Adam (11) observed that temperature of expansion was raised by 7 - 10°C.

It has been generally accepted (53) that the surface pressure-area relationship of these expanded films can be expressed by an equation of state of the Van der Waal's type as proposed by Langmuir (54)

$$(\pi - \pi_0)\ (\sigma - \sigma_0) \ = \ C \qquad \text{--(13)}$$

where π_0 is the negative spreading pressure of the chains, σ_0 is the co-area of the polar head group, and C is a constant equal to kT for un-ionised groups (55), k being the Boltzmann constant and T the absolute temperature.

From an earlier equation of Phillips and Rideal (56) of the form

$$\pi - E_\gamma - \sigma\frac{dE_\gamma}{d\sigma} + \frac{kT}{C_s} + \frac{dC_s}{d\sigma} \ = \ 0 \qquad \text{--(14)}$$

where

π = surface pressure

σ = surface area

k = Boltzmann constant

T = absolute temperature

C_s= surface concentration

E_γ= cohesive attraction energy

Hedge (57) has developed a modified form of Langmuir's equation. By analogy with the three dimensional system, the cohesive energy may be taken to be inversely proportional to the square of the surface area σ. Then $E_\gamma = a/\sigma^2$, a being the proportionality constant. Further since $C_s \propto 1/\sigma$, equation (14) becomes by appropriate substitution and simplification

$$(\pi + a/\sigma^2)\,\sigma = kT. \qquad \text{--(15)}$$

But in the case of liquid films, the area occupied by the molecules themselves σ_0 cannot be neglected. Inserting this quantity, equation (15) becomes

$$(\pi + a/\sigma^2)\,(\sigma - \sigma_0) = kT. \qquad \text{--(16)}$$

This form of Langmuir's equation has been verified with lecithin monolayers (57)

The expanded films may be classified into two types: liquid expanded and vapour expanded films.

Liquid expanded films are coherent, possessing a definite surface vapour pressure and tending to a definite limiting area (58). Harkins and Boyd (59) have called Adam's compressed vapor films the liquid expanded films. Liquid expanded films pass into the vapour expanded films if a certain critical temperature is exceeded irrespective of surface pressure. Vapour expanded films possess no definite limiting area and no constant surface vapour pressure. As the temperature is increased, they transform into "Gaseous Films" without discontinuity. Fatty acids, nitriles, alcohols, amides and ureas are typical of the substances forming liquid expanded films while esters, methyl ketones and long chain ketones which also form liquid expanded films transform to the vapour expanded type with increasing temperature.

A variety of theories have been proposed on the structure of expanded films. Cary and Rideal (58) suggested that the expansion of a film is a process of gradual hydration of the molecules in the film. Adam and Jessop (23) consider that the kinetic energy of the molecules in expanded films permits such a degree of agitation in the film that much of the orientation of the molecules is lost. A study of phenols has prompted Adam et al (60) to suggest another structure for the expanded films of ring compounds. They stated that the molecules remained in contact while the chains coil up in helices, the diameter of each coil of the helix being the same as the diameter of the cyclohexane ring. But an experimental study of chain structure compounds has proven the coiled chain theory to be untenable.

Langmuir (61) suggested that expanded films consist of chains which tend to adhere while the heads are in constant state of agitation, the chains tending to make a condensed and the heads a gaseous film. Experimental evidence has shown a decrease in area occurred when the chain length was increased as would be predicted by this view of film structure. Langmuir (54) further considered liquid expanded films as being formed of small two dimensional drops or micelles, the micelles growing in size and number on compression, until the sheet becomes a uniform duplex film, more than one molecule thick. Langmuir (62) and subsequently Adam (63) have treated liquid expanded films as duplex films with a satisfying degree of success.

(iii) <u>Gaseous Films</u>

Substances containing more than one polar group per molecule form a type of film called the gaseous film which obeys at least approximately an equation of state which is a two dimensional analogue of the ideal gas law. The equation has the form $\pi\sigma = kT$ in which π = surface pressure; σ = area of the film; T = temperature in degrees absolute; k = Boltzmann constant, 1.372 if area is expressed in sq. Å.U. The $\pi\sigma - \pi$ curves for gaseous films resemble curves of nearly perfect gases. The dip in the plots of

$\Pi\sigma - \sigma$ increases as the length of hydrocarbon chain increases (64). The diesters of dibasic acids give gaseous films exhibiting minimum deviations from ideality.

A gaseous film can be recognised by the fact that the surface pressure is continuous down to very small values. Adam and Jessop (23) investigated a number of gaseous films and concluded that all acids approach the perfect gaseous condition at sufficiently low pressures; but in the case of acids above C_8, the pressure must be less than one dyne/cm before gaseous films are obtained. Films of all the acids shorter than C_{12} are definitely gaseous in character and for acids shorter than C_8 above a surface pressure of 10 dynes/cm, the principal deviation from the perfect gas law is a function of the molecular size of the acid.

A very close similarity exists between gaseous films of insoluble substances and the adsorbed films of soluble substances. Langmuir, in case of adsorbed films, has shown that the energy of adsorption for each successive CH_2 in the molecule is constant and is equal to 710 calories per mol. This constancy could only be possible if the CH_2 groups have relatively the same geometric position in the film. An obvious conclusion from this fact is that in adsorbed films the chains are lying flat on the surface. Since the gaseous films resemble the adsorbed films, the molecules in the gaseous films probably lie flat, with their whole length more or less parallel to the surface.

(4) Phase changes in a Monolayer

The many improvements in the experimental technique of monolayer studies led to very accurate determinations of pressure-area relationships and the temperature dependence of these quantities. The work of Harkins and Nutting (65) was of particular importance in the development of high precision film studies. The attainment of reliable data on the physical properties of unimolecular films led naturally to a consideration of the thermodynamic properties of these films and calculations of their energy, entropy and phase relations (66). By applying the Clapeyron equation

$$\lambda = T\ (\partial\pi/\partial T)\ (A_F - A_S) \qquad\text{--(17)}$$

Where A_F and A_S are the areas of the film and solid respectively, λ the latent heat of spreading from the crystal to the monolayer could be determined for films of solids (58).

Devaux (6) was one of the first to point out that solids and liquids maintain their mechanical properties even when they are one molecule thick. By varying the temperature over a sufficient range, a given substance spread as a monolayer would show all the different states of matter common in three dimensions. When a gaseous surface film is compressed, it undergoes a change in phase analogous to a gas in three dimension condensing under pressure, even to the appearance of critical temperature conditions. When the temperature is varied, some intermediate phases occur however in two dimensional films which have no counterpart in three dimensional systems. Experimental investigations using pressure-area measurements, surface-potential and viscosity studies independently, have revealed that there are at least six possible surface phases in a monolayer.

The type of transition which may occur between these phases is not necessarily the ordinary transition occurring between gases, solids and liquids but may be of the diffuse type which Ehrenfest (67) called the higher order phase transition. According to Ehrenfest, the order of a phase change is determined by the lowest derivative of the free energy of the system which exhibits a discontinuity. In the study of surface phenomena, the energy quantity involved in a consideration of the order of the phase transition is the surface energy. The surface energy is defined as follows: If γ is the surface tension of a film covered surface and γ_0 that of the clean surface, the work done by an infinitesimal displacement of the barrier, which changes each of the two areas by $d\sigma$ and $-d\sigma$ respectively is

$$dw^s = (\gamma - \gamma_0)\, d\sigma \qquad \text{--(18)}$$

Introducing the surface pressure $\pi = \gamma_0 - \gamma$, the equation (18) becomes,

$$dw^s = -\pi\, d\sigma \qquad \text{--(19)}$$

This is analogous to the Pv work of gases

$$dw^v = -Pdv \qquad \text{--(20)}$$

If S represents the total entropy (surface and bulk) of the system, the variation of the total energy is defined by

$$dE = TdS - Pdv - \pi d\sigma \qquad \text{--(21)}$$

When T, P and π are considered as independent variables, the thermodynamic potential, G of Gibbs (including a term corresponding to the surface energy) can be written as,

$$G = A + Pv + \pi\sigma \qquad \text{--(22)}$$

where A, the Helmholtz free energy = E -TS.
Hence,

$$G = E - TS + Pv + \pi\sigma \qquad \text{--(23)}$$

and

$$dG = -SdT + vdP + \sigma d\pi \qquad \text{--(24)}$$

The successive partial derivatives can now be evaluated:

$$(\partial G/\partial \pi)_{P.T.} = \sigma \qquad \text{--(25)}$$

$$(\partial^2 G/\partial \pi^2)_{P.T.} = \partial\sigma/\partial\pi \qquad \text{--(26)}$$

An ordinary change of state is called a transformation of the first order, since it is characterised by a discontinuity in the area σ and consequently corresponds to a discontinuity in the first order derivative of G. Likewise a transformation in which σ does not undergo any variation but in which the compressibility

$$(k) = -d\sigma/\sigma d\pi \qquad \text{--(27)}$$

shows a discontinuity is a second order change, since according to equations (26) and (27) it corresponds to a discontinuity in the second derivative of G. Similarly, a discontinuity in the third derivative of G but not in the first two is indicative of a third order change.

Harkins has reclassified the types of films found at the air/water interface on the basis of their thermodynamic properties. Fig (1) represents a general phase diagram of Pentadecylic acid, over a range of temperatures below the critical. Table (1) shows the characteristics of the phases in a monolayer and the probable order of changes

<u>Figure 1</u>

<u>Figure 1</u>

(Reproduced from Harkins' Book.) (12)

General phase diagram of Pentadecylic acid monolayer over a range of temperatures below the critical. In the Fig L_1 is used for L_e and L_2 for L_c. Phases: FE or S, solid; ED or L_c, liquid condensed; DC or I, intermediate; CB or L_e, liquid expanded; BA or L_eG, gaseous film and L_e film in equilibrium; G, gaseous film. The temperatures given are those for Pentadecylic acid.

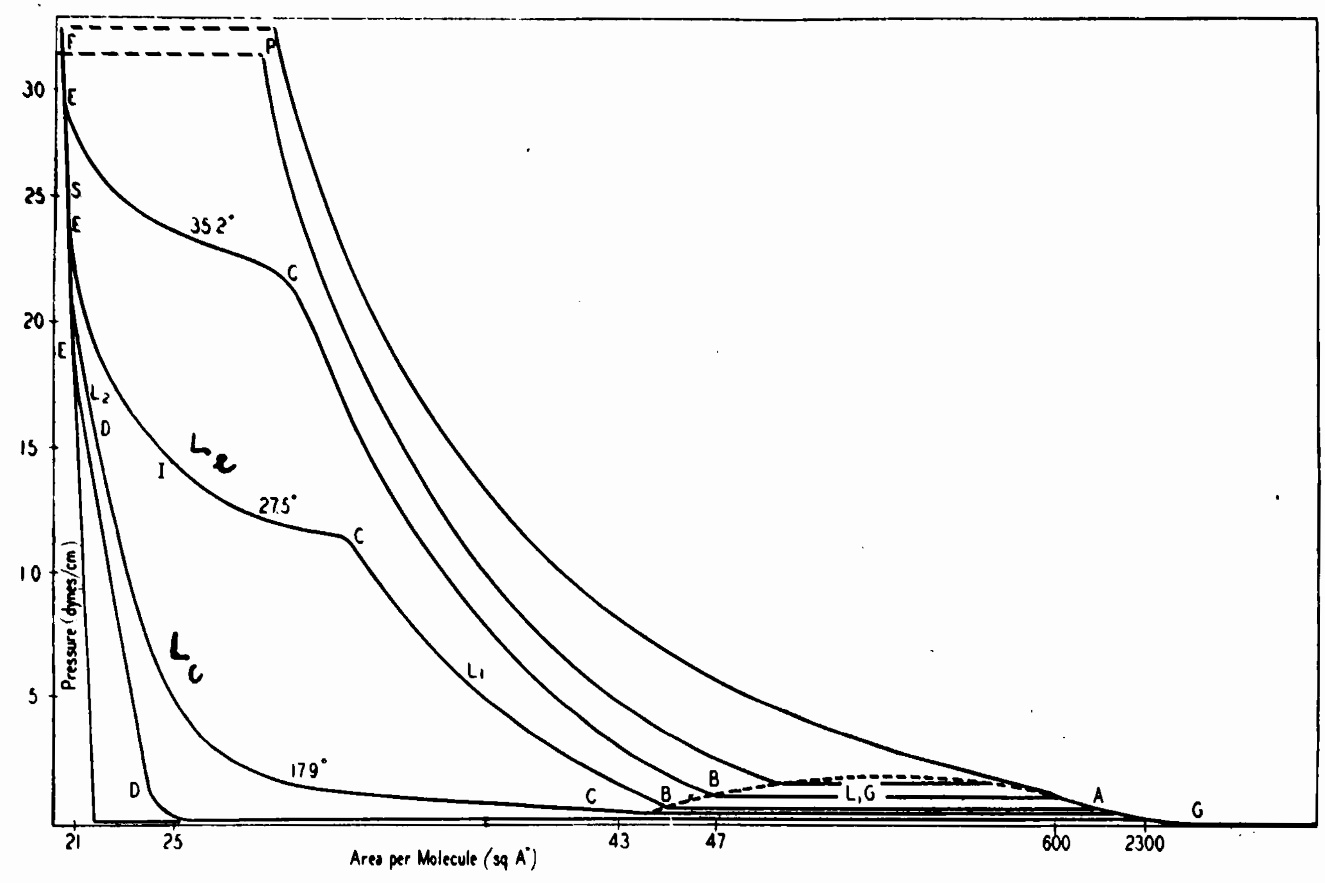
F
P
E
S
E
E
L2
D
I
35.2°
C
Le
27.5°
C
Lc
L1
179°
D
C
B
B
L1G
A
G
30
25
20
15
10
5
Pressure (dynes/cm)
21
25
43
47
600
2300
Area per Molecule (sq A°)

TABLE I

Type of Phase	Equation of State	Compressibility (k) cms/dyne	Order of change between them
1 Gas-G (Vapour expanded)	$\pi\sigma = kT$ if perfect	If perfect, (k) same as for L_1 films (0.04)	
2 Liquid L_e -BC (Liquid expanded)	$(\pi - \pi_o)(\sigma - \sigma_o) = kT$	2 to 7 x 10^{-7}	1 and 2: First (L_1G)
3 Intermediate I, or transition CE.		2 to 5 x 10^{-1} (long chain fatty acids) 2.2 x 10^{-1} (long chain esters)	1 or 2 and 3: Second (C)
			3 and 4: Third (D)
4 Liquid L_c -DE (L_2) (Liquid condensed)	$\pi = b - a\sigma$ $\log\eta = \log\eta_o + kT$ (a, b, are constants, η, η_o are viscosities of film and substrate respectively)	5 to 10 x 10^{-3}	
			4 and 5: First changing to second at higher temperatures.
5 Superliquid - L_s	$\pi = b - a\sigma$	.0005 to .0017.	
			4 and 6: Second 5 and 6: Second
6 S (Solid)	$\pi = b - a\sigma$	.0005 to .001	

between them. The corresponding nomenclature of Adam's classification considered previously is given in parenthesis.

The characteristics of each of these phases which have not been mentioned in Adam's classification will be briefly dealt with here. A gaseous monolayer subjected to compression and temperature variation, may directly condense to a solid film with-out undergoing the intermediate phase changes. Under proper conditions, any one of the six phases may change directly into any other one except possibly the changes between the liquid expanded and liquid condensed states which seem in general to go through the intermediate phase,

Gaseous film, represented by region L_1G have been shown by surface potential measurements of Harkins and Fischer (28) to be heterogeneous. The surface potential is roughly proportional to the number of molecules per unit area and since this number increases with pressure, the surface potential also increases. Harkins et al (20) showed that condensed films of tetrahydro d-pimeric acid, exhibit an increase from 203 to 220 mv, as the molecular area is decreased from 54 to 46 $Å^2$. The double bonds in d-pimeric acid reduces the potential due to the carboxyl group dipole by more than 50 per cent of the potential of the saturated analogue, tetrahydro d-pimeric acid. This indicates that the mutual dipole of the double bonds is opposed to that of the carboxyl group. The decrease of the potential on compression shows that a closer packing of the molecules, causing a more nearly vertical orientation to the surface, brings these dipoles into greater opposition.

In the case of myristic acid films (28) at 17°C, the gaseous film becomes entirely condensed to a liquid (L_1) state at 45 $Å^2$ per molecule. At a higher molecular area of 56.5 $Å^2$, an electrical survey shows that the region L_1G is heterogeneous. At an area of 37.1 $Å^2$, the film is in the intermediate state and remains in this state down to 25 $Å^2$.

The transition of a monolayer from a gaseous to a liquid state (L_1) is an ordinary change of the first order, accompanied by a latent heat of phase transformation. Thus it is analogous to the condensation of a gas to a liquid in a three dimensional system.

On compression the pressure of the liquid film (L_1) increases along a curve which has almost the form of an equilateral hyperbola. At C (fig 1) there is a phase transformation of a peculiar type to the intermediate liquid state (I). Just above the kink point, the π-σ curve is almost, but not quite horizontal. This is a region of considerable hysteresis. At D, a third order transition to a condensed monolayer (L_2) occurs and at E, the second order transition to a solid.

The compressibility (k) is characteristic of the phase, as is the increase of enthalpy which accompanies the spreading over unit area. In the present work, the compressibility is chosen as the basis for characterisation of the various phases.

(5) Surface Potentials of Monolayers

The surface potential technique was first introduced in a study of monolayers by Guyot (68) and Frumkin (69). They measured the changes in contact potential at the air-water interface in the presence and absence of a film. For their measurements an air electrode was used, a probe covered with a small amount of radioactive deposit which caused the gap of air between the probe and the surface to become conducting. The air electrode was used in conjunction with a standard calomel electrode and an electrometer. The difference between the potential at the clean surface and at the film covered surface was termed the surface potential and related to n, the number of molecules per sq. cm of film by the Helmholtz equation,

$$\Delta V = 4\pi n \mu \qquad \text{--(28)}$$

In this equation μ is the average electric moment of the effective vertical component possessed by each molecule. By determining Δv experimentally, μ, can be evaluated. The value of μ gives information about the orientation of the molecules in the film and hence information on the film properties in general.

A combination of the surface pressure apparatus of Adam and Jessop (23) and the surface potential apparatus of Schulman and Rideal (70) was constructed by Adam and Harding (71). With the aid of this apparatus, it was possible to study the surface potential for various states of the film. These workers studied the fatty acids containing from 14 to 22 C atoms in the chain. This study showed that the value of μ increased slightly as the expanded film was compressed and decreased as the condensed film was compressed. This showed that the orientation of the head groups (especially -COOH in case of acids) did not change on compressing either a liquid expanded film or a condensed film. Adam and Harding concluded from this that in expanded films, the end groups tend to adhere while the chains rotate about C-C linkages.

Schulman and Rideal studied the Π-σ and Δv-σ curves of a monolayer of myristic acid on 0.1 N HCl. They noted that the transition from expanded to gaseous film took place at 47 Å^2 and as soon as this area was exceeded, the value of μ decreased. The decrease in the value of μ corresponded to a change in the orientation of the film forming molecules. In the expanded film, the molecules were more or less vertical; as soon as the film became gaseous after exceeding the limiting area 47 Å^2, some of the molecules would be flat on the surface as indicated by the decrease in μ.

As a result of a detailed study of condensed films, Schulman and Hughes (72) concluded that the values of lateral surface pressure reflected the behaviour of hydrocarbon chains in the film, while the values of the surface potential in general reflected the behaviour of the polar groups in the film molecules.

Hughes (73) investigated surface potentials of monolayers of the unsaturated acids, oleic, petroselenic and chaulmoogric. Harkins et al (20) studied monolayers of d-pimeric and tetra-hydro d-pimeric acids by the surface potential technique. These experiments indicated that the surface potential is sensitive to the orientation of the double bond and the surface potential of condensed films of unsaturated compounds is lower (100mv) than that for saturated compounds (200mv).

Marsden and Schulman (74) made a study of the surface potential as a function of the pH of the substrate on both unicomponent films and mixed films. They concluded that the film properties of one component monolayers on substrates of different pH depended on the degree of ionisation of the polar groups and the electrical force acting between these polar groups. If the repulsive forces between the polar groups were large, then ionisation of the heads occurred and the film became the expanded type. The changes in the film properties of mixed monolayers were also attributed to the changes in the electrical forces between the polar groups.

(6) Chemical reactions in Surface Films

The study, by the monolayer technique, of reactions at the air/water interface is essentially due to Rideal and coworkers. Reactions can be followed by change of area or surface potential at constant surface pressure. The various types of surface chemical reactions which have been studied fall into the following categories: 1) Oxidation reactions, 2) Hydrolysis of lactones and esters, 3) Lactonisation of hydroxy acids and 4) Isotopic exchange reactions by radioactive techniques. In almost all of these reactions, it has been shown that the rate of reaction of a substance present in a film at a liquid surface may be influenced by the special conditions prevailing at the surface which permits the changes in the accessibility of the reacting groups of the molecules in the film to the reagents in the substrate.

(a) Oxidation reactions:

In a study of the oxidation of fatty acids containing a double bond in the hydrocarbon chain, by permanganate in the underlying water, Hughes and Rideal (75) found the accessibility of the film molecules for the substrate permanganate to influence markedly the reaction velocity. The kinetics of such oxidation of double bonds was studied by these workers using changes in the surface potential with time to follow the reaction. Assuming the reaction to be bimolecular, the bimolecular reaction constant K_2 was given by the equation,

$$K_2 = \frac{1}{t.c} \ln \frac{\Delta v_o - \Delta v_\infty}{\Delta v_t - \Delta v_\infty} \qquad \text{--(29)}$$

where c = concentration of MnO_4^- ions in the substrate, Δv_o, Δv_t, and Δv_∞ representing the surface potentials at times t = o, t, and ∞ respectively.

It was found that oleic and petroselenic acids were much more rapidly oxidised on dilute acid permanganate when the films were under low surface pressure than when compressed to a higher surface pressure. Prior to oxidations, these acids formed liquid expanded films, but after oxidation, they passed into gaseous films. The rate of oxidation of the double bond could be reduced to a measurable extent by compression of the film, so that the degree of accessibility of the molecules to the underlying solution reactant was diminished by removing double bonds from the surface. That the reaction velocity is extremely sensitive to variations in pressure was also established by studies of the rate of autoxidation of the maleic anhydride compound of β-elaeo-stearin by Gee and Rideal (76).

Mittelman and Palmer (77) investigated the permanganate oxidation of triolein monolayers. The interpretation of results are given by these workers in terms of a model which attempted to account for the changing accessibility of film molecules to substrate reactant. The velocity constant K is proportional to the fraction of chains in a position to react. Considering all the possible configurations of the hydrocarbon chains as members of a series of L shapes, the velocity constant K is given by

$$K = \text{Constant x a function of } \pi$$

$$= \text{Constant x} \, \phi(\pi) \qquad \text{--(30)}$$

where

$$\phi(\pi) = \sum_{l_1}^{l_2} \exp\left(\frac{-\pi al+E'}{kT}\right) \Bigg/ \sum_{0}^{l_2} \exp\left(\frac{-\pi al+E'}{kT}\right)$$

In the above equation, l is the distance between the carboxyl and the corner of L in the chains, π= film pressure, a = width of the chain, E' = energy required to twist the hydrocarbon chain at the corner of the L,E' = 800 cal per mol (78), k = Boltzmann constant, T = absolute temperature.

Keichi Eda (79) investigated the kinetics of permanganate oxidation of unsaturated acid monolayers by measuring changes of the film area with time at constant pressure as an alternative technique to the surface potential method.

(b) Hydrolysis reactions

(i) Alkaline hydrolysis of lactones and esters

Monolayers of long chain fatty acid lactones and esters undergo hydrolysis when spread on alkaline substrates. The hydrolysis reactions of these films again reflected the effect of molecular orientation on the reaction velocities.

Adam (80) showed that a film of γ-stearo lactone on the surface of N NaOH rapidly underwent hydrolysis with the formation of γ-hydroxy stearic acid. As the reaction proceeded, the initially condensed or liquid-expanded film of γ-stearo lactone passed over to the gaseous film of γ-hydroxy stearic acid. The kinetics of this reaction was first followed by Fosbinder and Rideal (81) using the surface potential method developed by Schulman and Rideal (70). The bimolecular reaction constant was given by the equation developed for oxidation reactions. The apparent energy of activation has been calculated for these reactions from the expression

$$\frac{d \ln K}{dt} = \frac{E}{RT^2} \qquad \text{--(31)}$$

The hydrolysis of short chain fatty acid esters on an alkaline substrate have been investigated by Alexander and Rideal (82) and Alexander and Schulman (83), using the surface potential technique. Adam and Miller (84) studied the hydrolysis of soaps of long chain fatty acids on strongly alkaline substrates. These soaps were found to form expanded films, the stability of which was increased by greater chain length of the film molecules and higher alkalinity of the substrate.

(ii) Acid hydrolysis of esters

The velocity of hydrolysis of films of esters on acid substrates is markedly slow and the effect of molecular orientation on the reaction velocity is difficult to follow. However the velocity for the hydrolysis of an expanded film of ethyl palmitate on acid substrate was determined on all but condensed films. In this latter case the changes of area and potential were too small for confident measurement.

In bulk hydrolysis, it is well established that the H^+ ion is a much less powerful catalyst than the OH^- ion. A confirmation of this fact was observed with films of the long chain esters. Octadecyl acetate on a substrate of 5N HCl was hydrolysed very slowly at 26° C and $\pi = 3$ dynes/cm. The velocity constant was found to be 3.30×10^{-3} l/g. mol per minute, some hundred times lower than the value obtained for this constant on alkaline substrates.

Recently Havinga (85) has reported the acid hydrolysis of mixed films of Alpha-diazo-stearic methyl ester (DME) and stearyl phosphoric acid and DME and lignocerylamine on dilute HCl. The course of each reaction was followed by ultraviolet absorption analysis, with time, of the reacting samples. Havinga concluded that the surface reactions are not only dependent upon the pH of the substrate but are considerably influenced by the potential shifts in the electrical double layer at the interface (86).

(c) Lactonisation

The rate of lactonisation of films of ω- hydroxy ethyl stearyl malonic acid and γ- hydroxy stearic acid were studied by Kögl and Havinga (87). The rate of lactonisation of ω- hydroxy ethyl stearyl malonic acid in a film is 10^3 to 10^4 times greater than in bulk under identical pH conditions. The rapid rate in the film may be attributed to the close approach of the hydroxy and the carboxyl group in the compressed film of stearic acid derivative.

Lactonisation of γ- hydroxy stearic acid on the other hand is slower in a film than in bulk. This fact is attributed again to a stearic factor, the inability of the two reacting groups to come close to each other in films of this compound. Lactonisation of monolayers of γ- hydroxy stearic acid was also studied by Davies (88), using pressure-area and potential-area measurements. The second order velocity constant K was evaluated from the usual expression:

$$K = \frac{1}{t[H^{+}]} \ln \frac{\Delta V_0 - \Delta V_\infty}{\Delta V_t - \Delta V_\infty} \qquad \text{--(32)}$$

where $[H^{+}]$ represents the concentration of acid in the substrate and the rest of the terms have their usual significance. Davies found that the rate is practically unchanged till the film pressure exceeds about 9 dynes/cm; thereafter decreasing as the film condenses, being reduced to less than half the former value at π= 26 dynes/cm. The slower reactions at higher pressures may be attributed to the inaccessibility of the -OH or -COOH group to the substrate. Davies explains the decrease in rate at higher pressures in terms of concentrations of reacting groups in the surfaces, without considering electrical redistributions in the molecule, changes of mechanism of reaction, potential barriers at the surface or the charged energy of activation.

(d) Isotopic Exchange reaction

(i) History

The study of isotopic exchange reactions using tracer technique in bulk phase or in monolayers is of comparatively recent origin. Mc Kay (89) reported preliminary experiments on isotopic exchange reactions in solutions using radioactive iodine. In general there are certain unique characteristics of exchange reactions. The reaction products are chemically identical with the reactants; hence the energy diagram of the reacting molecular system must be a completely symmetrical one; an energy of activation but no heat of reaction characterises the exchange reaction. Moreover there are no complications due to changes in the chemical composition of the reacting mixture as the reaction proceeds.

The literature contains many references to isotopic exchange reactions using radioactive iodine as the tracer element. Mc Kay (90) made a somewhat detailed study of the kinetics of I^{128} exchange reactions in alcoholic solution, the general reaction being given by the equation

$$RI + I^{128-} \rightleftarrows RI^{128} + I^-$$

The kinetics of the exchange reaction was developed as follows: if the concentration of RI and I^- be a and b respectively and x be the concentration of RI* at any time, t, then the total rate of the reaction V, is given by,

$$-\ln (1-x/x_{\infty}) = V (a+b) t/ab \qquad --(33)$$

where x_{∞} is the limiting value of x when exchange is complete, that is, at $t = \infty$, if the exchange reaction is a simple bimolecular reaction, then,

$$V = K(ab) \qquad --(34)$$

Therefore

$$-\ln (1-x/x_{\infty}) = K (a+b) t \qquad --(35)$$

where K = velocity constant of the reaction.

This equation is valid only for the homogeneous exchange reaction and assumes that no appreciable side reactions occur. When ethyl iodide was exchanged with the iodide ion of NaI, the effect of initial concentration of both reacting species was studied as a means of determining the order of the reaction. Three series of experiments were studied, varying the concentration of sodium iodide in the first two series at constant ethyl iodide concentration and varying the ethyl iodide concentration at constant NaI concentration in the third set. The results illustrated the bimolecular nature of the reaction. A one hundred-fold increase in the concentration of sodium iodide doubled the velocity constant and a four-fold change in the ethyl iodide concentration resulted in a 20% change in the velocity constant. An approximate straight line was obtained on plotting the velocity constant against the logarithm of the concentration. The energy of activation was determined graphically by the usual plot of log K versus 1/T.

Since the work of McKay, many investigators have reported studies on iodine exchange reactions (91,92,93) using I^{131}. Behrens and Maddock (94) studied the thermal exchange between I^{131} and methyl iodide. Rapid exchange between I^{131} and stannic iodide in carbon tetrachloride at $0^{o}C$ was studied by Kahn and Freedman (95). The exchange was complete in 7 seconds, possibly due to the formation of positive halide ions (96). All the above mentioned reactions were studied in non-aqueous medium.

The exchange reaction between organic iodides and inorganic iodine in aqueous solution has been studied by Van der Straaten and Aten (92), using I^{131} as the tracer element. In this work, the sodium salt, methyl ester and free iodoacetic acid were each exchanged with iodide ions. The reaction rate was determined from the expression (97):

$$R = (axb/a+b)\ (0.69/T_{\frac{1}{2}}) \qquad \text{--(36)}$$

a and b being the concentrations in moles per litre of the reactants; $T_{\frac{1}{2}}$, the time of half exchange in seconds (The time for the specific activity of the originally inactive fraction X, to become one half of the specific activity at total exchange, X); R = reaction rate in moles litre^{-1} sec^{-1}.

For a second order reaction, the reaction rate would be related to the concentration of the reactants by the expression

$$R = abK \qquad \text{--(37)}$$

K being rate constant in litre moles^{-1} sec^{-1}.

As a result of the many investigations (98-101) of isotopic halogen exchange with aliphatic halides, it has been proposed that the exchange reaction proceeds through the mechanism of the Walden inversion. It is assumed that inversion takes place when the entrant group attaches itself to the side of the asymmetric carbon atom opposite that occupied by the group to be expelled. The negative ion approaches the carbon-halogen dipole at its positive end.

(ii) Isotopic exchange reactions in monolayers.

The exchange reaction between halogen substituted fatty acid labelled with I^{131} and substrate potassium iodide ions was originally reported by Robertson et al (102). The reaction investigated was an exchange between Alpha-Iodo stearic acid (AIS), tagged with I^{131} and substrate potassium iodide. The reaction taking place was summarized by the equation

$$CH_3(CH_2)_{15}CHI^{*}\ COOH + I^{-} \longrightarrow CH_3(CH_2)_{15}CHI\ COOH + I^{*-}$$

The kinetics of the homogeneous exchange reaction were studied (103). In general for a reaction of m^{th} order in concentration of reactant a and n^{th} order in concentration of reactant b, the over all reaction velocity V can be expressed in the form

$$V = K_{m+n}\ (a)^{m}\ (b)^{n} \qquad \text{--(38)}$$

where K_{m+n} is the exchange constant for $(m+n)^{th}$ order reaction. The monolayer exchange reaction could be considered as first order in fatty acid concentration b and n^{th} order in the substrate iodide ion concentration a. The above equation then becomes

$$V = K_{n+1}\ (b)\ (a)^{n} \qquad \text{--(39)}$$

It has been shown by Robertson that the total rate of reaction in terms of measured radioactivity could be written

$$V = \frac{(b)}{t}\ \ln\ \frac{c_o}{c_t} \qquad \text{--(40)}$$

where

c_o = counts per minute at t = o

c_t = counts per minute at any time t.

Hence from the above equations,

$$K_{n+1} (b) (a)^n = \frac{(b)}{t} \ln \frac{c_o}{c_t} \qquad \text{--(41)}$$

or

$$K_{n+1} = \frac{1}{a^n t} \ln \frac{c_o}{c_t} \qquad \text{--(42)}$$

The pseudo first order reaction constant K^1 from which the activation energy could be determined once the temperature dependence was established is given by the expression,

$$K^1 = \frac{1}{t} \ln \frac{c_o}{c_t} \qquad \text{--(43)}$$

K^1 is related to K_{n+1} by the relation

$$K^1 = K_{n+1} \quad a^n \qquad \text{--(44)}$$

Taking logarithms,

$$n \ln a + \ln K = \ln K^1 \qquad \text{--(45)}$$

The slope of the plot of ln a against ln K^1 will give n, the order of reaction in substrate ion concentration.

The activation energy E can be determined by the

Arrhenius equation,

$$K^1 = A e^{-E/RT} \qquad \text{--(46)}$$

then,

$$\ln K^1 = \ln A - (E/RT) \qquad \text{--(47)}$$

The slope of the line obtained by plotting ln K^1 against the reciprocal of the temperature will give the activation energy for reaction required by the molecules.

(iii) Early work in Monolayer exchange reactions

Robertson (103) followed the exchange reaction between I^{131} and AIS spread as a monolayer at the air/water interface and substrate iodide ions. This work indicated that the exchange constant was independent of surface pressure except in the critical region (18°C) for the transition from liquid expanded to liquid condensed films. The activation energy for exchange in liquid condensed and liquid expanded films was found to be 10 and 8 K. calories per mole showing a discontinuity in the activation energy plot. The change in the temperature coefficient of the rate constant was attributed to a reorientation in the film resulting in a change in the accessibility of I^{131} atoms in the alpha position to the substrate iodide.

The investigations of the isotopic exchange reaction between monolayers of active alpha iodo(I^{131}) stearic acid and substrate iodide ions was continued in the work of Rabinovitch (104) where the effect on the exchange kinetics, of pH, substrate cations and temperature were determined. Exchange reactions of active AIS acid monolayer on 1 N KI substrate solutions were performed under both acid and alkaline conditions. Simultaneous automatic recordings of $\pi-\sigma$ diagrams were made. The results of these investigations showed that a rapid exchange was associated with a liquid expanded film on an acid substrate and a slow exchange was associated with a gaseous film on an alkaline substrate.

Exchange reactions were also studied in which barium ions were present in the substrate. The results of these exchange reactions showed that alkaline substrates retard the exchange rate to a marked extent.

By a systematic study of the effect of variations of pH at 18°C, 16°C and 35°C on the exchange rate constant, Rabinovitch showed that the rate constant K passes through a maximum near pH 1 to 2 and drops slowly to about one fourth the maximum at pH = 4.5. At 25°C, the maximum occured between pH 2-3 and at this temperature the exchange rate constant was 8 to 25 times higher at pH 2 to 3 than at pH 11-12, irrespective of the presence of cations.

II EXPERIMENTAL

(1) Apparatus

(a) Trough

The troughs employed by the earlier workers in surface film studies were usually constructed of a non rusting material such as brass or stainless steel. The desired non-wetting properties of the trough were then achieved by coating the inside and edges of the trough with paraffin or some other suitable water repellant. It was essential that the non-wetting agent chosen was itself free of any surface active contamination; hence laborious purification and testing was necessary before a particular material was applied to the trough. Further, the coating of water repellant had to be renewed frequently if the trough was in constant use. The introduction of silica troughs by Adam (page 28,11) served the two-fold purpose of reducing the amount of non-wetting agent required and minimizing contamination of the substrate by the metallic ions of the trough itself.

Rabinovitch (104) used a trough with internal dimensions 21" x 8" x 1/2". This trough was constructed of stainless steel, perfectly milled out and heat treated and coated with several layers of teflon.

The same trough with a teflon sheet covering has been used in the present work. This teflon covered trough can be cleaned very thoroughly. Using such a trough, results in fair agreement with earlier work have been obtained.

(b) Barrier and barrier drive mechanism

Early workers employed as barriers, paper, glass or brass strips coated evenly with highly purified paraffin. The use of such barriers, besides necessitating the tedious paraffin treatment to render them non-wetting,also required that great care be exercised in their use to prevent contamination of the surface and leakage of the film forming material past the barriers. In the work of Rabinovitch (104) and the present work an improved type of barrier has been used. These barriers consist of rectangular stainless steel strips, cushioned with soft foam rubber and the whole wrapped in a layer of teflon sheet. In the very large number of experiments performed this type of barrier eliminated the usual problems of leakage. The dimensions of the steel barrier strips were 3/16" x 5/8" x 10½" for the stationary barrier and 3/16" x 5/8" x 15" for the movable barrier.

The stationary barrier rests on the trough at a fixed distance away from the drive mechanism. The 15" long barrier rests on the trough with the ends carried in the rectangular yokes of a barrier moving device connected to a worm gear below the trough. The distance between the movable and the immovable barrier was known in terms of the number of revolutions, registered on a Veeder Root revolution counter connected to the worm-gear. The area corresponding to one turn of the revolution counter was determined by direct measurements. Usually the films were spread on a surface enclosed by the two barriers 170 revolutions apart, corresponding to an area of 8.8094×10^{18} Å^2.

A fast barrier drive mechanism on a suitably geared 700 R.P.M., 1/10 H.P., D.C. motor was used for surface contamination tests and the removal of old films. The movable barrier traversed the distance of 170 revolutions to come in contact with the other barrier in roughly 19 seconds. This fast compression barrier drive mechanism was not used for any experimental determinations of π-σ isotherms of fatty acids.

For the experimental work a variable speed Graham-drive was installed (104) to obtain a wide range of expansion and compression rates. With this modification of the barrier moving device, the study of hysteresis effects and relaxation effects in spread monolayers was greatly facilitated.

(c) Temperature control of the system

Temperature control in the experimental investigations was achieved by enclosing the film trough assembly in a double walled chamber(Fig 2a). The details of construction have been dealt with in detail by Robertson (103). A sheet of blotting paper held by magnets against the ceiling of the inner box enclosing the trough assembly prevented condensed water from dripping from the ceiling of the box into the trough, a problem of serious concern in earlier studies. The temperature of the substrate was ascertained by a one-tenth degree Eimer and Amend thermometer (-10° C to 60° C) whose bulb was kept immersed in the substrate. By circulation of water from an outer constant temperature source through copper tubing in the box and the water jacket on which the trough rested, the temperature of the substrate could be controlled to ±0.1° C of the desired value.

(d) Surface pressure measurement

The measurements of surface pressure in these investigations were made by an automatic recording device based on the Wilhelmy dipping plate (21) previously used by Dervichian (105) and Harkins and Anderson (29). These workers measured the development of surface pressure by using a thin rectangular microscope slide, partly immersed in the substrate and suspended by a thin wire from one arm of an analytical balance. The deflection of a light beam from a mirror mounted at the fulcrum of the balance beam resulting from the vertical displacement of the slide, gave the surface pressure measurements.

Figure 2a

(With the kind permission of Dr. R.F. Robertson)

Figure 2a

Constant Temperature box.

1. Outer glass wool insulation
2. Chamber containing copper coils (not shown) for constant temperature water
3. Constant temperature air chamber
4. Cork supports
5. Stone pedestal
6. Windows (triple glass)

Film Trough.

A	Trough
A_1	Trough support
A_2	Barrier moving device
A_3	Adjustable Feet
A_4	Handle and revolution counter of barrier moving device.

Geiger Tube Assembly.

B	Geiger Tube
B_1	Tube carriage
B_2	Tracks for carriage
B_3	Handle for moving tube carriage
B_4	Shielded lead to Rate Meter

Surface balance.

C	Sleeve for wire of surface balance

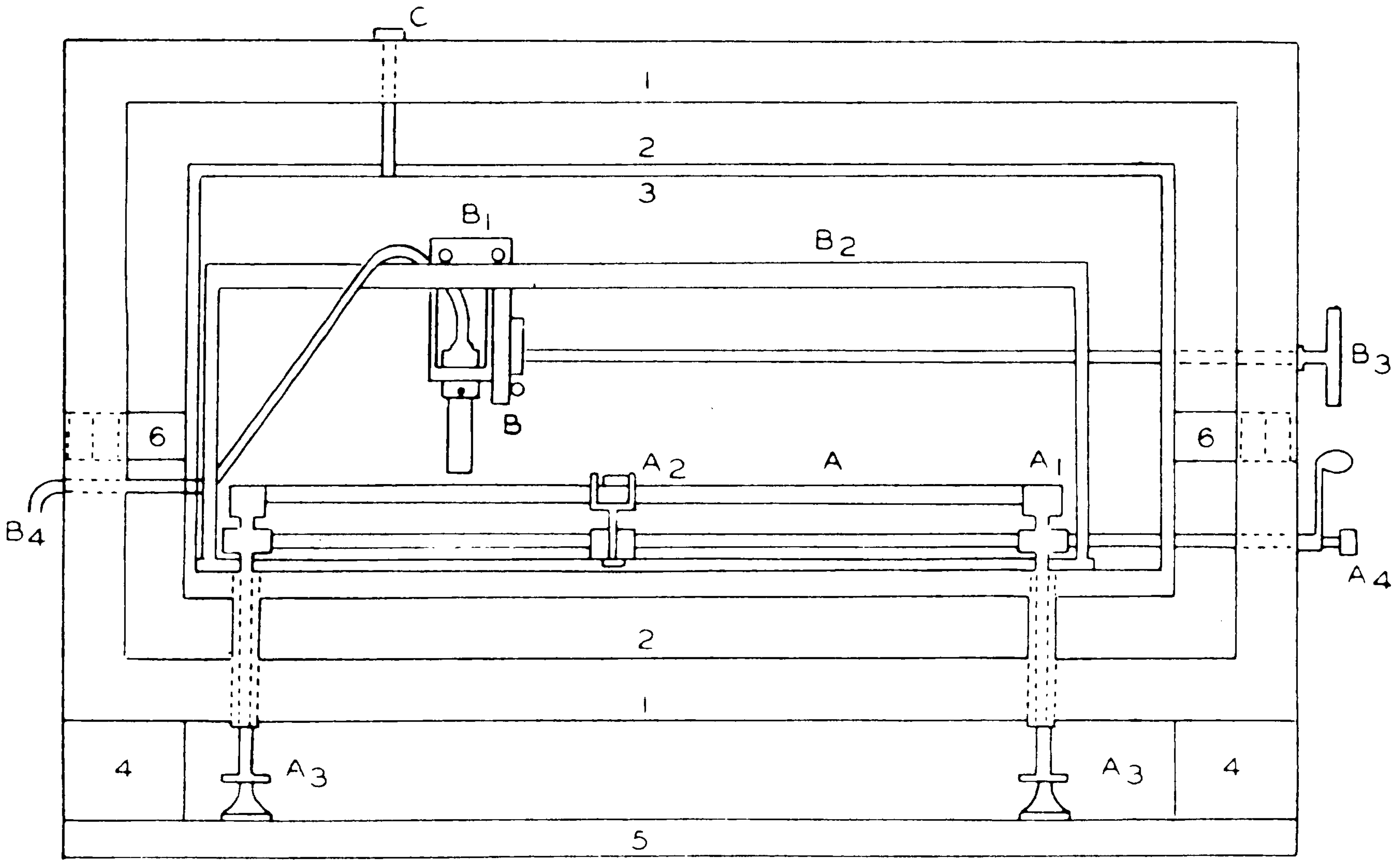
C
1
2
3
B1
B2
B3
B
6
6
A2
A
A1
B4
A4
2
1
4
A3
A3
4
5

In the present work, the same principle of a dipping plate was used, but an automatic analytical balance designed by Mauer (106) for recording rapid changes in weight was adopted for instantaneous balancing and strip-chart recording of the surface pressure. This method, first used by Rabinovitch (104) is superior to either the vertical pull balance of Harkins and Anderson (29) or other types of horizontal pull balances. The balance provides continuous recording of the film pressure as a function of molecular area either during compression or expansion. Since only the perimeter of the slide and not the thickness as in Harkins and Anderson (29) enters into measurement of the surface pressure, the experimental error of 0.5% in the older method is reduced to 0.1%. In contrast to the technique of Harkins and Anderson, the vertical displacement of the slide in the present balance is practically zero. Consequently, the crystallisation of salt from substrates (if potassium iodide solutions are employed) is avoided and accurate measurements can be made during film expansion on the salt substrates. This was not possible in the early work on exchange reactions (103) because of fouling of the slide surface on emerging from the KI substrate. Fig 2b is a sketch of the entire recording unit. The components of this unit are as follows:

(1) Microscope slide, partially dipping in the substrate.

Figure 2b

Figure 2b

Sketch of the entire η-σ-recording unit.

1 Microscope slide

2 Christian-Becker chainomatic balance

3 Light source

4 Photo tube and bridge circuit

5 Solenoid

6 Decade resistance box

7 Weight recording amplifier

8 Electronic recorder

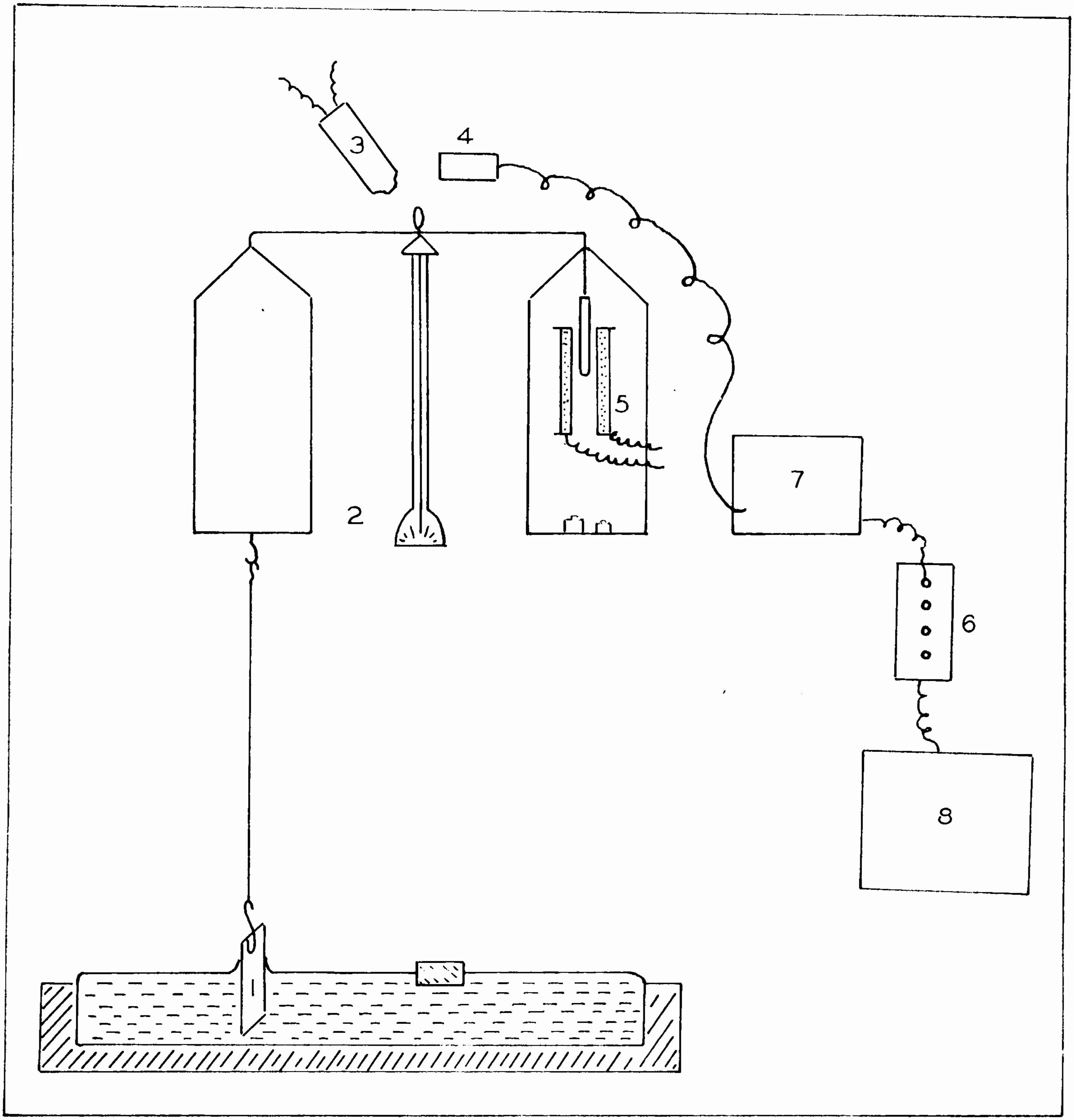
3
4
2
5
7
6
8
1

Corning cover glass #1, 24 x 40 mm, suspended from a nichrome wire fixed to the right hand pan of the balance.

(2) Christian-Becker chainomatic balance.

(3) Light source: A 6 v Mazda bulb connected to a storage battery.

(4) Photo-tube and bridge circuit.

(5) Solenoid: with a ¼" x 3" magnet as the core.

(6) Decade resistance box.

(7) Weight recording amplifier, amplifying the output of the bridge circuit to provide current in the solenoid.

(8) Electronic recorder (Minneapolis-Honeywell Reg.Co. Brown Instruments Division - Type 153 x 12v -x-30. Single span).

The voltage drop across the decade resistance box in series with the solenoid, was measured and traced by the recorder. Once the unit was calibrated, the film pressure could be read from the tracing as a linear function of the pen displacement. The recorder required 4½ seconds to traverse the entire range of 0 - 50 dynes on the full scale of 10 inches on the chart paper (type 5839 - N - R). Another interesting feature of this recorder was a multi-speed Insco-Brown chart drive installed directly on the change gear hubs of the recorder, to permit the selection of eight different chart speeds. A detailed account of the theory, function and calibration of this type of balance has been given by

Rabinovitch (104).

(e) Radioactivity measurements

A geiger end-window counter (Amperex 200 NB) was used as the detector for the radioactive films. This type of fused mica end-window (1.4 mgm/cm^2) geiger tube was found to be capable of surviving in the atmosphere of saturated water vapour present in the constant temperature box of the film balance and trough. The plateau region for each tube employed was determined from a standard uranium source. Usually the operating voltage was between 750 - 900 volts and increased slightly with aging. The tube was positioned in a specially designed holder over the film.

The count rate of the film was measured by an Electronics Associates Count Ratemeter (type EA - 172 S). This ratemeter was frequently calibrated (because of possible tube failure) using a pulse generator or a Berkeley scalar. By incorporating a fine control in the circuit, the ratemeter was found to have a linear response. The count-rate was recorded on an Esterline-Angus 10 milliamp recorder. A plot of count-rate as a function of time was thus obtained directly. A chart speed of 3/4" per hour was usually employed for exchange studies but higher speeds could be selected when required.

(f) Maintenance and precautions to be observed

(i) The electronic tubes in the EA ratemeter, weight recording amplifier had to be tested frequently. The 6J6 tubes in the EA ratemeter usually lasted from 2 to 3 months if continuously used. The weight recording amplifier tubes, rectifier 80, 5691 (6SL7) and 5692 (6SN7) seemed to last fairly long; but if defective gave an erratic trace on the recorder making calibration difficult.

(ii) The potentiometer wire in the Honeywell recorder had to be kept clean by brushing and washing with petroleum ether, otherwise the response sensitivity was seriously affected.

(iii) The Honeywell recorder had to be oiled monthly to insure satisfactory performance.

(iv) Any extraneous source of light, particularly fluorescent fixtures near the photo-tube affected the automatic surface balance to such an extent that it was found advantageous to turn all unnecessary lights off during pressure measurements.

(v) Vibrational disturbances markedly affected the surface balance. Any unnecessary vibrations had to be eliminated for satisfactory operation of the balance.

(g) Surface potential measurements

The air electrode used for surface potential measurements consisted of a 5 mc polonium ^{210} plated source positioned near the stationary barrier about half an inch above the film. The other electrode was a standard calomel electrode dipping into the substrate behind the movable barrier. The two electrodes along with a Beckmann pH meter (Model G) were used for the surface potential measurements. The whole box of the air thermostat was well grounded and electrical disturbances around the apparatus were kept at a minimum.

(2) Materials

(a) $I^{131}\alpha$-Iodo-stearic acid

For exchange reactions, 20 mg of AIS prepared by Robertson (103) were dissolved in 5 ml of absolute alcohol and acidified with 2 drops of constant boiling hydrochloric acid. One ml of I^{131} as aqueous sodium iodide (10 millicurie) was then added to the above mixture and the whole was refluxed for 1½ to 2 hours. The refluxed solution was cooled and 50-75 cc of 0.01N HCl was added and the mixture was allowed to stand overnight for good crystal growth. The I^{131} AIS crystals were filtered, dried by suction for about twelve hours and dissolved in benzene and stored in 10 ml volumetric flasks in a lead castle.

This procedure yielded a very highly active I^{131} AIS in contrast to the preparations of Robertson (103) and Rabinovitch (104). Carrier free I^{131} (as aqueous NaI) was obtained from Commercial Products Division of Atomic Energy Commission of Canada Ltd.

(b) Chain substituted stearic acids

The chain substituted stearic acids used were obtained from Dr. I.E. Puddington, Director, Applied Chemistry Division, National Research Council, Ottawa. The stearic acids were

NAME	Melting point (in °C)
(1) Stearic acid	69.61
(2) 2-Methyl stearic acid	54.6 - 55.1
(3) 3-Methyl stearic acid	50.8 - 51.3
(4) 3-Ethyl stearic acid	47.5 - 48.1
(5) 10-Phenyl stearic acid	Not available
(6) 12-Hydroxy stearic acid	80 - 81
(7) 12-Keto stearic acid	81 - 82

(c) Other materials

Fischer's reagent grade thiophene free benzene was used as the spreading solvent for all the fatty acids employed. The solvent was used without further purification if found, on testing, to be free of surface active contaminants.

Chemically pure potassium chloride and iodide and sodium bisulphite were employed without further purification.

(3) Procedure

(a) Exchange reactions

(i) Preparation of Trough

Before use, the teflon trough was cleaned twice with hot chromic acid solution. When the cleaning solution was removed, the trough was rinsed with profuse quantities of high grade distilled water. After this treatment the trough was satisfactorily free of any surface active contamination.

(ii) Preparation of substrate solutions

Substrates of the desired concentrations were prepared by dissolving calculated quantities of potassium iodide and potassium chloride in distilled water. The iodide substrates could be used repeatedly after the free iodine from atmospheric oxidation was removed by a trace sodium bisulphite or by active charcoal.

(iii) Positioning of barriers

After filling the trough with the substrate, clean barriers were positioned on the trough in the following manner: The movable barrier was placed in its carrier and advanced to a point corresponding to 180 revolutions of the revolution counter. The stationary barrier was then placed against the forward edge of the movable barrier. The movable barrier was then brought back to a position corresponding to 10 revolutions on the counter. The barriers were thus separated by 170 revolutions from which could be determined the initial area available for spreading the monolayer. This procedure of moving the barriers apart from zero area to the initial area also served to sweep the water surface free of surface active contaminants before the film was spread,

(iv) Final preparations for an experiment

The surface balance was then calibrated to read 0-50 dynes/cm for full scale deflection by the method of Rabinovitch (104). A test for surface contaminations was performed by compressing the surface to 1/8 its original area and noting the surface pressure developed. A pressure less than 0.1 dynes/cm at maximum compression was a sufficient criterion of the absence of surface contamination.

If radioactive measurements were to be made on the film, the geiger tube was positioned over the clean surface and the background count rate of the substrate was recorded. Once the background count was determined the radioactive acid was then spread dropwise from a suitable microliter pipette, and the pressure adjusted, by compression or expansion, to the desired value and the count rate recorded.

(b) The pressure area isotherms of the chain substituted stearic acids

A calculated quantity of each of the acids to be studied was accurately weighed out and dissolved in benzene, in a 10 ml volumetric flask. The volumetric flasks were then stored in an atmosphere of benzene to minimise changes in concentration from evaporation of the solvent. The weight of acid required to prepare the stock solution was related to the initial area per molecule for the individual experiment.

A typical calculation follows for the preparation of a 10 ml solution of 12 keto-stearic acid (molecular weight = 298.45), so that 50 microlitres will give an area per molecule of 65 $Å^2$ when spread on a surface of $8.8094\text{x}10^{18} Å^2$.

Total area of surface = $8.8094\text{x}10^{18}\ Å^2$.

65 $Å^2$ are occupied by 1 molecule.

$8.8094\text{x}10^{18}\ Å^2$ . . . . . $\dfrac{8.8094\text{x}10^{18}}{65}$ molecules

or

$$= \frac{8.8094\text{x}10^{18}}{65} \text{ X } \frac{298.45}{6.023\text{x}10^{23}} \text{ gms}$$

where 298.45 = molecular weight of 12 ketostearic acid and $6.023\text{x}10^{23}$ = Avogadro number. This weight should be present in 50 1 or 0.05 ml. Therefore 0.05 ml of solution should contain $\dfrac{8.8094\text{x}10^{18}}{65} \text{ X } \dfrac{298.45}{6.023\text{x}10^{23}}$ = 0.01352 gm

= 13.52 mgm.

For each of the chain substituted stearic acids, the required weight was calculated by the above method and the benzene solutions prepared.

The rate of compression was interpreted as the rate of change of area per molecule with time, $d\sigma/dt$. This derivative could be related to (i) the initial area per molecule $\underline{x}$, (ii) the total area of surface expressed as the number of revolutions on the counter B, and (iii) the rate of motion of the barrier (in terms of number of revolutions per minute) w,

$$d\sigma/dt = \underline{x}/B \times w \qquad \text{--(48)}$$

The value of B was arbitrarily held constant at 170 revolutions for all the experiments. In any individual experiment where a specific compression rate was required, w could be easily evaluated from the known or chosen values of $\underline{x}$ and $d\sigma/dt$. The Graham drive speed control could then be set to give the calculated value of w and hence the required rate of compression.

A typical pressure-area experiment was performed as follows: A 0.01 N HCl solution was prepared by diluting constant boiling hydrochloric acid with distilled water (checked for surface active contamination). This substrate solution was then added to the clean trough until the trough was filled to the brim. The substrate was swept several times with the clean barriers as described earlier. The slide, dipping into the substrate was suspended from the wire attached to the balance and the surface pressure measuring unit was then calibrated to measure a pressure of 0-50 dynes/cm for full scale pen deflection on the Honeywell recorder.

The surface was then checked for surface active contamination as described earlier and if no contamination was detected, the film was spread.

Usually 50 microlitres of the benzene solution of the particular acid under investigation was spread drop by drop from a micropipette at various points on the surface. A period of ten to fifteen minutes, depending on the temperature, was allowed for evaporation of benzene from the surface.

The film was then compressed at the desired rate of compression and the pressure-time curve recorded on the Minneapolis-Honeywell recorder. From the known chart speed of the recorder and the known rate of the movement of the barrier, the time axis of the recorder chart could be directly converted to area per molecule. Thus the pressure area curves could be directly recorded.

III RESULTS

(1) Radioactive work

(a) Exchange reactions

Exchange reactions were performed at approximately pH = 2 and at 25°C and 14°C between an active AIS monolayer and 1 N KI substrate. These experiments were in fair agreement with similar experiments of Robertson (103) and Rabinovitch (104) and a comparative table of the results is shown below:-

TABLE II

Temp	pH of substrate	10^4K^1 min^{-1}		
		Robertson	Rabinovitch	Present
25°C	2.0	25.3, 24.7	24.4	24.9, 24.9
14°C	2.1	6.8, 7.0	5.5	7.5

In an attempt to determine the order of exchange rate with respect to the substrate, exchange reactions were studied between an active AIS monolayer and various substrate concentrations of KI and KCl mixtures of approximately constant ionic strength. This series of experiments was performed at hydrogen ion concentrations equivalent to pH = 2 and pH = 3 at a temperature of 25°C.

The results of these experiments are collected in tables III to XXII. In these tables C.P.M. stands for counts per minute after the background correction has been applied; c_o and c_t represent counts per minute at zero time and at any time t respectively. The exchange constant K^1 was computed from the equation,

$$K^1 = \frac{2.303 \times \log (c_o / c_t)}{t_{\text{min}}} \qquad \text{--(49)}$$

Figures 3 - 6 are plots of logarithm of relative counting rates along ordinate and time in hours along the abscissa. The pseudo first order exchange constant was calculated for each curve and tabulated in tables XXIII to XXVI.

The order of the reaction in substrate concentration was determined from plots of logarithm of concentration of the substrate iodide against logarithm of exchange constant. Figures 7 and 8 represent these plots. The plots are apparently linear for all concentrations in 1 N solutions (pH = 2) and for 2 N solutions (pH = 3) up to 1 N KI concentration in the solution. Above 1 N KI concentrations in the 2 N solution deviations from linearity appear at pH = 3. It must be pointed out however that even for 1 N KI solutions with no KCl present the first order rate constant is somewhat higher than is to be expected for linearity.

TABLE III

Substrate KI concentration dependence

π = 4.0 dynes/cm. Temperature 25°C pH = 2.0

Substrate 0.25 N KI + o.75 N KCl (1 N Solution)

Time (hrs.)	C.P.M.	c_o/c_t
0.0	12860	1.000
1.0	11860	1.085
2.0	10860	1.118
3.0	10360	1.240
4.0	9860	1.300
5.0	9110	1.410
6.0	8610	1.500
7.0	8110	1.590
8.0	7860	1.640
9.0	7360	1.750
10.0	6860	1.870

TABLE IV

Substrate KI concentration dependence

π = 4.0 dynes/cm. Temperature 25°C pH = 2.0

Substrate 0.50 N KI + 0.50 N KCl (1 N Solution)

Time (hrs.)	C.P.M.	c_o/c_t
0.0	11850	1.000
1.0	10600	1.120
2.0	9600	1.240
3.0	8600	1.380
4.0	7850	1.510
5.0	7100	1.670
6.0	6350	1.870
7.0	6100	1.940

TABLE V

Substrate KI concentration dependence

π = 4.0 dynes/cm. Temperature 25°C pH = 2.0

Substrate o.75 N KI + 0.25 N KCl (1 N solution)

Time (hrs.)	C.P.M.	c_o/c_t
0.0	11560	1.000
1.0	9560	1.210
2.0	8310	1.390
3.0	7310	1.580
4.0	6310	1.830
5.0	5810	1.990
6.0	5060	2.280
7.0	4560	2.540
8.0	4060	2.840
9.0	3560	3.240
10.0	3060	3.780

TABLE VI

Substrate KI concentration dependence

π = 4.0 dynes/cm. Temperature 25°C pH = 2.0

Substrate 1.00 N KI + 0.00 N KCl (1 N solution)

Time (hrs.)	C.P.M.	c_o/c_t
0.0	5860	1.000
1.0	4960	1.180
2.0	4260	1.380
3.0	3760	1.560
4.0	3260	1.800
5.0	2960	1.98
6.0	2560	2.30

TABLE VII

Substrate KI concentration dependence

π = 4.0 dynes/cm. Temperature 25°C pH = 2.0

Substrate 0.25 N KI + 1.75 N KCl (2 N solution)

Time (hrs.)	C.P.M.	c_o/c_t
0.0	10350	1.000
1.0	9350	1.110
2.0	8600	1.200
3.0	8100	1.280
4.0	7350	1.410
5.0	6600	1.570
6.0	6100	1.700
7.0	5600	1.850
8.0	5100	2.040

TABLE VIII

Substrate KI concentration dependence

$\pi = 4.0$ dynes/cm. Temperature 25°C pH = 2.0

Substrate 0.50 N KI + 1.5 N KCl (2 N solution)

Time (hrs.)	C.P.M.	c_o/c_t
0.0	7420	1.000
1.0	6320	1.170
2.0	5420	1.370
3.0	4820	1.540
4.0	4420	1.680
5.0	4020	1.850
6.0	3620	2.040
7.0	3220	2.300
8.0	2820	2.630
9.0	2420	3.060

TABLE IX

Substrate KI concentration dependance

π = 4.0 dynes/cm. Temperature 25°C pH = 2.0

Substrate 0.75 N KI + 1.25 N KCl (2 N solution)

Time (hrs.)	C.P.M.	c_o/c_t
0.0	6700	1.000
1.0	5700	1.175
2.0	5000	1.340
3.0	4200	1.590
4.0	3700	1.810
5.0	3000	2.230
6.0	2600	2.580
7.0	2200	3.040
8.0	1800	3.720
9.0	1700	3.940
10.0	1400	4.780

TABLE X

Substrate KI concentration dependence

π = 4.0 dynes/cm. Temperature 25°C pH = 2.0

Substrate 1.0 N KI + 1.0 N KCl (2 N solution)

Time (hrs.)	C.P.M.	c_0/c_t
0.0	7580	1.000
1.0	6180	1.225
2.0	5280	1.430
3.0	4380	1.730
4.0	3780	2.000
5.0	3280	2.300
6.0	2880	2.630
7.0	2480	3.050
8.0	2080	3.640
9.0	1880	4.030
10.0	1680	4.500

TABLE XI

Substrate KI concentration dependence

$\pi = 4.0$ dynes/cm. Temperature 25°C pH = 2.0

Substrate 1.5 N KI + 0.5 N KCl (2 N solution)

Time (hrs.)	C.P.M.	c_o/c_t
0.0	7870	1.000
1.0	6270	1.250
2.0	4970	1.580
3.0	3870	2.040
4.0	3070	2.560
5.0	2570	3.070
6.0	2070	3.800
7.0	1770	4.410
8.0	1470	5.350
9.0	1270	6.200
10.0	1070	7.350

TABLE XII

Substrate KI concentration dependence

π= 4.0 dynes/cm. Temperature 25°C pH = 2.0

Substrate 2.0 N KI + 0.0 N KCl (2 N solution)

Time (hrs.)	C.P.M.	c_o/c_t
0.0	6500	1.000
1.0	4700	1.380
2.0	3800	1.710
3.0	2900	2.240
4.0	2300	2.820
5.0	1900	3.420
6.0	1500	4.340
7.0	1200	5.420
8.0	1100	5.920
9.0	900	7.230
10.0	700	9.300

TABLE XIII

Substrate KI concentration dependence

$\pi =$ 4.0 dynes/cm. Temperature 25°C pH = 3.0

Substrate 0.25 N KI + 0.75 N KCl (1 N solution)

Time (hrs.)	C.P.M.	c_o/c_t
0.0	13350	1.000
1.0	12350	1.080
2.0	11600	1.150
3.0	10850	1.230
4.0	10350	1.290
5.0	9850	1.360
6.0	9350	1.430
7.0	8850	1.500
8.0	8600	1.550
9.0	8100	1.650

TABLE XIV

Substrate KI concentration dependence

π = 4.0 dynes/cm. Temperature 25°C pH = 3.0

Substrate 0.5 N KI + 0.5 N KCl (1 N solution)

Time (hrs.)	C.P.M.	c_o/c_t
0.0	13850	1.000
1.0	12850	1.080
2.0	11600	1.190
3.0	10850	1.275
4.0	10350	1.335
5.0	9600	1.440
6.0	8850	1.570
8.0	7850	1.770
9.0	7600	1.820
10.0	7150	1.940

TABLE XV

Substrate KI concentration dependence

π= 4.0 dynes/cm. Temperature 25°C pH = 3.0

Substrate 0.75 N KI + 0.25 N KCl (1 N solution)

Time (hrs.)	C.P.M.	c_o/c_t
0.0	13300	1.000
1.0	11050	1.200
2.0	10050	1.330
3.0	9050	1.470
4.0	8300	1.600
5.0	7300	1.820
6.0	6800	1.960
7.0	6050	2.220
8.0	5550	2.400

TABLE XVI

Substrate KI concentration dependence

π = 4.0 dynes/cm. Temperature 25°C pH = 3.0

Substrate 1.0 N KI + 0.0 N KCl (1 N solution)

Time (hrs.)	C.P.M.	c_o/c_t
0.0	4700	1.000
1.0	4000	1.175
2.0	3400	1.380
3.0	2800	1.670
4.0	2400	1.960
5.0	2200	2.140
6.0	1900	2.460
7.0	1700	2.760
8.0	1500	3.120
9.0	1400	3.360
10.0	1200	3.920

TABLE XVII

Substrate KI concentration dependence

π= 4.0 dynes/cm. Temperature 25°C pH = 3.0

Substrate 0.25 N KI + 1.75 N KCl (2 N solution)

Time (hrs.)	C.P.M.	c_o/c_t
0.0	6530	1.000
1.0	6030	1.080
2.0	5630	1.160
3.0	5330	1.230
4.0	5130	1.270
5.0	4830	1.350
6.0	4630	1.410
7.0	4330	1.510
8.0	4130	1.580
9.0	3930	1.660
10.0	3530	1.850

TABLE XVIII

Substrate KI concentration dependence

π = 4.0 dynes/cm. Temperature 25°C pH = 3.0

Substrate 0.5 N KI + 1.5 N KCl (2 N solution)

Time (hrs.)	C.P.M.	c_o/c_t
0.0	5400	1.000
1.0	4900	1.100
2.0	4500	1.200
3.0	4100	1.320
4.0	3700	1.460
5.0	3300	1.640
6.0	3000	1.800
7.0	2600	2.080

TABLE XIX

Substrate KI concentration dependence

π = 4.0 dynes/cm. Temperature 25°C pH = 3.0

Substrate 0.75 N KI + 1.25 N KCl (2 N solution)

Time (hrs.)	C.P.M.	c_o/c_t
0.0	5080	1.000
1.0	3880	1.310
2.0	3480	1.460
3.0	3080	1.650
4.0	2680	1.900
5.0	2380	2.140
6.0	2080	2.440
7.0	1880	2.700
8.0	1680	3.020
9.0	1380	3.680
10.0	1280	3.960

TABLE XX

Substrate KI concentration dependence

π = 4.0 dynes/cm. Temperature 25°C pH = 3.0

Substrate 1.0 N KI + 1.0 N KCl (2 N solution)

Time (hrs.)	C.P.M.	c_o/c_t
0.0	7760	1.000
1.0	6360	1.220
2.0	5660	1.370
3.0	4860	1.590
4.0	4160	1.860
5.0	3660	2.120
6.0	3260	2.380
7.0	2960	2.620
8.0	2560	3.020
9.0	2360	3.280
10.0	2160	3.600

TABLE XXI

Substrate KI concentration dependence

π= 4.0 dynes/cm. Temperature 25°C pH = 3.0

Substrate 1.5 N KI + 0.5 N KCl (2 N solution)

Time (hrs.)	C.P.M.	c_o/c_t
0.0	5310	1.000
1.0	4610	1.150
2.0	3910	1.360
3.0	3310	1.600
4.0	2910	1.830
5.0	2410	2.200
6.0	2110	2.520
7.0	1810	2.920
8.0	1610	3.300
9.0	1410	3.770

TABLE XXII

Substrate KI concentration dependence

π= 4.0 dynes/cm. Temperature 25°C pH = 3.0

Substrate 2.0 N KI + 0.0 N KCl (2 N solution)

Time (hrs.)	C.P.M.	c_0/c_t
0.0	6100	1.000
1.0	4800	1.270
2.0	3900	1.565
3.0	3100	1.970
4.0	2600	2.350
5.0	2100	2.900
6.0	1800	3.390
7.0	1500	4.060
8.0	1200	5.100
9.0	1000	6.100
10.0	800	7.640

<u>Figure 3</u>

Figure 3

Pseudo-first order plots (Concentration dependence)

1 N solution pH = 2.0

1 0.25 N KI + 0.75 N KCl

2 0.50 N KI + 0.50 N KCl

3 0.75 N KI + 0.25 N KCl

4 1.00 N KI + 0.00 N KCl

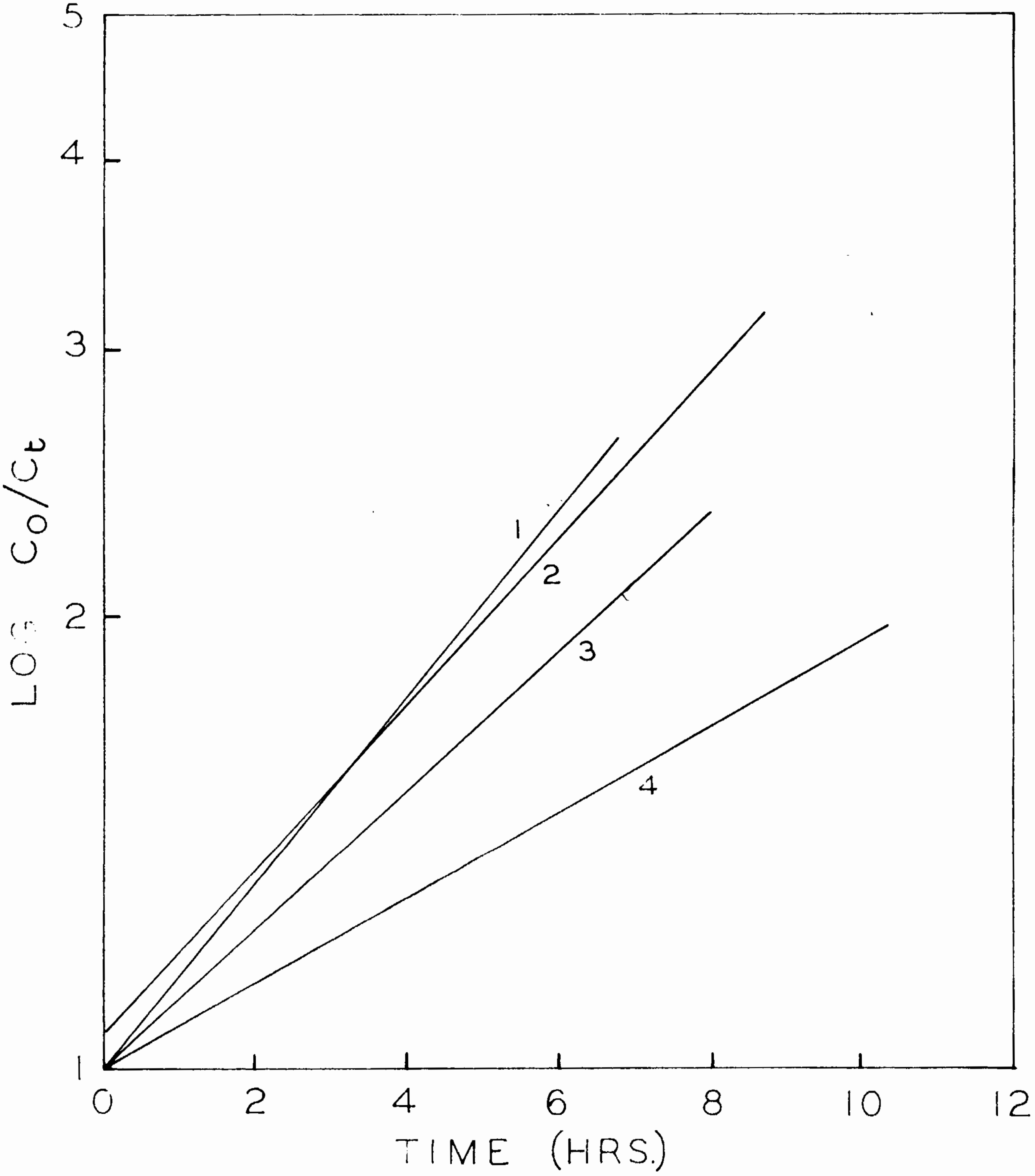
5
4
3
2
1
LOG C_o/C_t
0
2
4
6
8
10
12
TIME (HRS.)
1
2
3
4

Figure 4

Figure 4

Pseudo-first order plots (Concentration dependence)

2 N solution pH = 2.0

1.7

1 0.25 N KI + 1.25 N KCl

2 0.50 N KI + 1.50 N KCl

3 0.75 N KI + 1.25 N KCl

4 1.00 N KI + 1.00 N KCl

5 1.50 N KI + 0.50 N KCl

6 2.00 N KI + 0.00 N KCl

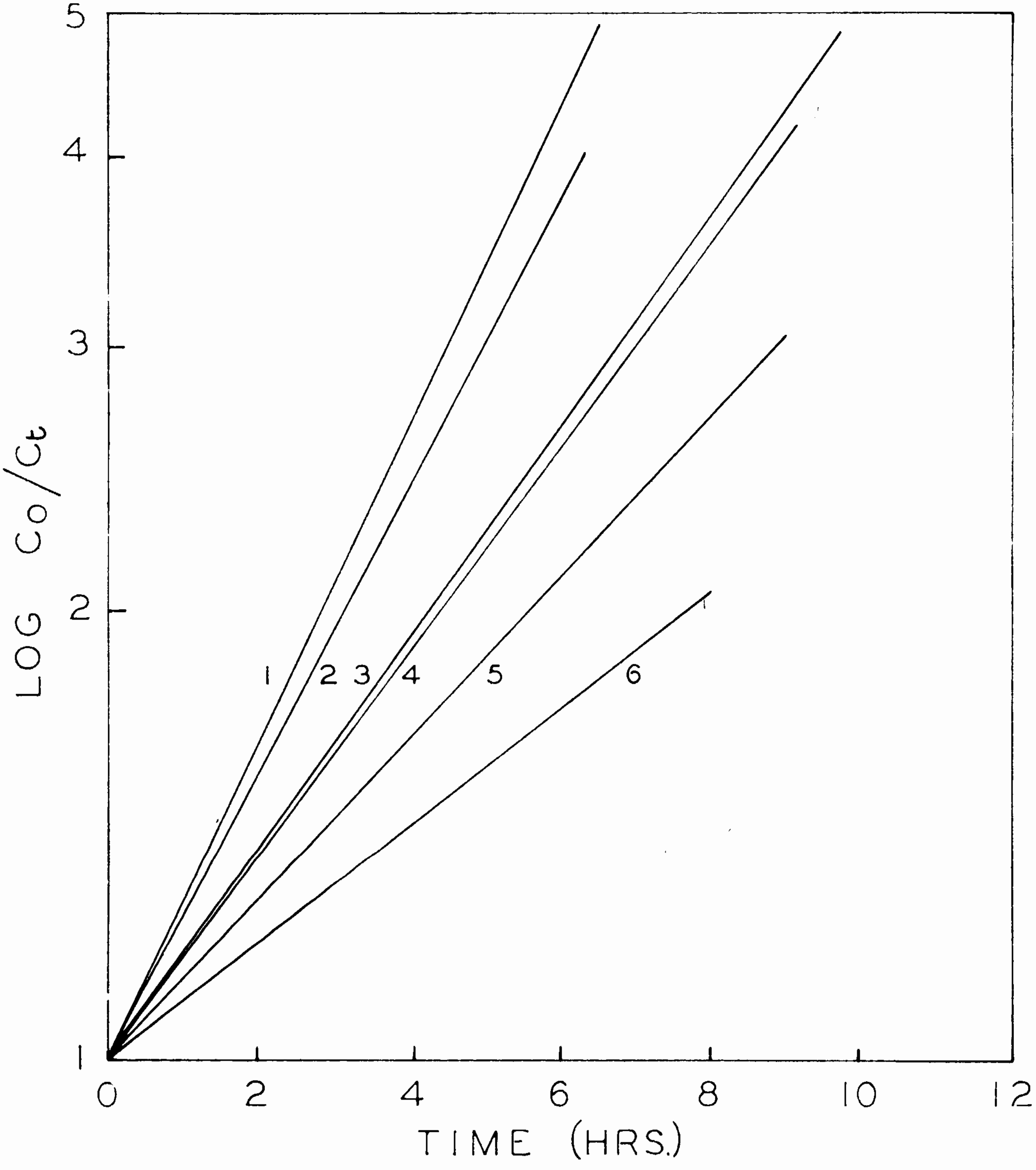
LOG Co/Ct
5
4
3
2
1
0
2
4
6
8
10
12
TIME (HRS.)
1
2
3
4
5
6

Figure 5

Figure 5

Pseudo-first order plots (Concentration dependence)

1 N solution pH = 3.0

1 0.25 N KI+ 0.75 N KCl
2 0.50 N KI + 0.50 N KCl
3 0.75 N KI + 0.25 N KCl
4 1.00 N KI +0.00 N KCl

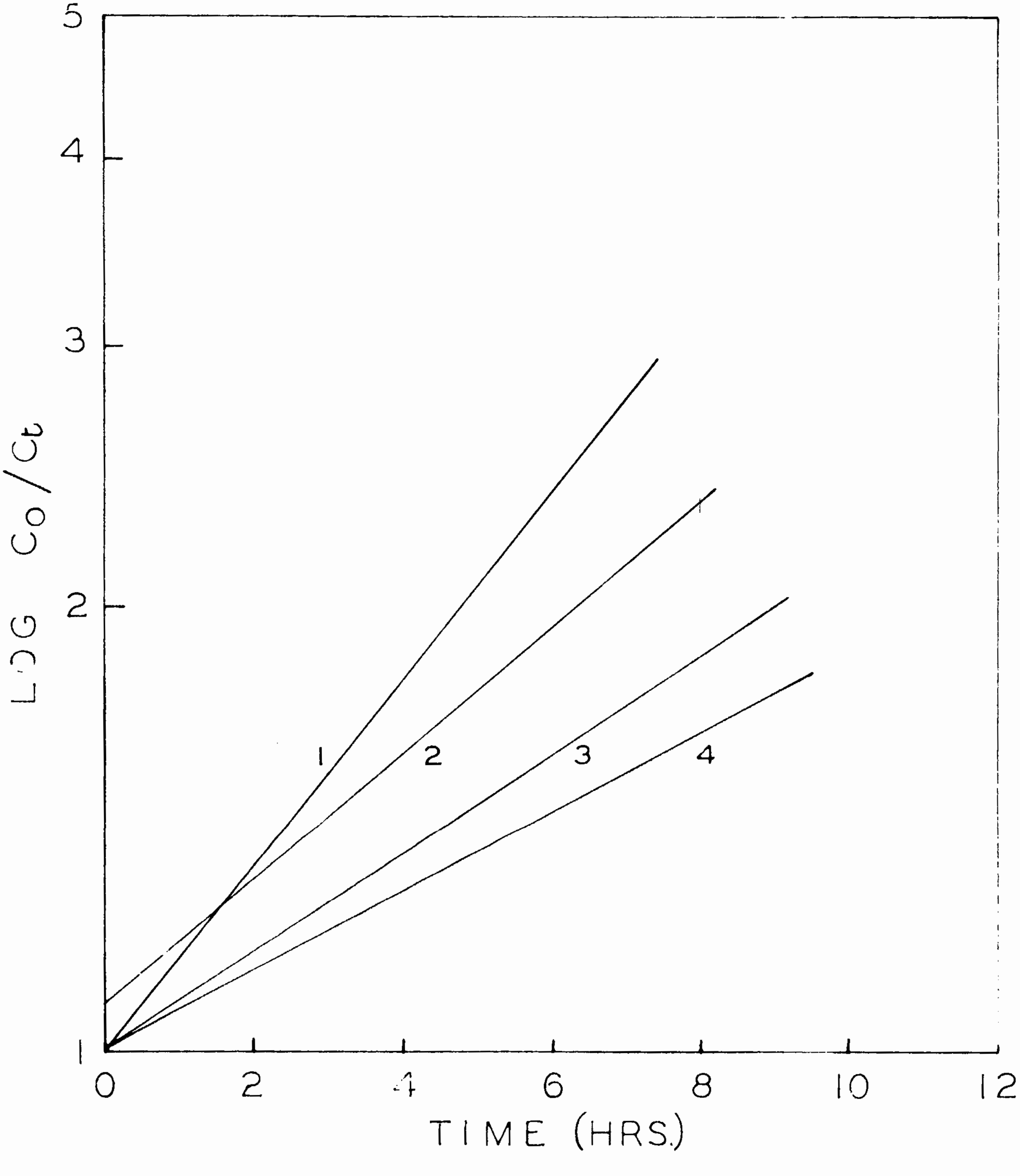
5
4
3
2
1
LOG Co/Ct
1
2
3
4
0
2
4
6
8
10
12
TIME (HRS.)

Figure 6

Figure 6

Pseudo-first order plots (Concentration dependence)

2 N solution pH = 3.0

1 0.25 N KI + 1.75 N KCl
2 0.50 N KI + 1.50 N KCl
3 0.75 N KI + 1.25 N KCl
4 1.00 N KI + 1.00 N KCl
5 1.50 N KI + 0.50 N KCl
6 2.00 N KI + 0.00 N KCl

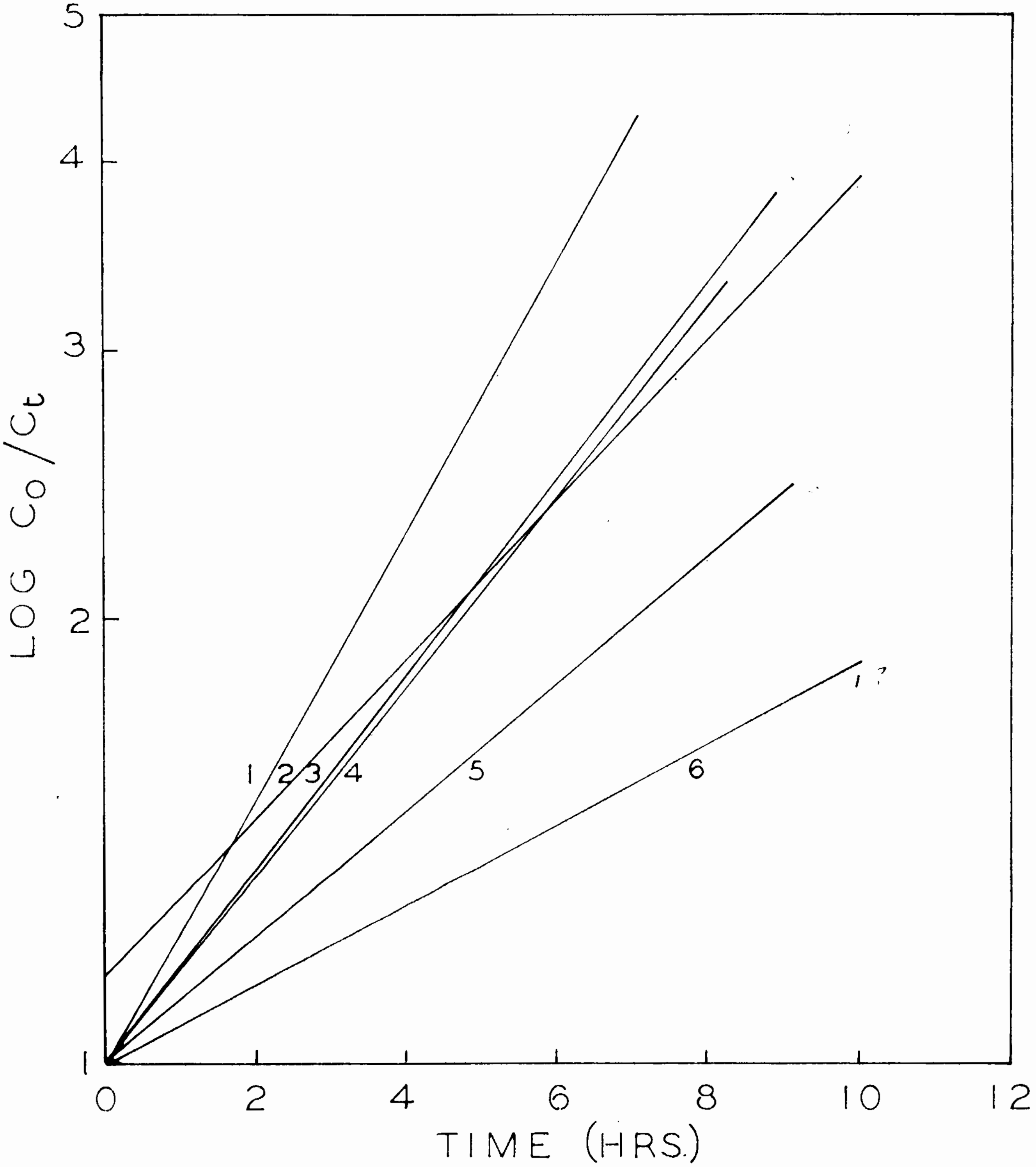
LOG C_O/C_t
5
4
3
2
1
0
2
4
6
8
10
12
TIME (HRS.)
1
2
3
4
5
6

TABLE XXIII

Exchange constants(concentration dependence)(Figure 3)

1 N solution pH = 2.0

Substrate concentration	Exchange constant $10^4 K^1 \text{min}^{-1}$
1 0.25 N KI + 0.75 N KCl	11.21
2 0.50 N KI + 0.50 N KCl	17.70
3 0.75 N KI + 0.25 N KCl	23.10
4 1.00 N KI + 0.00 N KCl	24.00

TABLE XXIV

Exchange constants (concentration dependence)(Figure 4)

2 N solution pH = 2.0

Substrate concentration	Exchange constant $10^4 K^1$ min-1
1 0.25 N KI + 1.75 N KCl	15.15
2 0.50 N KI + 1.50 N KCl	20.50
3 0.75 N KI + 1.25 N KCl	26.30
4 1.00 N KI + 1.00 N KCl	27.10
5 1.50 N KI + 0.50 N KCl	37.18
6 2.00 N KI + 0.00 N KCl	40.80

TABLE XXV

Exchange constants (concentration dependance)(Figure 5)

1 N solution pH = 3.0

	Substrate concentration	Exchange constant $10^4 K^1 min^{-1}$
1	0.25 N KI + 0.75 N KCl	10.62
2	0.50 N KI + 0.50 N KCl	13.00
3	0.75 N KI + 0.25 N KCl	19.60
4	1.00 N KI + 0.00 N KCl	23.90

TABLE XXVI

Exchange constants (concentration dependence)(Figure 6)

2 N solution pH = 3.0

	Substrate concentration	Exchange constant $10^4 K^1 min^{-1}$
1	0.25 N KI + 1.25 N KCl	10.25
2	0.50 N KI + 1.50 N KCl	16.30
3	0.75 N KI + 1.25 N KCl	25.22
4	1.00 N KI + 1.00 N KCl	25.60
5	1.50 N KI + 0.50 N KCl	25.60
6	2.00 N KI + 0.00 N KCl	34.34

Figure 7

Figure 7

Concentration - Exchange constant plots.

pH = 2.0

○ 1 N solution

● 2 N solution

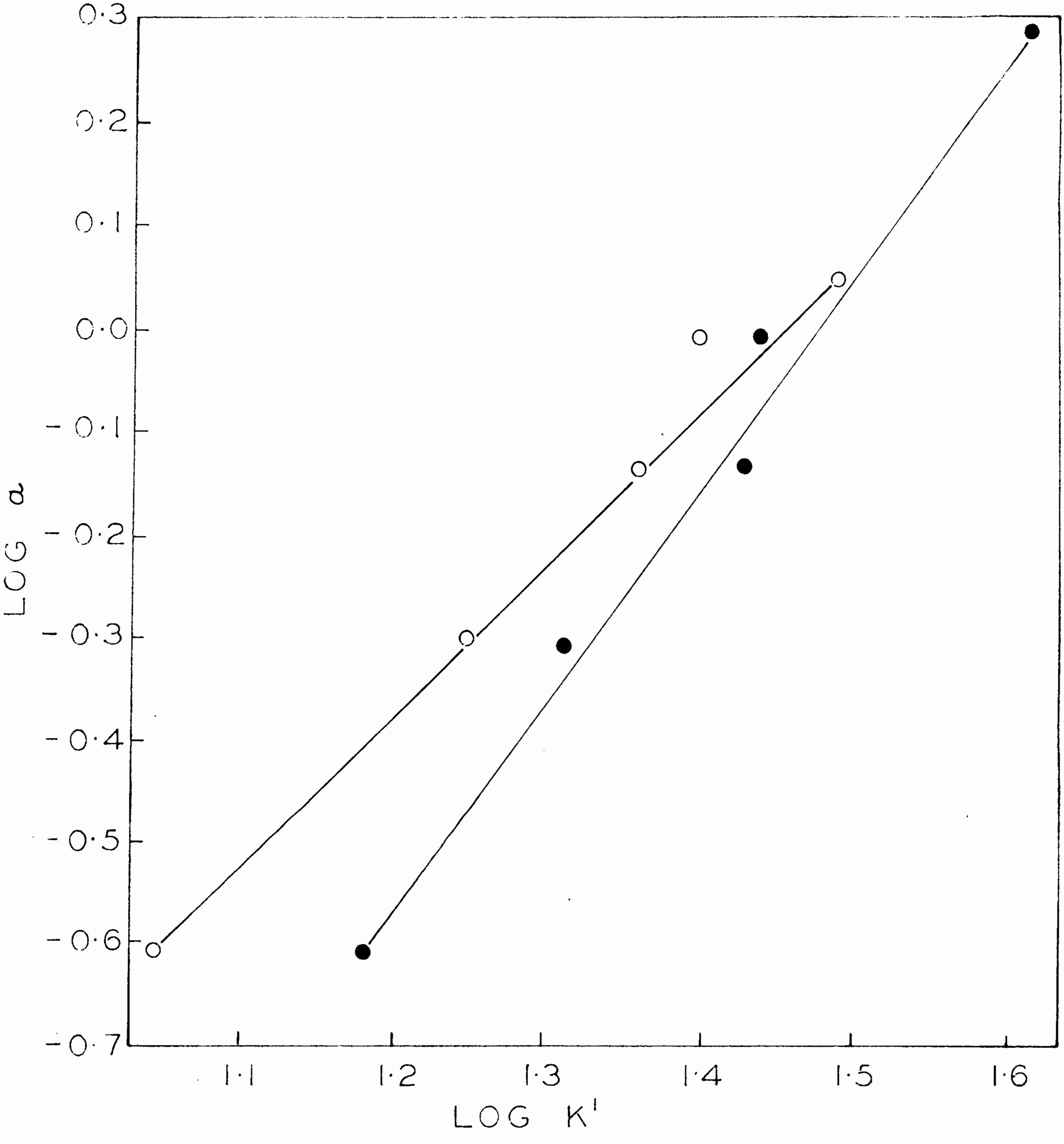
0·3
0·2
0·1
0·0
- 0·1
- 0·2
- 0·3
- 0·4
- 0·5
- 0·6
- 0·7
LOG α
1·1
1·2
1·3
1·4
1·5
1·6
LOG K'

Figure 8

Figure 8

Concentration - Exchange constant plots.

pH = 3.0

○ 1 N solution

● 2 N solution

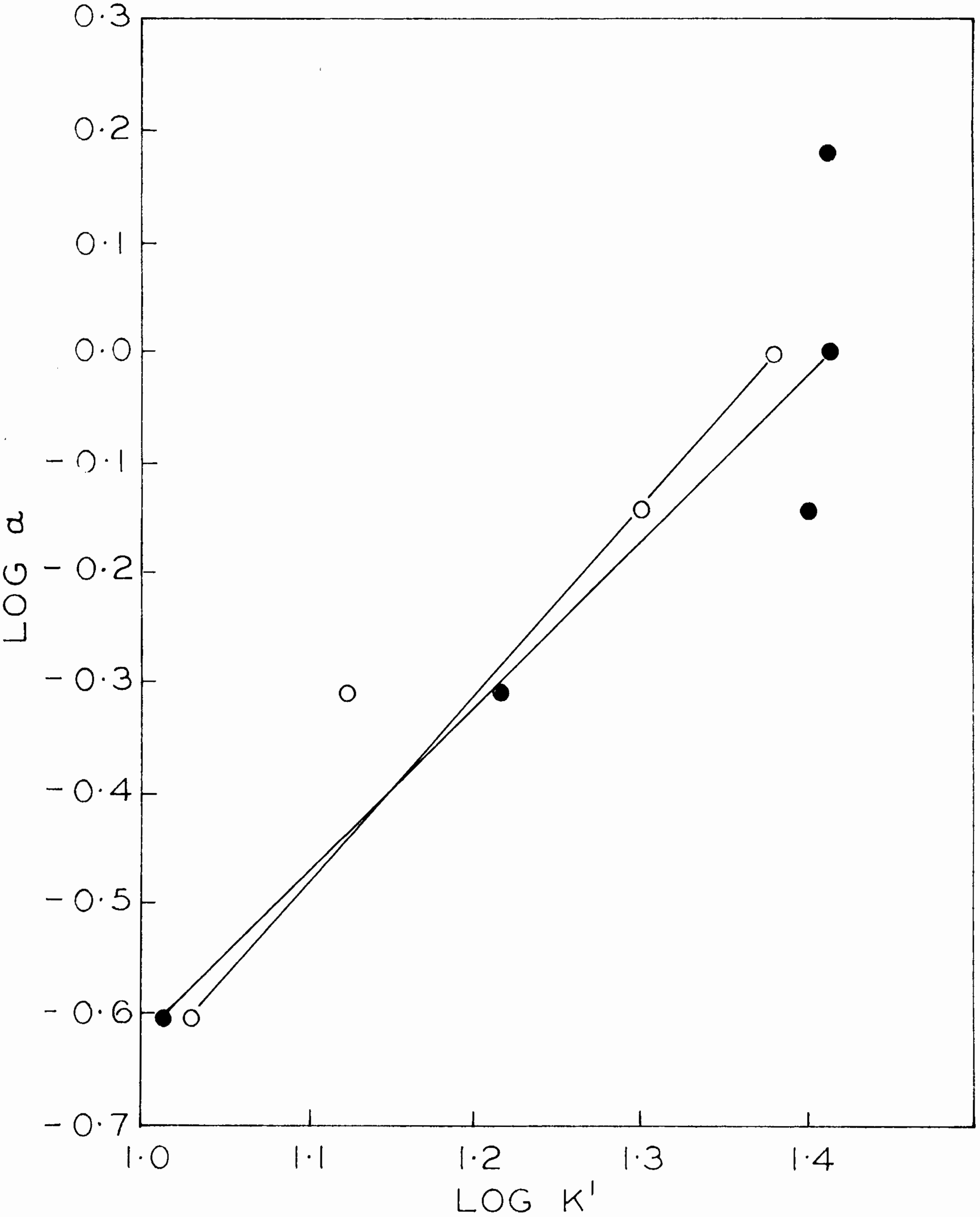
0·3
0·2
0·1
0·0
−0·1
−0·2
−0·3
−0·4
−0·5
−0·6
−0·7
LOG α
1·0
1·1
1·2
1·3
1·4
LOG K'

The order of reaction n, is given by the equation (45). The value of n was calculated from the slopes of log a versus log K^1 plots. The values of n and logarithm of over-all reaction constant K have been collected for all the cases investigated in Table XXVII.

TABLE XXVII

Values of n and K for various substrate concentrations.
Temperature 25°C.

Total substrate concentration	pH	n	log K
1) 1.0 N	2.0	0.6695	1.4527
	3.0	0.5848	1.3782
2) 2.0 N	2.0	0.4819	1.4706
	3.0	0.6637	1.4103

(b) Experiments on the variation of count rate with change in area per molecule

It has been shown by Rabinovitch (104) that the relative counting rate c_t/c_o is a function of the reciprocal area per molecule, c_t and c_o being count rates at time t and time = 0. This relation can be expressed in the form,

$$(c_t/c_o) = A\ (1/\sigma) \qquad \text{--(50)}$$

The ratio c_t/c_o becomes unity as σ, the area per molecule tends to A, the initial area per molecule. It is imperative from the above equation that for compression or expansion c_t/c_o versus $1/\sigma$ plots give a straight line passing through the origin if the radioactivity is homogeneously distributed in the surface.

Experiments were performed by compressing an active AIS film on 0.01 N HCl and 0.01 N NaOH, using various surface concentrations of active acid. Here results of spreading 50λl of active acid on 0.01 N HCl and 0.01 N NaOH are given in the Tables XXVIII and XXIX. Plots corresponding to these results as well as plots corresponding to 100 λl active acid on 0.01 N HCl and 0.01 N NaOH are given in Figure 9. In all these experiments, the initial area per molecule was estimated by comparison with the corresponding π-σ relationships of inactive AIS film.

Radioactive films both before and after compression were scanned by the Geiger tube to determine the degree of inhomogeneity. On examining an uncompressed monolayer of 100λl of active acid, with Geiger tube situated at three different collinear positions, it was noted that the count rate remained roughly constant with a variation of 100 - 300 C.P.M. in an over-all count rate of 30000 C.P.M. In the study of count rate during compression, at the point of first transition in the π-σ

curve of the film, viz., the plot at which the surface pressure begins to rise rapidly, a corresponding abrupt increase in count rate could be noticed. At high surface pressures, sometimes even beyond collapse, the count rate was studied as a function of pressure at constant area. At high surface pressure (collapse or beyond) π decreases gradually with time, while the count rate appeared to remain constant. During decompression of a previously compressed film of active AIS, the count rate decreased proportionally as the area per molecule was increased. Figure 10 is a π-σ curve of 50λl of active AIS. Figure 11 is the corresponding count rate versus area curve. A comparison of the two curves of Figure 10 and Figure 11 shows clearly the influence of constant and of variable area on the surface pressure and on the count rate.

(c) Surface potential as function of pH of 1 N KI substrate

As an additional study of exchange reactions, surface potential measurements were made on monolayers of inactive AIS on various substrates at two different temperatures. Figure 12 gives the π-σ and ΔV-σ curves on 0.01 N HCl substrates at 25°C. The corresponding curves for 17.5°C are given in Figure 13. The data of these two figures are given in Tables XXX and XXXI.

Rabinovitch (104) carried out exchange reaction on KI substrates of varying pH and found that at 25°C the exchange rate constant attained a maximum between pH = 2 and pH = 3. In an attempt to investigate the point further, surface potential measurements were made on films as a function of pH of the KI substrate solutions. Figures 14 to 18 are plots of ΔV-σ and the simultaneous π-σ curves for the following range of pH values of 1 N KI substrates, pH = 2.05, 2.8, 3.2 and 3.8. The corresponding numerical data of ΔV, π, σ are given in Tables XXXII to XXXVI. Figure 19 represents ΔV-pH curves at areas of 100 $Å^2$, 75 $Å^2$, 50 $Å^2$ and 35 $Å^2$ per molecule.

(d) Surface potential measurements of some exchange reactions.

Exchange reactions on 1.0 N KI (pH = 2) were followed by surface potential measurements. The numerical results of these experiments with active AIS monolayers on 1.0 N KI (pH = 2 and 25°C) are given in Table XXXVII. The exchange reaction at 17.3°C, where the transition of AIS monolayer from L_e to L_c takes place, was followed by surface potential measurements at hourly intervals. Numerical data are given in Tables XXXVIII and XXXIX. The exchange reaction of a collapsed monolayer of active AIS on 1.0 N KI was investigated with simultaneous measurements of surface potentials. Results of this investigation are given in Table (XL).

TABLE XXVIII

Variations of count rate with compression

50λl of active AIS on 0.01 N HCl substrate

Temperature 25^{0}C

Time (Min.)	(σ) Area/molecule	C.P.M.
0	64.10	13550
1	60.90	13650
2	57.69	13700
3	54.49	13750
4	51.28	14000
5	48.08	14750
6	44.87	15750
7	41.67	16250
8	38.46	17250
9	35.26	18250
10	32.06	19750
11	28.85	20750
12	25.65	20950
13	22.44	21950
14	19.24	25750

TABLE XXIX

Variations of count rate with compression

50λl of active AIS on 0.01 N NaOH substrate

Temperature 25°C

Time (min.)	(σ) Area/molecule	C.P.M.
0	64.10	5850
1	60.90	6350
2	57.69	6750
3	54.49	7350
4	51.28	7850
5	48.08	8350
6	44.87	8550
7	41.67	9350
8	38.46	9600
9	35.26	10100
10	32.05	11350
11	28.85	11850
12	25.64	12600
13	22.44	13600
14	19.23	14850

Figure 9

Figure 9

Variations of count rate with compression.

Various values of c_o were chosen for the same

$10^3\sigma = 31.2$

● 50λl of active AIS on 0.01 N HCl c_o = 19750 C.P.M.

△ 50λl of active AIS on 0.01 N NaOH c_o = 11350 C.P.M.

○ 100λl of active AIS on 0.01 N HCl

▲ 100λl of active AIS on 0.01 N NaOH

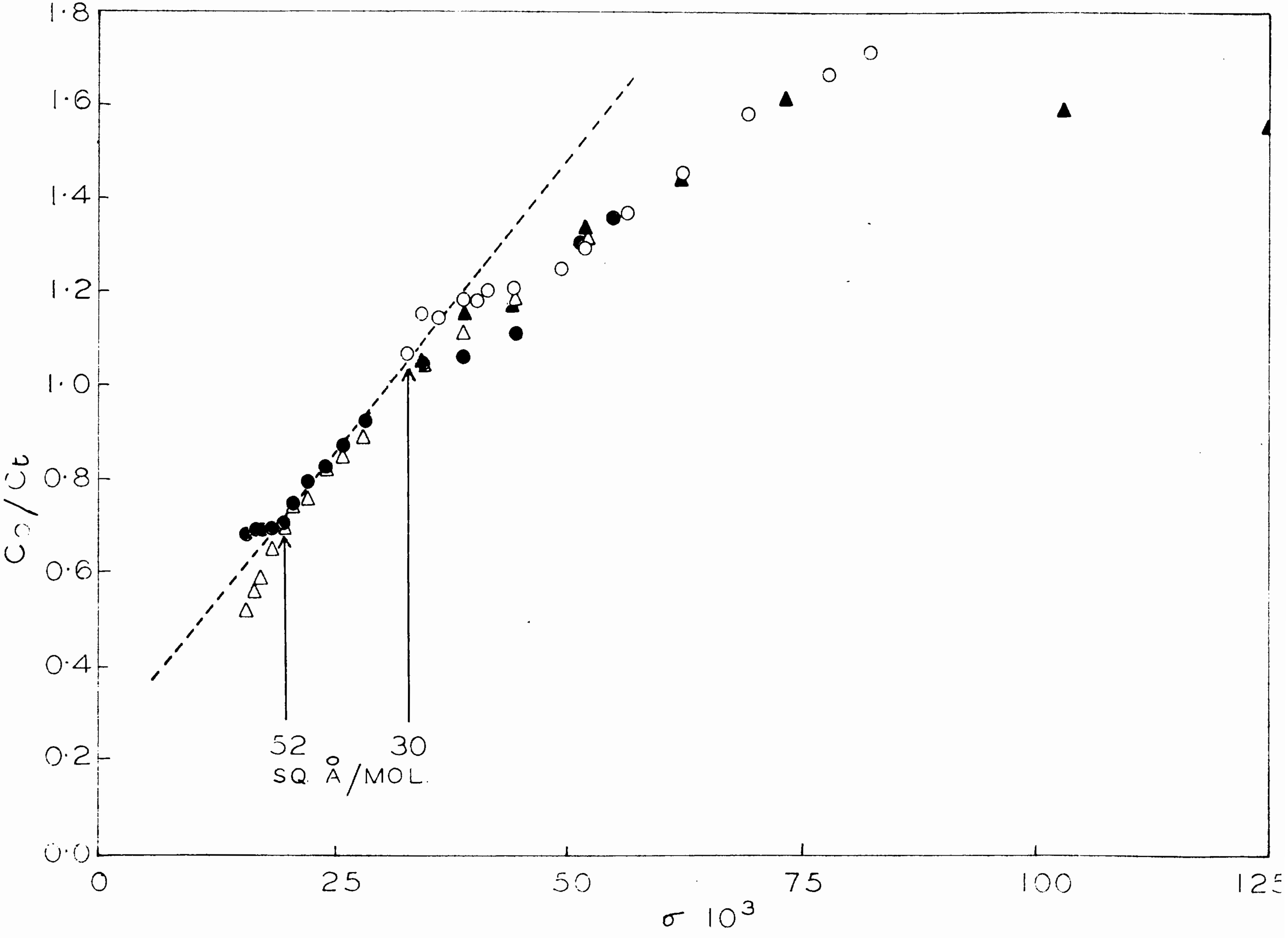
1·8
1·6
1·4
1·2
1·0
0·8
0·6
0·4
0·2
0·0
C_o / C_t
0
25
50
75
100
125
$\sigma\ 10^3$
52
30
SQ. Å/MOL.

Figure 10

Figure 10

π-σ curve of 50λl of active AIS

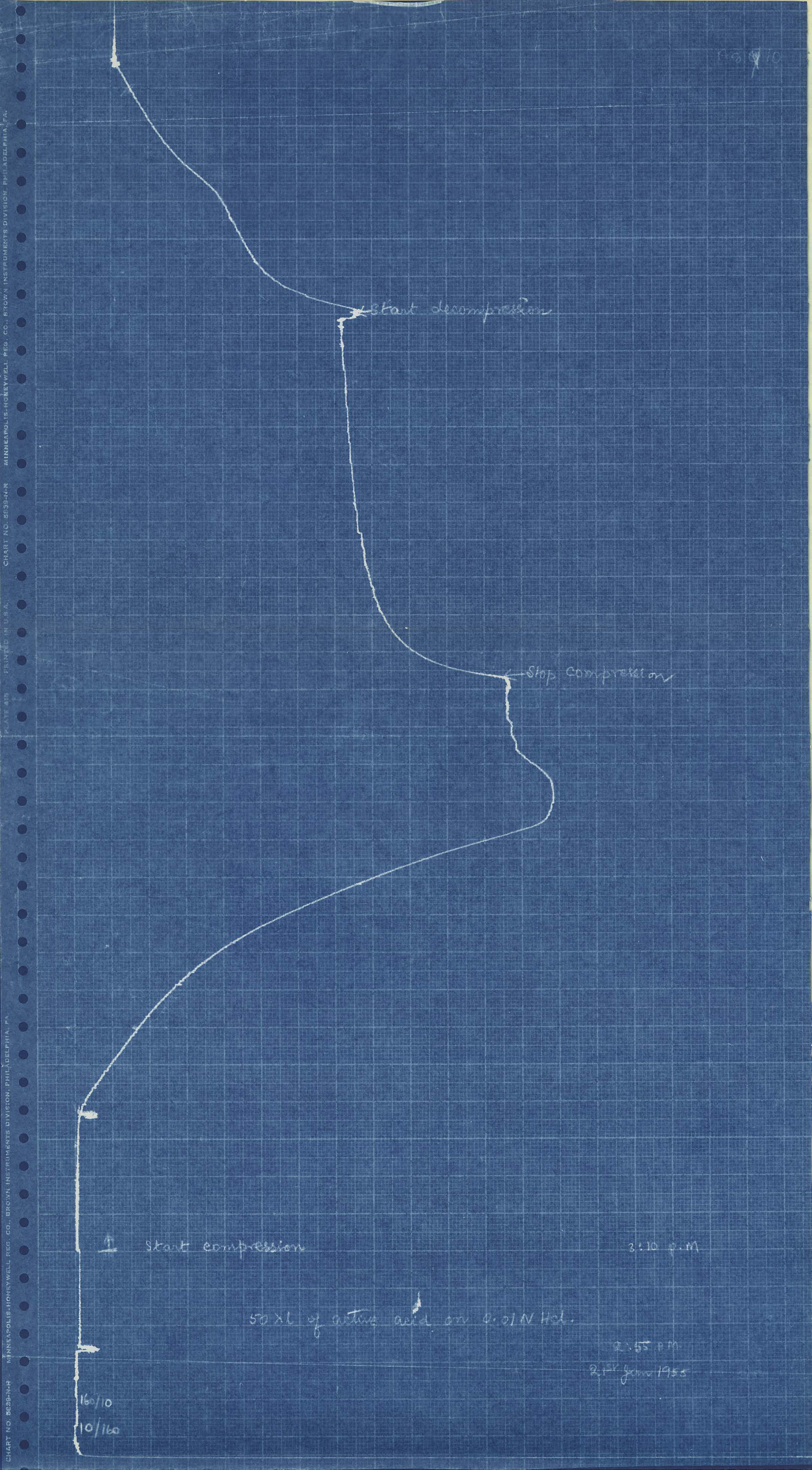

Start decompression

Stop compression

Start compression 3:10 p.M

50 λl of active acid on 0.01N HCl.

2:55 p.M.
21st Jan 1955

Figure 11

Figure 11

Count rate versus area (time) curve corresponding to Figure 10

Start decompression

Stop compression

Counter at the centre of the trough

Start compression

0-5000 C.P.M

Background Count

0-5000 C.P.M

Figure 12

Figure 12

Inactive AIS monolayer on 0.01 N HCl

Initial area = 100 Å^2. Temperature 25^{0}C.

Compression rate 5 Å^2/molecule per minute

●—● $\Delta V - \sigma$ curve

c —— $\pi - \sigma$ curve

<u>Figure 13</u>

Figure 13

Inactive AIS monolayer on 0.01 N HCl

Initial area = 100 Å^2. Temperature 17.5°C.

Compression rate 5 Å^2/molecule per minute

●—● $\Delta V - \sigma$ curve

—— $\pi - \sigma$ curve

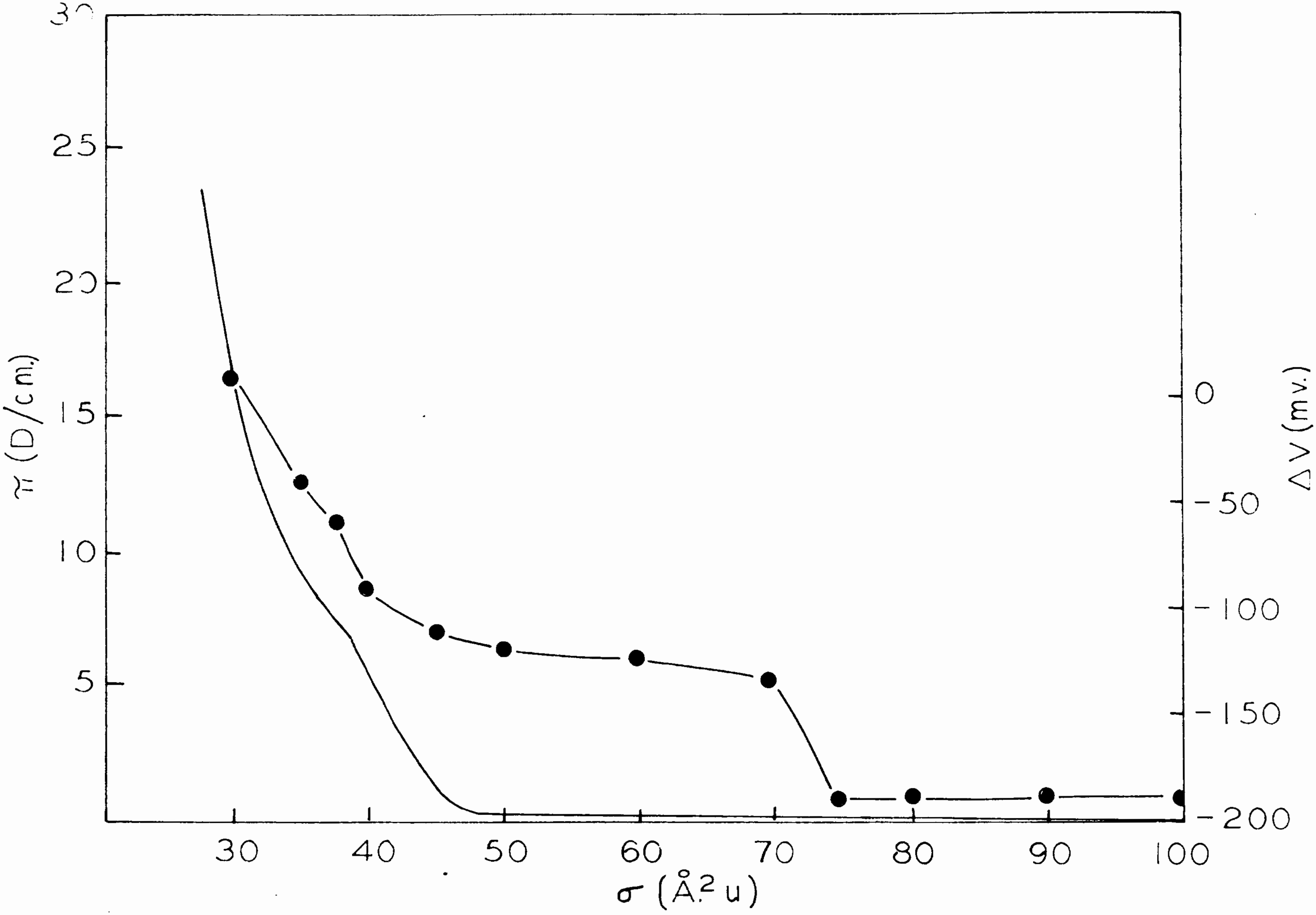
30
25
20
15
10
5
π (D/cm.)
0
-50
-100
-150
-200
ΔV (mv.)
30
40
50
60
70
80
90
100
σ (Å.² u)

TABLE XXXI

σ- π- ΔV measurements of inactive AIS monolayer on 0.01 N HCl substrate

Temperature 17.5°C.

σ (Å^2/ molecule)	π (dynes/cm.)	$-\Delta V$(millivolts)
100	0.05	190
90	0.05	190
80	0.05	190
75	0.05	190
70	0.05	135
60	0.10	125
50	0.25	120
45	1.25	110
40	5.00	90
37.5	7.25	60
35	9.00	40
30	16.00	10

Figure 14

Figure 14

$\Delta V - \sigma$, $\pi - \sigma$ diagrams of an inactive monolayer of AIS on 1.0 N KI substrate (pH = 1.2) Temperature 25°C.

●—●	$\Delta V - \sigma$	diagram
—	$\pi - \sigma$	diagram

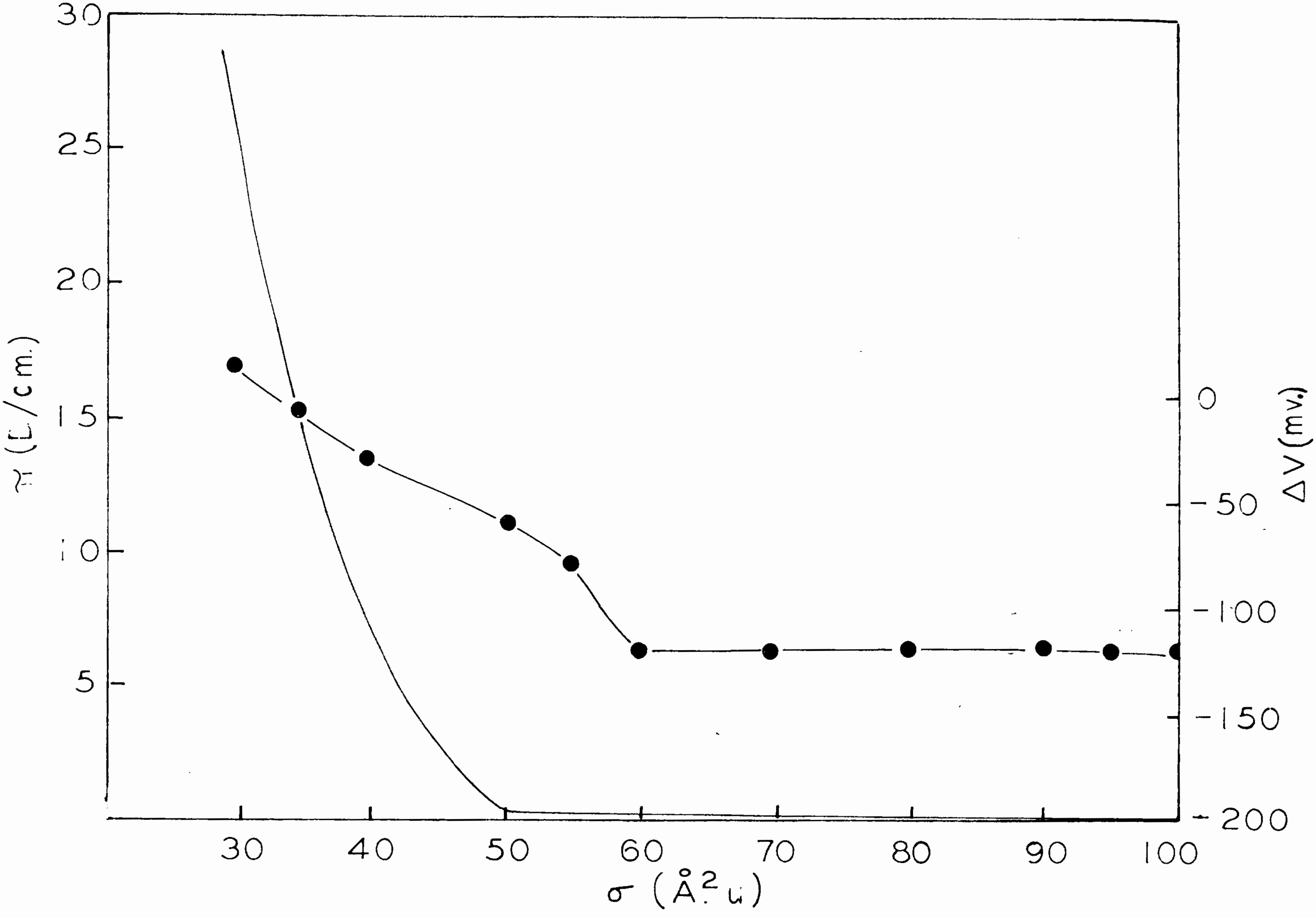
30
25
20
15
10
5
π (E/cm.)
0
-50
-100
-150
-200
ΔV (mv.)
30
40
50
60
70
80
90
100
σ (Å² ω)

Figure 15

Figure 15

ΔV-σ, π-σ diagrams of an inactive monolayer of AIS on 1.0 N KI substrate (pH = 2.05)

Temperature 25^{0}C.

●—● ΔV - σ diagram

—— π - σ diagram

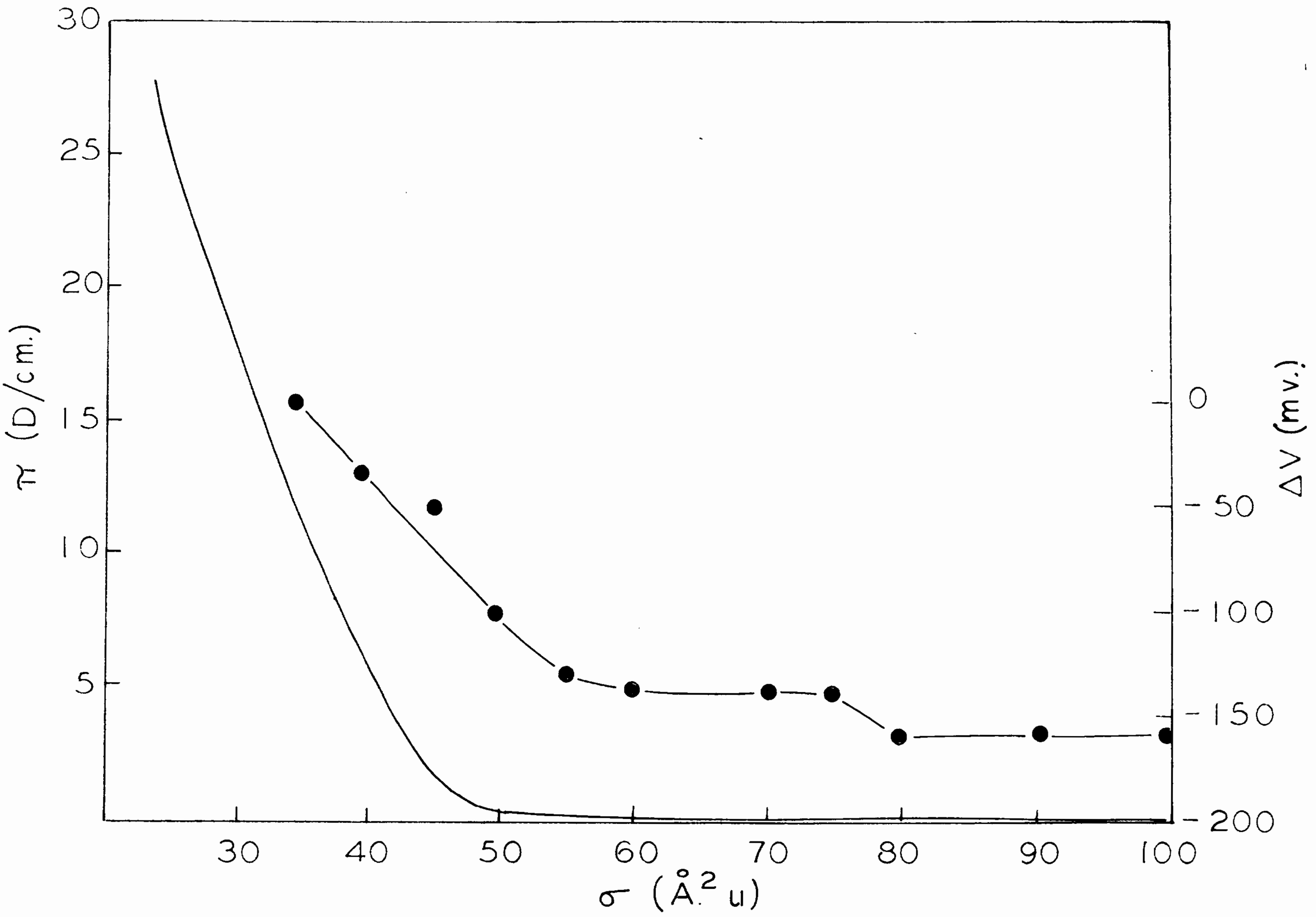
30
25
20
15
10
5
π (D/cm.)
0
- 50
-100
-150
-200
ΔV (mv.)
30
40
50
60
70
80
90
100
σ (Å² u)

Figure 16

Figure 16

ΔV-σ, π-σ diagrams of an inactive monolayer of AIS on 1.0 N KI substrate (pH = 2.8)
Temperature 25^{0}C.

●—● ΔV - σ diagram

—— π - σ diagram

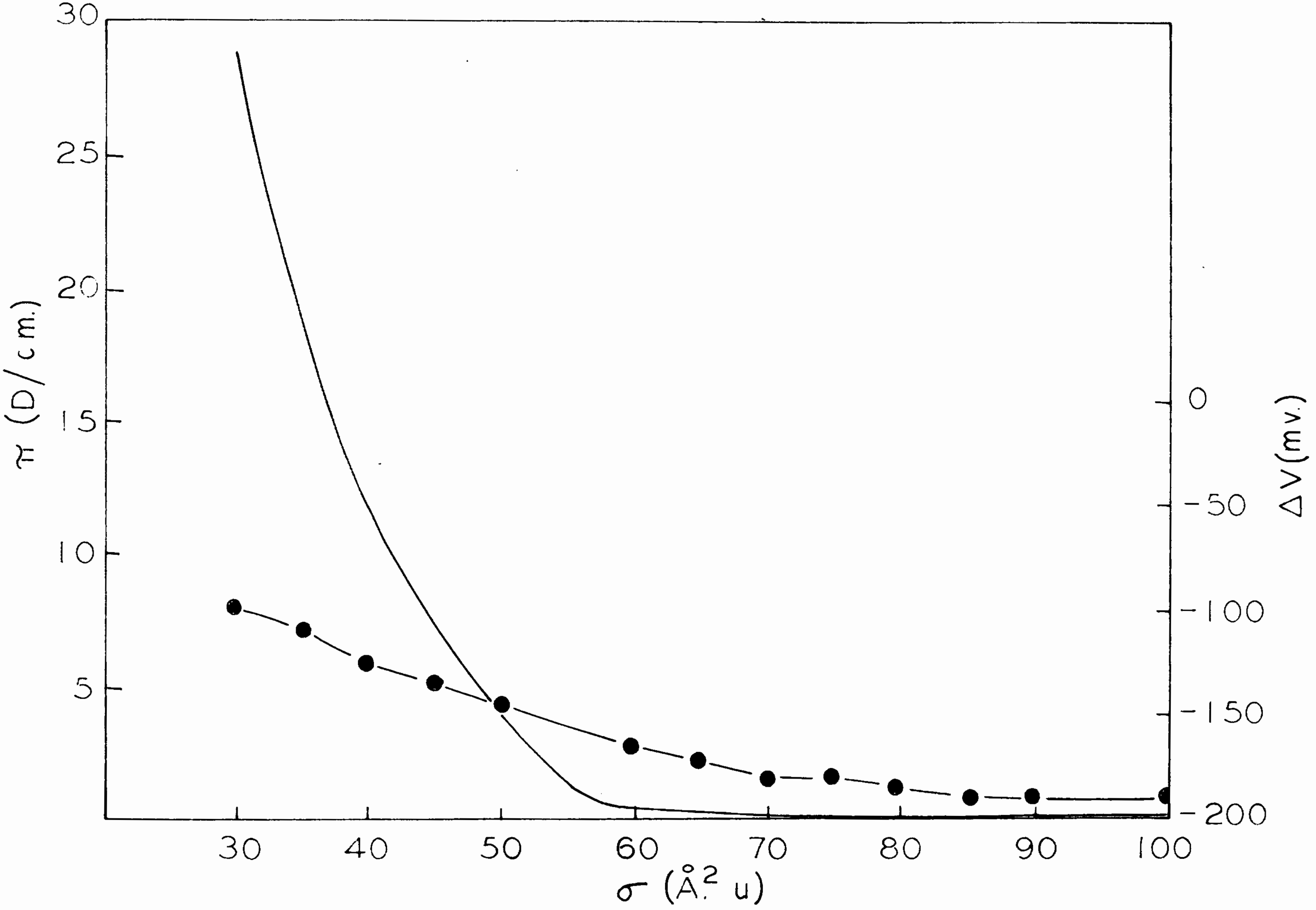
30
25
20
15
10
5
π (D/cm.)
0
-50
-100
-150
-200
ΔV(mv.)
30
40
50
60
70
80
90
100
σ (Å.² u)

Figure 17

Figure 17

$\Delta V-\sigma$, $\pi-\sigma$ diagrams of an inactive monolayer of AIS on 1.0 N KI substrate (pH = 3.2)

Temperature 25°C.

●—● $\Delta V-\sigma$ diagram

—— $\pi-\sigma$ diagram

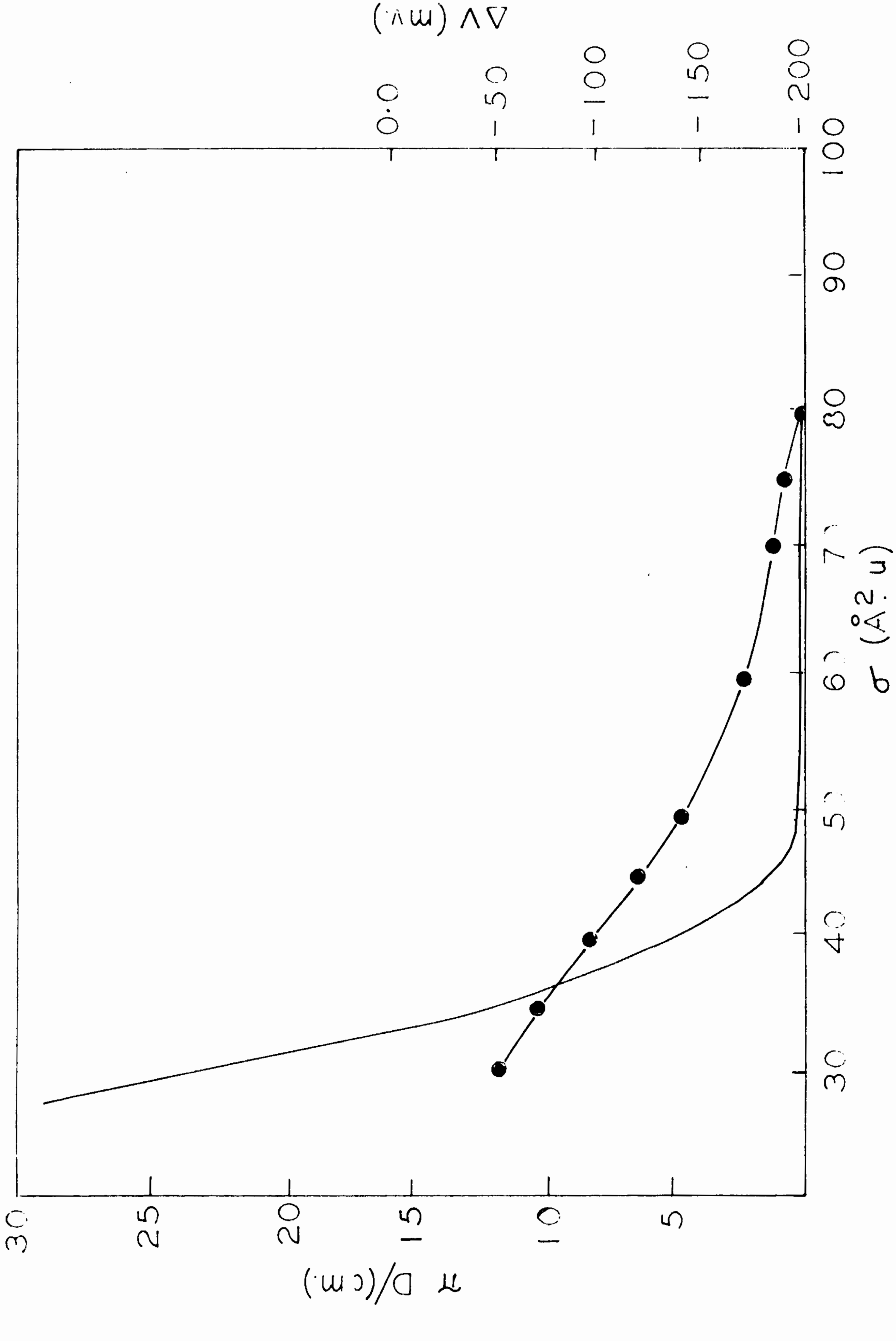

π D/(cm.)
30
25
20
15
10
5
ΔV (mV.)
0.0
−50
−100
−150
−200
σ (Å² u)
30
40
50
60
70
80
90
100

<u>Figure 18</u>

Figure 18

$\Delta V - \sigma$, $\pi - \sigma$ diagrams of an inactive monolayer of AIS on 1.0 N KI substrate (pH = 3.8)

Temperature 25°C

●—● $\Delta V - \sigma$ diagram

— $\pi - \sigma$ diagram

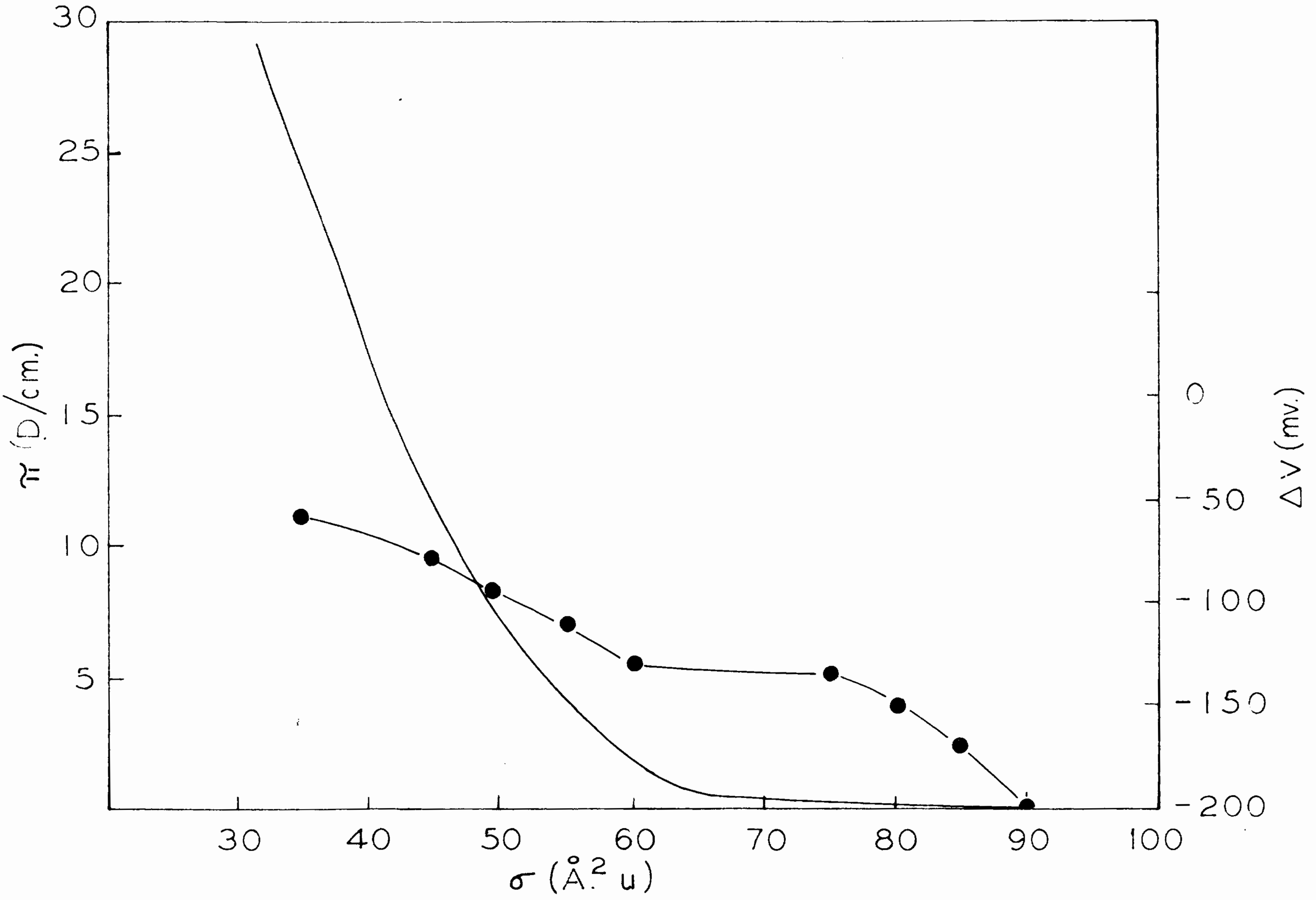

30
25
20
15
10
5
π (D/cm.)
0
- 50
- 100
- 150
- 200
ΔV (mv.)
30
40
50
60
70
80
90
100
σ (Å² u)

Figure 19

Figure 19

Surface potential of a monolayer of AIS as a function of pH of substrate 1.0 N KI at various molecular areas.

Temperature 25°C.

○ 100 Å^2 per molecule
● 75 Å^2 per molecule
△ 50 Å^2 per molecule
▲ 35 Å^2 per molecule

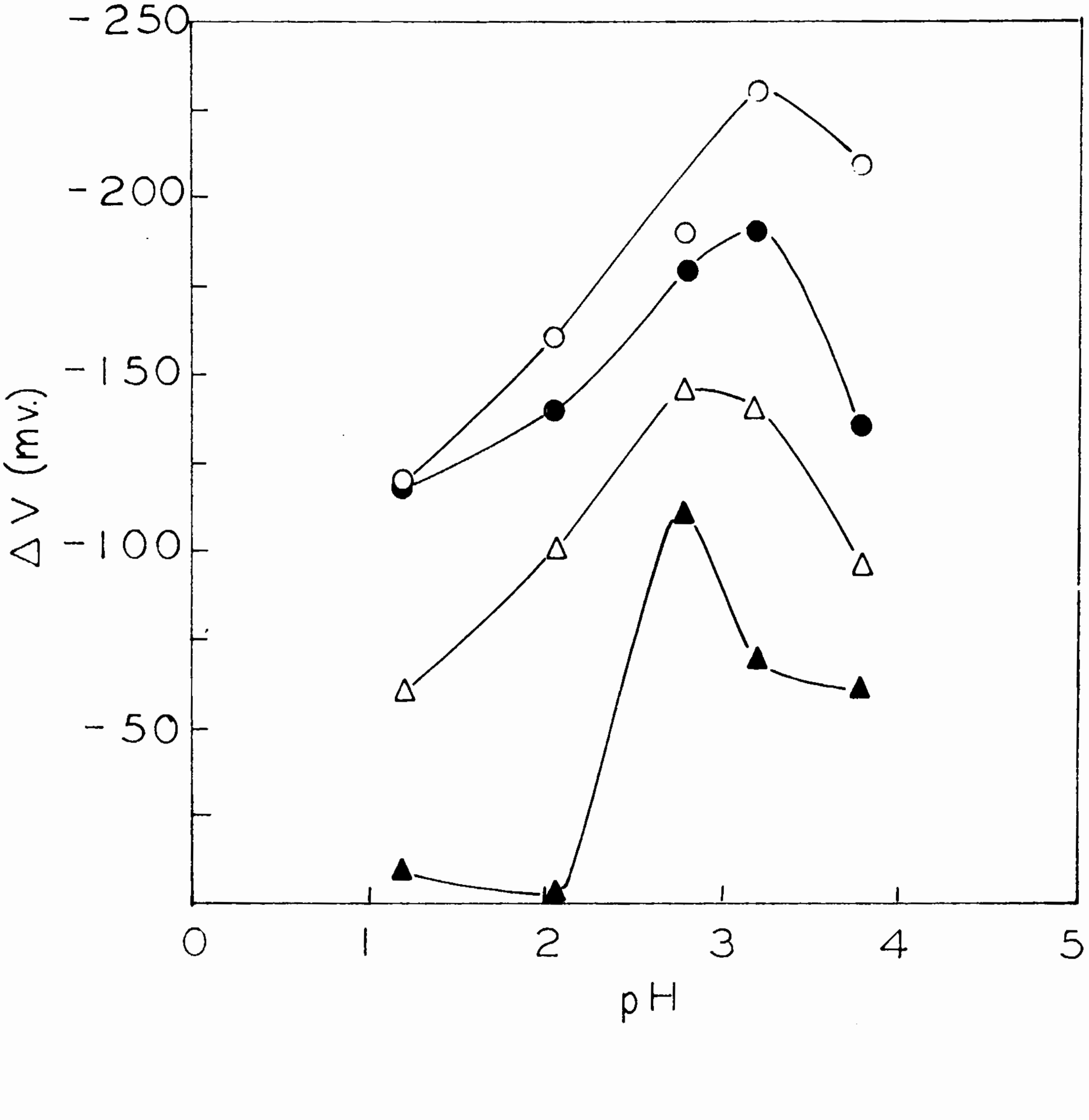
-250
-200
-150
-100
-50
ΔV (mv.)
0
1
2
3
4
5
pH

TABLE XXXII

σ- π- ΔV measurements of inactive AIS monolayer on 1.0 N KI (pH = 1.2)

Temperature 25°C.

σ (Å^2/ molecule)	π (dynes/cm)	$-\Delta V$ (millivolts)
100	0.00	120
95	0.00	120
90	0.00	120
85	0.00	120
80	0.00	120
75	0.00	120
70	0.00	120
60	0.15	120
55	0.10	80
50	0.50	60
40	3.00	30
35	14.50	10
30	26.25	15

TABLE XXXIII

σ- π- ΔV measurements of inactive AIS monolayer on 1.0 N KI (pH = 2.05) Temperature 25°C.

σ (Å^2/ molecule)	π (dynes/cm)	$-\Delta V$(millivolts)
100	0.10	160
90	0.10	160
85	0.10	160
80	0.10	160
75	0.10	140
70	0.10	140
60	0.10	140
55	0.15	130
50	0.25	100
45	2.00	50
40	5.75	35
35	12.50	0
30	18.25	5

TABLE XXXIV

σ-π-ΔV measurements of inactive AIS
monolayer on 1.0 N KI (pH = 2.8)
Temperature 25°C.

σ (Å^2/ molecule)	π (dynes/cm)	$-\Delta V$ (millivolts)
100	0.00	190
95	0.00	190
90	0.10	190
85	0.10	190
80	0.15	185
75	0.15	180
70	0.20	180
65	0.25	170
60	0.50	165
55	1.50	160
50	4.00	145
45	7.50	135
40	12.50	125
35	19.00	110
30	29.50	100

TABLE XXXV

σ-π-ΔV measurements of inactive AIS
monolayer on 1.0 N KI (pH = 3.2)
Temperature 25°C.

σ (Å^2/ molecule)	π (dynes/cm)	$-\Delta V$(millivolts)
100	0.00	230
95	0.10	225
90	0.10	215
85	0.10	210
80	0.10	200
75	0.10	190
70	0.10	185
60	0.15	170
50	0.25	140
45	1.00	120
40	5.00	95
35	11.25	70
30	22.50	50

TABLE XXXVI

σ-π-ΔV measurements of inactive AIS
monolayer on 1.0 N KI (pH = 3.8)
Temperature 25°C

σ(Å^2/ molecule)	π(dynes/cm)	$-\Delta V$(millivolts)
100	0.10	210
90	0.20	200
85	0.25	170
80	0.25	150
75	0.25	135
70	0.35	140
60	1.75	130
55	4.25	110
50	7.25	95
45	11.75	80
40	17.50	70
35	25.00	60

TABLE XXXVII

Simultaneous exchange - surface potential measurements of an active AIS monolayer on 1.0 N KI substrate (pH = 2.0)

Temperature 25°C π = 4.0 dynes/cm.

Time (hrs.)	C.P.M.	c_o/c_t	$-\Delta v$(mv)
0.0	38900	1.000	115
1.0	33600	1.155	188
2.0	28900	1.345	230
3.0	24400	1.595	225
4.0	21400	1.785	210
5.0	18900	2.030	230
6.0	16400	2.335	220
7.0	14900	2.610	215

$10^4\ K^1\ \text{min}^{-1} = 25.95$

TABLE XXXVIII

Simultaneous exchange - surface potential measurements of an active AIS monolayer on 1.0 N KI substrate (pH = 2.0)

Temperature 17.3°C π = 4.0 dynes/cm.

Time (hrs.)	C.P.M.	c_o/c_t	$+\Delta v$(mv)
0.0	28200	1.000	35
0.5	27450	1.035	40
1.0	26450	1.075	60
1.5	25950	1.100	70
2.0	25450	1.120	140
2.5	24450	1.160	100
3.0	23450	1.210	115
3.5	22450	1.270	130
4.0	21450	1.320	140

$10^4 K^1 \text{min}^{-1} = 9.66$

TABLE XXXIX

Simultaneous exchange - surface potential measurements of an active AIS monolayer on 1.0 N KI substrate (pH = 2.0)

Temperature 17.3°C π = 22.5 dynes/cm.

Time (hrs.)	C.P.M.	c_o/c_t	$-\Delta V$(mv)
0.0	30000	1.000	165
0.5	29000	1.035	210
1.0	27500	1.090	240
1.5	26500	1.130	290
2.0	25500	1.175	285
2.5	25000	1.200	235
3.0	24000	1.250	240
3.5	23500	1.280	238
4.0	22500	1.330	220

10^4 K^1 min^{-1} = 13.45

TABLE XL

Simultaneous exchange - surface potential measurements of a collapsed active AIS film on 1.0 N KI substrate (pH = 2.0)
Temperature 25°C π = 30 dynes/cm.

Time (hrs.)	C.P.M.	c_o/c_t	$-\Delta V$(mv)
0.0	7800	1.000	430
0.5	7600	1.025	435
1.0	7300	1.070	530
1.5	7100	1.100	-
2.0	6900	1.130	400
2.5	6700	1.160	-
3.0	6600	1.180	455
3.5	6500	1.200	290

$10^4\ K^1\ \text{min}^{-1} = 10.19$

(2) π-σ curves of chain substituted stearic acids.

Stearic acid (SA), 2 methyl stearic acid (2 MSA), 3 methyl stearic acid (3 MSA), 3 ethyl stearic acid (3 ESA), 10 phenyl stearic acid (10 PSA), 12 hydroxy stearic acid (12 HSA), and 12 keto stearic acid (12 KSA) were studied as monolayer films at the air/water interface and the pressure area isotherms were determined for each of these acids. The effects of compression rates on the characteristics of the π-σ curves were investigated. After maximum pressure was attained during compression, decompression curves for the monolayers were recorded, the rate of compression and of decompression being the same.

In order to select suitable conditions for the experiments, a number of pressure-area curves were determined on 0.01 N HCl substrates for SA, 10 PSA, 12 HSA, and 12 KSA, with 35 $Å^2$, 100 $Å^2$, 160 $Å^2$ and 150 $Å^2$ per molecule respectively as the initial areas. Three series of experiments at 11.4°C, 18°C and 25°C were performed. The results of these preliminary investigations can be summarized as follows: Stearic acid showed the usual values of 25 $Å^2$ per molecule and 20.5 $Å^2$ per molecule at zero compressions for the two well known transition points. In case of 10 PSA, the surface pressure rapidly increased when the surface area reached 58 $Å^2$

per molecule and attained a maximum surface pressure of 24 dynes/cm before collapse of the monolayer occured. π remained constant with time at constant area per molecule after this point had been reached.

12 HSA spread as an expanded film at large molecular areas of the order of 160 Å^2 per molecule. As the monolayer of 12 HSA was compressed, the pressure rose gradually to about 5 dynes/cm. At this value a small maximum was obtained in the π-σ curve, the pressure decreasing slightly with decreasing area per molecule before the appearance of the equilibrium region. This maximum was imperceptible at 25°C particularly at low compression rates. As the temperature was decreased however the maximum became more and more pronounced and thus seemed to be temperature dependent. (See Figure 38)

12 KSA at large molecular areas of the order of 150 Å^2 per molecule appeared to spread as a gaseous monolayer. In the condensed region of the π-σ diagram of 12 KSA, at low temperature and beyond 25 dynes/cm, a marked transition region was observed. This transition region is shown in Figure 41.

At 25°C both 12 HSA and 12 KSA could be compressed to surprisingly low molecular areas with the pressure still rising and without the film showing signs of collapse. At 11.4°C however, both 12 HSA and 12 KSA monolayers manifested maximum π values near 18 Å^2 per molecule, followed by rapid collapse. This suggested that π-σ curves obtained at higher temperatures may be complicated by a slow concomitant collapse.

As a consequence of this preliminary investigation, it was concluded that the π-σ study of these stearic acid derivatives should be made under the following conditions and with the following purposes.

(1) The initial area for each acid should be the same. On the basis of the preliminary data a value of 65 $\AA^2$ per molecule was chosen as the initial area for each acid.

(2) π-σ isotherms should be obtained at $12.1^{\circ}C \pm 0.1$ and $25.0^{\circ}C \pm 0.1$.

(3) The compression rates to be employed should in each case be 1.848 $\AA^2$, 2.413 $\AA^2$ and 4.5 $\AA^2$ per molecule per minute.

(4) A preliminary study of the apparent hysteresis phenomena should be made for each acid.

The results of the studies of the π-σ relationships of the various fatty acid derivatives will be dealt with individually for each acid. The types of films as determined from the isotherms will be characterised by the compressibility coefficient, (k)

$$(-k) = (1/\sigma)\ (d\sigma/d\pi)$$

calculated in the manner of Dervichian (107)

(a) Stearic acid (SA): $CH_3 - (CH_2)_{16} - COOH$

The films of SA were spread on a 0.01 N HCl substrate from a stock solution in benzene. 50 microliters of this stock solution were spread drop wise over an area of 8.8094×10^{18} $Å^2$ to give an initial area of 65 $Å^2$ per molecule. π-σ curves were obtained for temperatures of 12.1°C and 25°C and at compression rates of 1.848 $Å^2$, 2.413 $Å^2$, 4.5 $Å^2$ per molecule per minute at each temperature. The corresponding pressure-area curves are given in Figures 20 to 22. The pertinent experimental data is given in Table XLI. In this Table the letters P and Q represent the areas at which the first and second transitions take place in the film.

TABLE XLI

π-σ curve for various compression rates at 12.1°C and 25°C.

Compression rate $Å^2$/ mol/ min.	Temp. °C	P $Å^2$	Q $Å^2$
1) 1.848	12.1	26.19	20.28
	25.0	25.64	20.10
2) 2.413	12.1	25.91	20.85
	25.0	25.91	20.36
3) 4.5	12.1	26.08	21.13
	25.0	26.03	20.90

Figure 20

Figure 20

π-σ diagram of stearic acid at a compression rate of 1.848 Å^2 / molecule / minute.
Initial area 65 Å^2 per molecule.

1 obtained at 25°C

2 obtained at 12.1°C

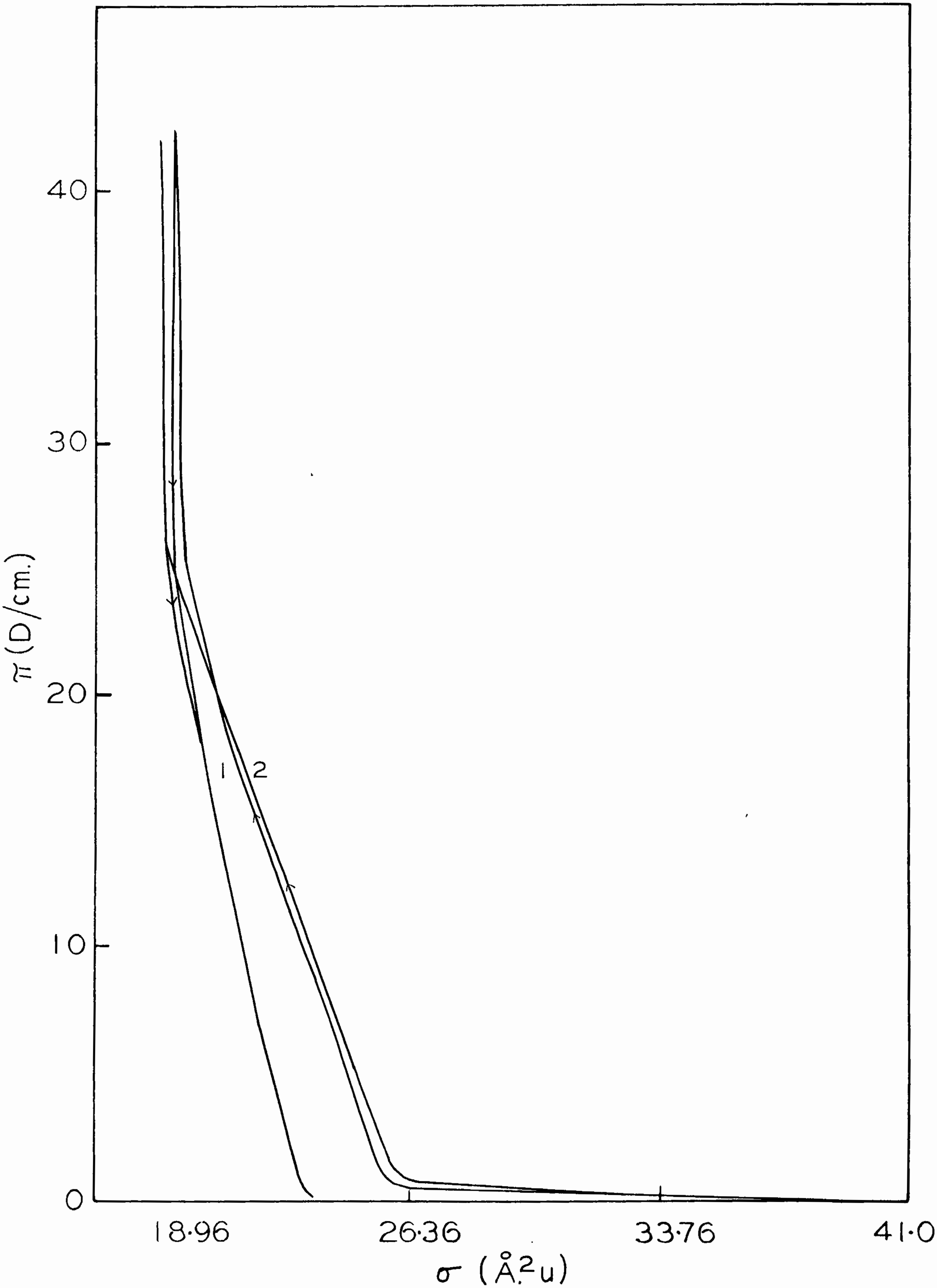
40
30
20
10
0
π (D/cm.)
1
2
18·96
26·36
33·76
41·0
σ (Å.²u)

<u>Figure 21</u>

Figure 21

π-σ diagram of stearic acid at a compression rate of 2.413 Å^2 / molecule / minute. Initial area 65 Å^2 per molecule.

1 obtained at 25°C

2 obtained at 12.1°C

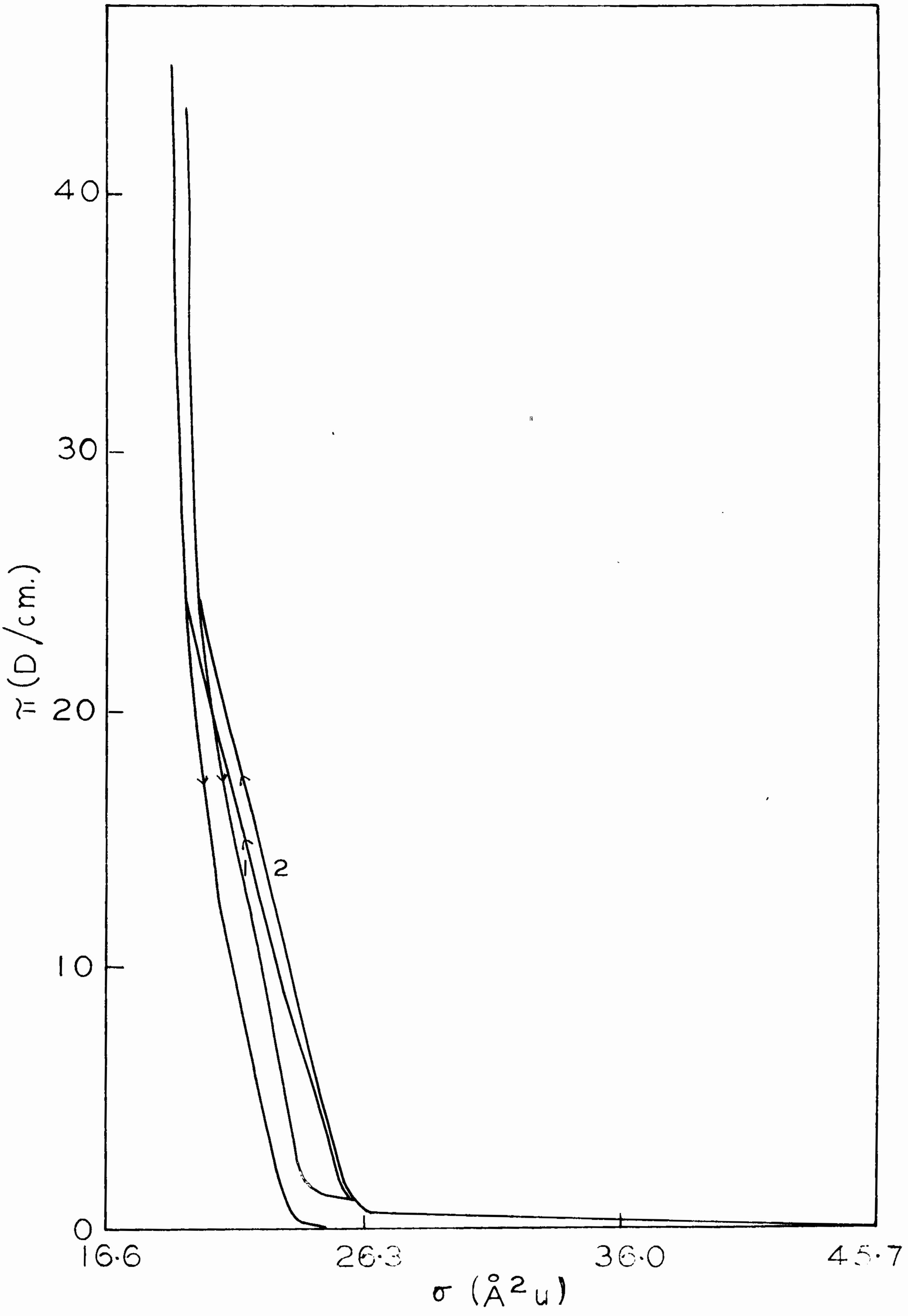

40
30
20
10
0
π (D/cm.)
1
2
16·6
26·3
36·0
45·7
σ (Å²u)

Figure 22

Figure 22

π-σ-diagram of stearic acid at a compression rate of 4.5 Å^2 / molecule / minute.
Initial area 65 Å^2 per molecule.

1 obtained at 25°C

2 obtained at 12.1°C

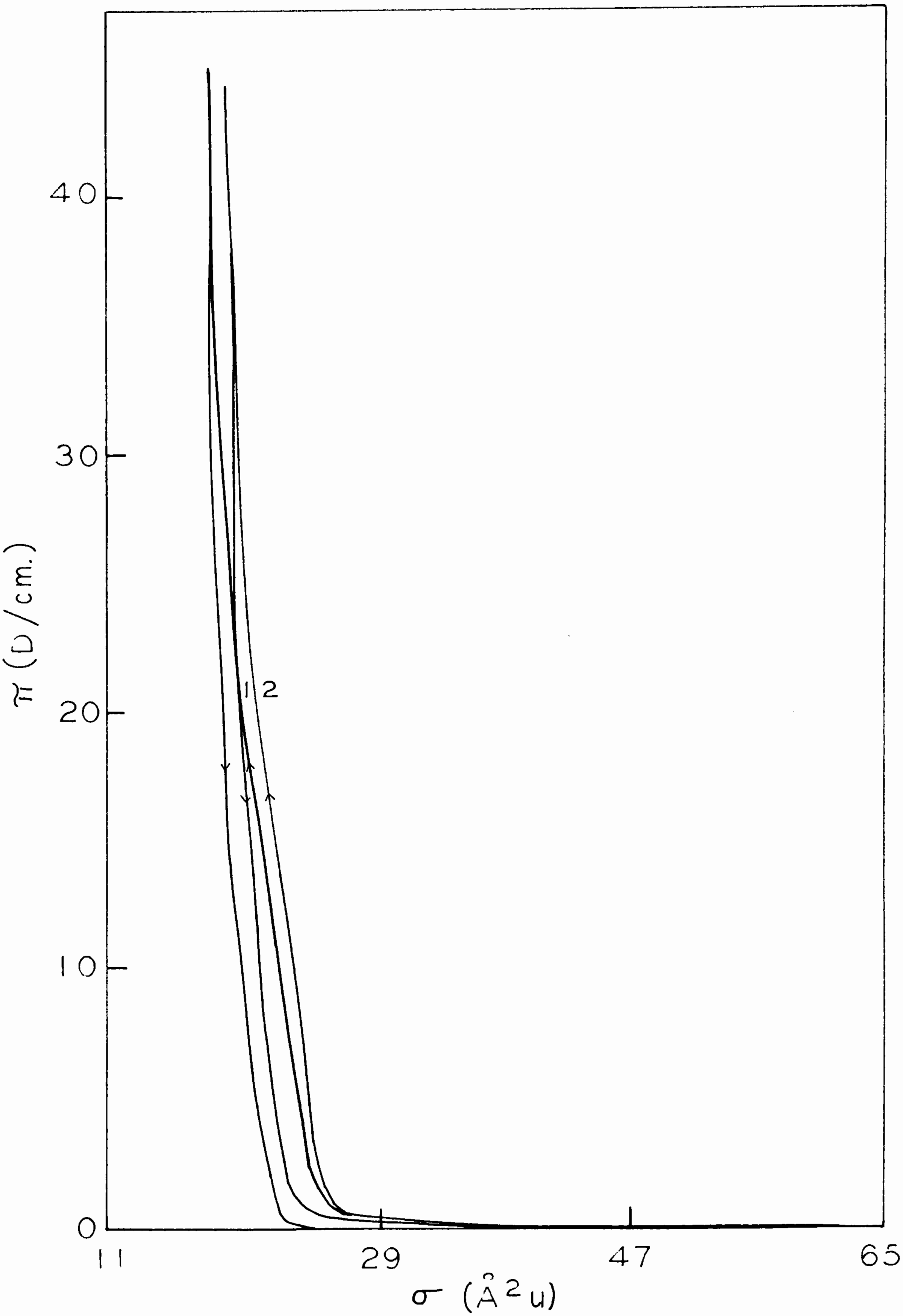

40
30
20
10
0
π (D/cm.)
11
29
47
65
σ (Å²u)
1
2

The compressibilities of the SA monolayer as calculated from the π-σ plots of the film under a compression rate of 2.413 Å^2 per molecule per minute are given in Table XLII.

TABLE XLII

Film characteristics of SA monolayer

	12.1°C		25°C	
	(-k)cms/dyne	Film type	(-k)cms/dyne	Film type
Below Q	0.0099 (at 23.98 Å^2, 8 d/cm)	L_c	0.0115 (at 23.98 Å^2, 8 d/cm)	L_c
Above Q	0.0014 (at 19.90 Å^2, 27.5 d/cm)	L_s	0.0013 (at 19.40 Å^2, 35.0 d/cm)	L_s

It can be seen from these data that in general the surface pressure attains higher values at higher temperatures and at higher rates of compression. The compressibilities also vary with temperature and compression rate, being higher at higher temperatures and higher rates of compression.

(b) <u>2 Methyl stearic acid (2 MSA)</u>:

$CH_3 - (CH_2)_{14} - (CH_3)\ CH - CH_2 - COOH$

Pressure area isotherms of 2MSA monolayers with an initial area of 65 Å^2 per molecule were recorded during both compression and decompression and are reproduced in Figures 23 to 25. The compressibilities of a monolayer of 2 MSA have been computed from π-σ curves at 25°C and compression rate 1.848 Å^2 per molecule per minute and given in Table XLIII. P_1 in this table is the point at which the surface pressure first begins to rise and Q_1 is the transition point in the curve. The point Q_1 appears during compression only at higher temperatures and at higher compression rates; but during decompression this transition point appears at correspondingly lower pressures and areas.

TABLE XLIII

Film characteristics of 2 MSA monolayer

Rate of compression Å^2/mol/min	Temp. °C	P_1 Å^2		(-k) cms/dyne
1) 1.848	12.1	33.22		
	25.0	50.22	Below Q (L_e)	0.0278 (at 39.13 Å^2, 5.25 d/cm)
			Above Q (L_c)	0.0161 (at 29.37 Å^2, 12.5 d/cm)
2) 2.413	12.1	33.03		
	25.0	49.32		
3) 4.5	12.1	33.50		
	25.0	50.02		

Figure 23

Figure 23

π-σ diagram of 2 MSA at a compression rate of 1.848 Å^2 / molecule / minute. Initial area 65 Å^2 per molecule.

1 obtained at 25°C

2 obtained at 12.1°C

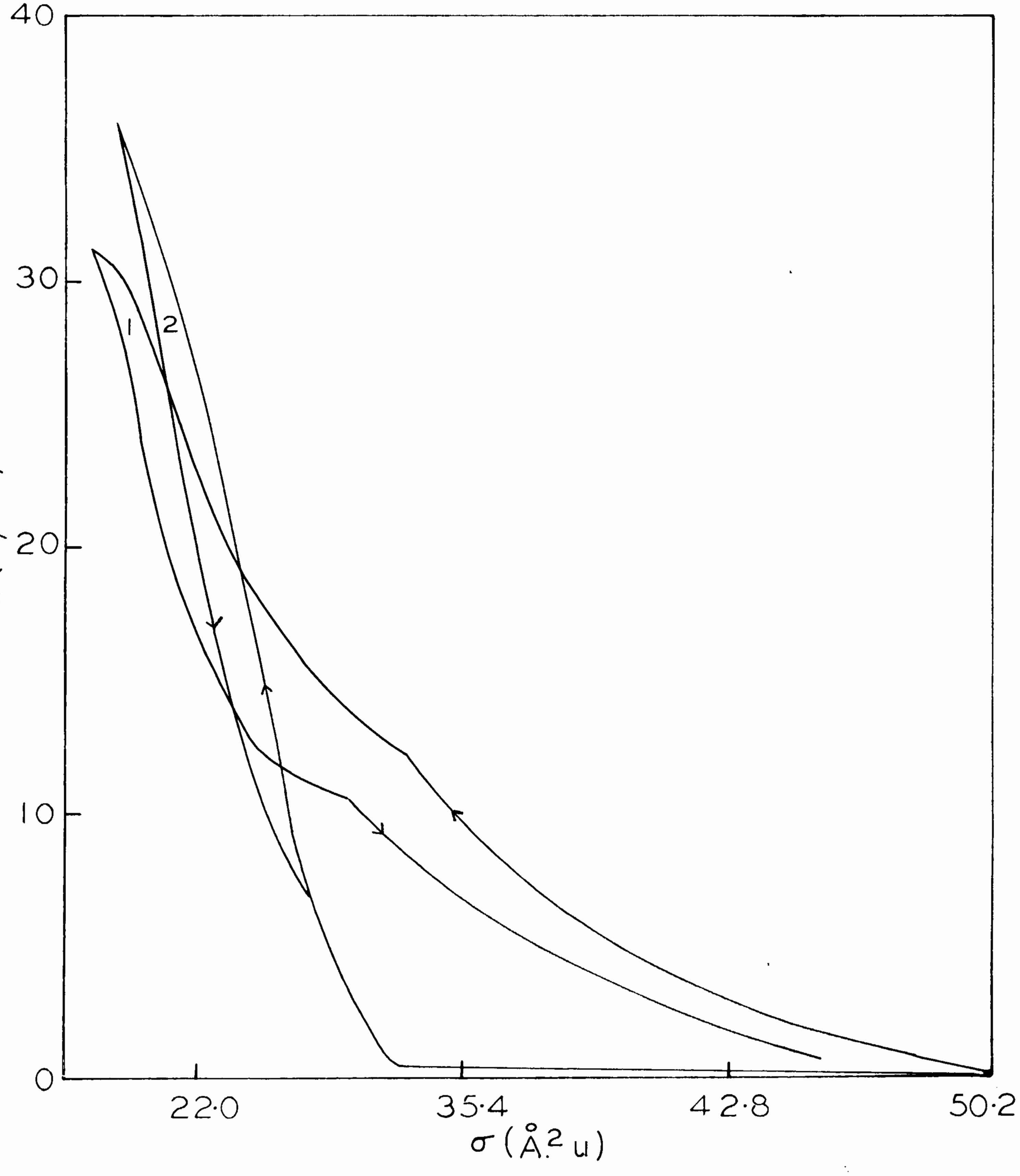

40
30
20
10
0
1
2
22·0
35·4
42·8
50·2
π (D/cm.)
σ (Å.² u)

Figure 24

Figure 24

π-σ diagram of 2 MSA at a compression rate of 2.413 Å^2 / molecule / minute. Initial area 65 Å^2 per molecule.

1 obtained at 25°C

2 obtained at 12.1°C

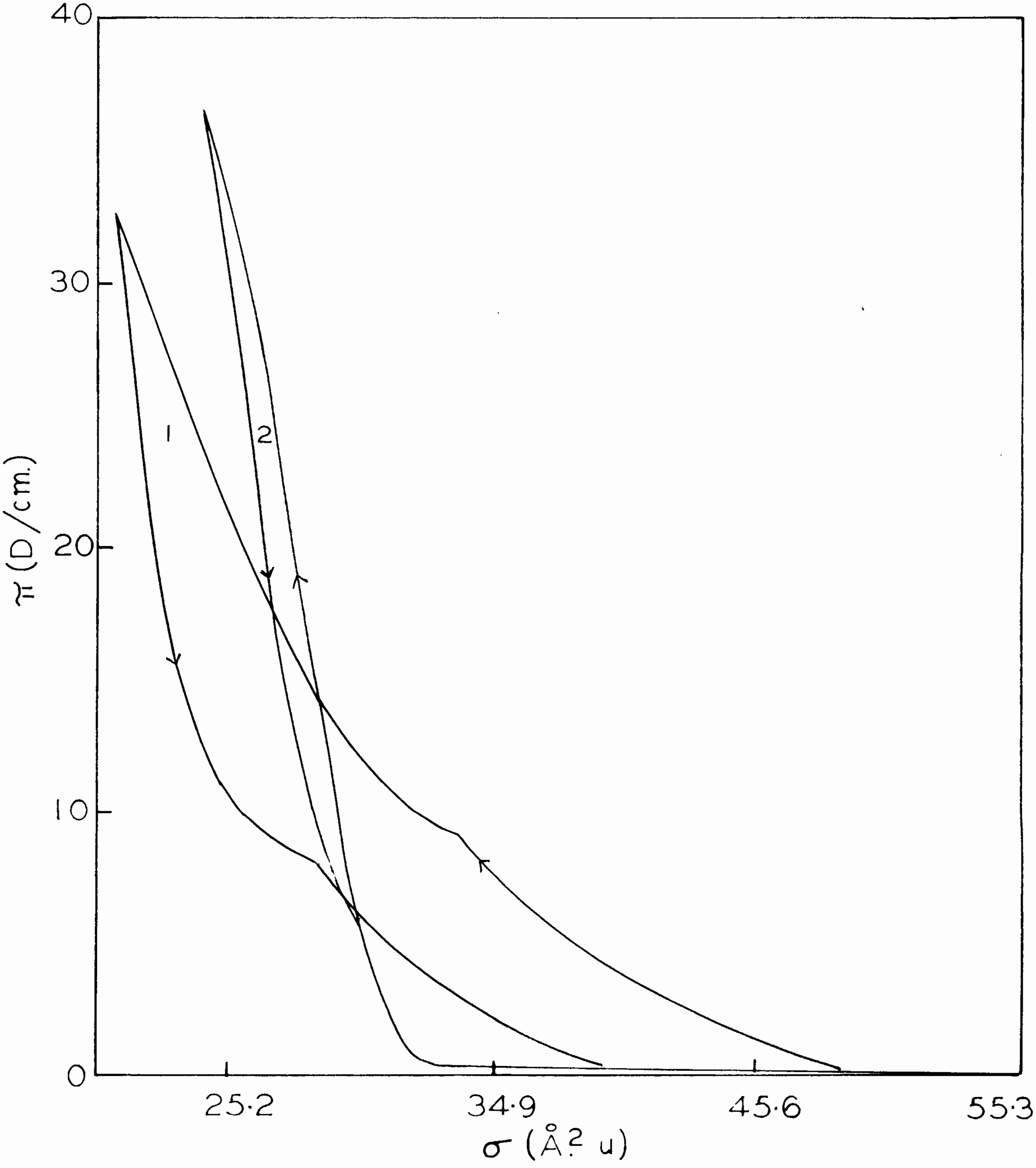

40
30
20
10
0
π (D/cm.)
1
2
25·2
34·9
45·6
55·3
σ (Å² u)

Figure 25

<u>Figure 25</u>

π-σ diagram of 2 MSA at a compression rate of 4.5 Å^2 / molecule / minute. Initial area 65 Å^2 per molecule.

1 obtained at 25°C

2 obtained at 12.1°C

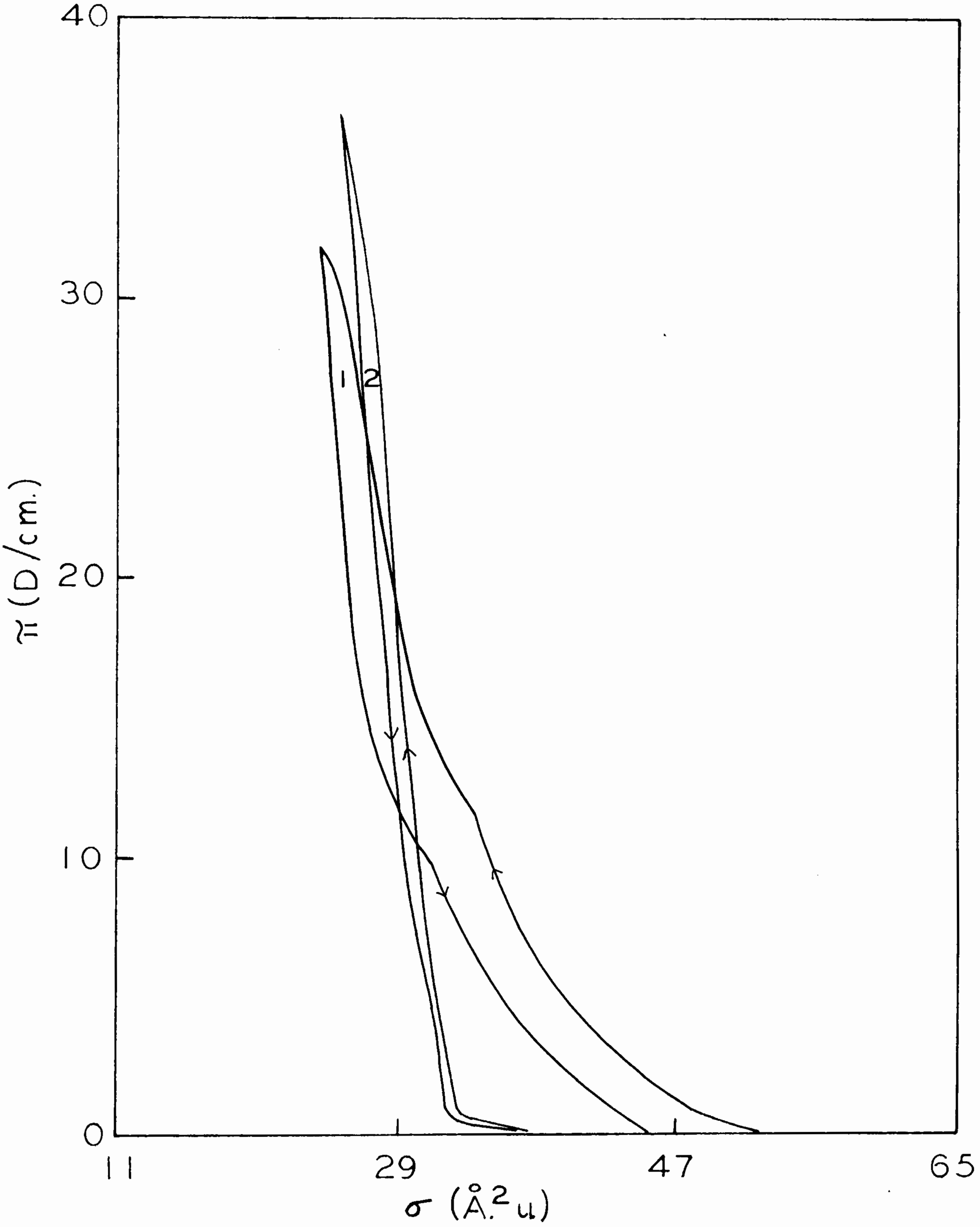
40
30
20
10
0
π (D/cm.)
11
29
47
65
σ (Å.²u)
1
2

(c) 3 Methyl stearic acid (3 MSA):

$CH_3 - (CH_2)_{13} - (CH_3)\ CH - (CH_2)_2 - COOH.$

Recording of the π-σ curves of 3 MSA have been reporduced in Figures 26 to 28. Numerical data read from these π-σ diagrams are given in Table XLIV. P_1 and Q_1 have the same significance as mentioned earlier.

TABLE XLIV

π-σ curve of 3 MSA for various compression rates at 12.1°C and 25°C.

Compression rate Å^2 / mol / min	Temp. °C	P_1 Å^2	Q_1 Å^2
1) 1.848	12.1	33.95	30.63
	25.0	55.76	35.43
2) 2.413	12.1	34.23	29.29
	25.0	50.52	33.87
3) 4.5	12.1	34.40	29.00
	25.0	51.50	33.55

The compressibility coefficient (-k) calculated from the isotherms at 4.5 Å^2/mol/min. compression rate are given in Table XLV.

TABLE XLV

Film characteristics of 3 MSA monolayer

	12.1°C		25°C	
	(-k)cms/dyne	Film type	(-k)cms/dyne	Film type
Below Q_1	0.0083 (at 33.5 Å^2, 5 d/cm)	L_c	0.0433 (at 40.2 Å^2, 4 d/cm)	L_e
Above Q_1	0.0065 (at 26.8 Å^2, 23.8 d/cm)	L_c	0.0081 (at 26.8 Å^2, 20 d/cm)	L_c

(d) <u>3 Ethyl stearic acid (3 ESA):</u>

$CH_3 - (CH_2)_{13} - (C_2H_5)\ CH - (CH_2)_2 - COOH$

The pressure area isotherms are reproduced for 3 ESA in Figures 29 to 31. The experiments were performed as in the previous cases. The experimental results are given in Table XLVI.

<u>Figure 26</u>

Figure 26

π-σ diagram of 3 MSA at a compression rate of 1.848 $Å^2$ / molecule / minute. Initial area 65 $Å^2$ per molecule.

1 obtained at 25°C

2 obtained at 12.1°C

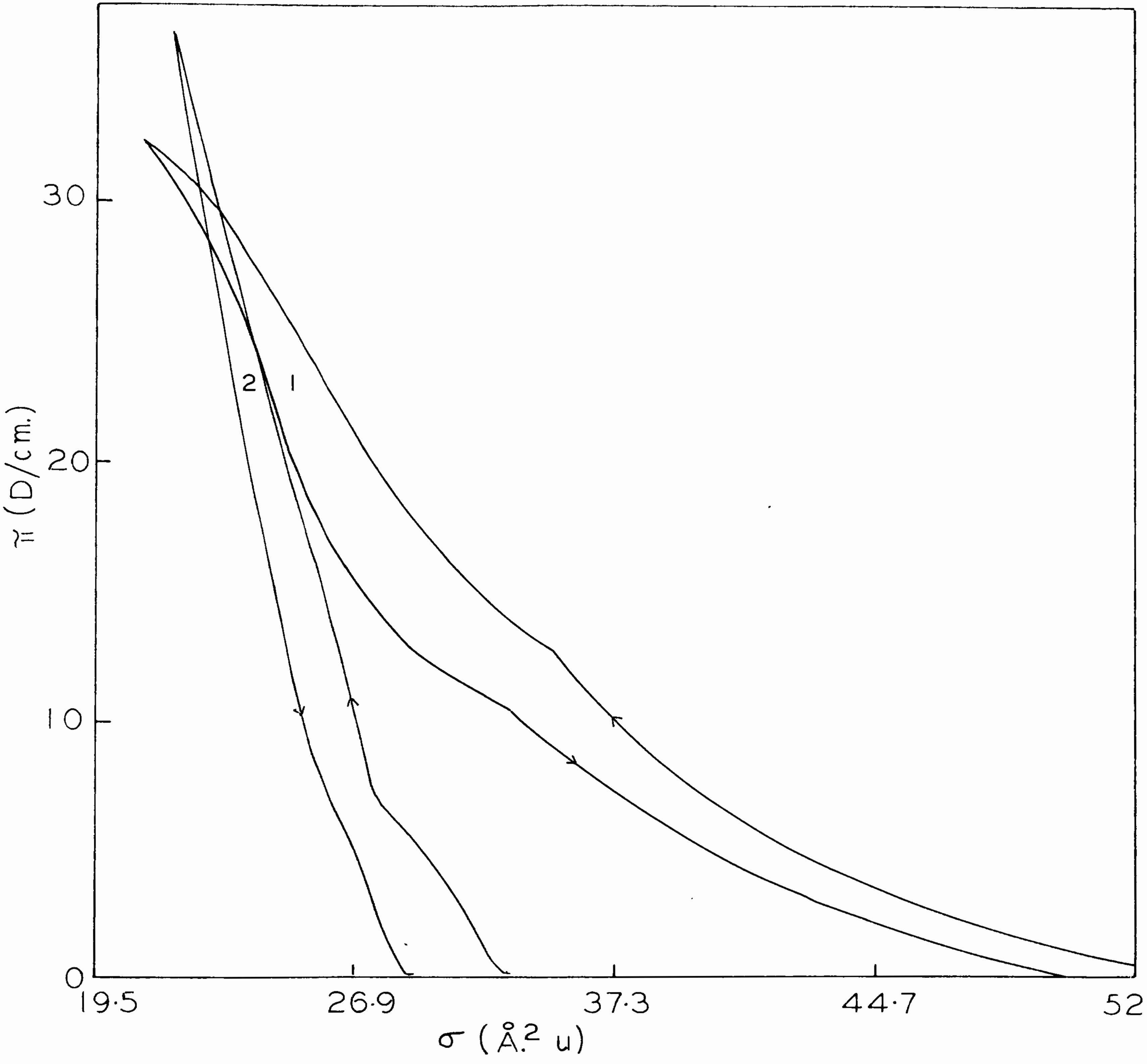
30
20
10
0
π (D/cm.)
19·5
26·9
37·3
44·7
52·1
σ (Å.² u)
2
1

<u>Figure 27</u>

Figure 27

$\pi - \sigma$ diagram of 3 MSA at a compression rate of 2.413 $Å^2$ / molecule / minute. Initial area 65 $Å^2$ per molecule.

1 obtained at 25°C

2 obtained at 12.1°C

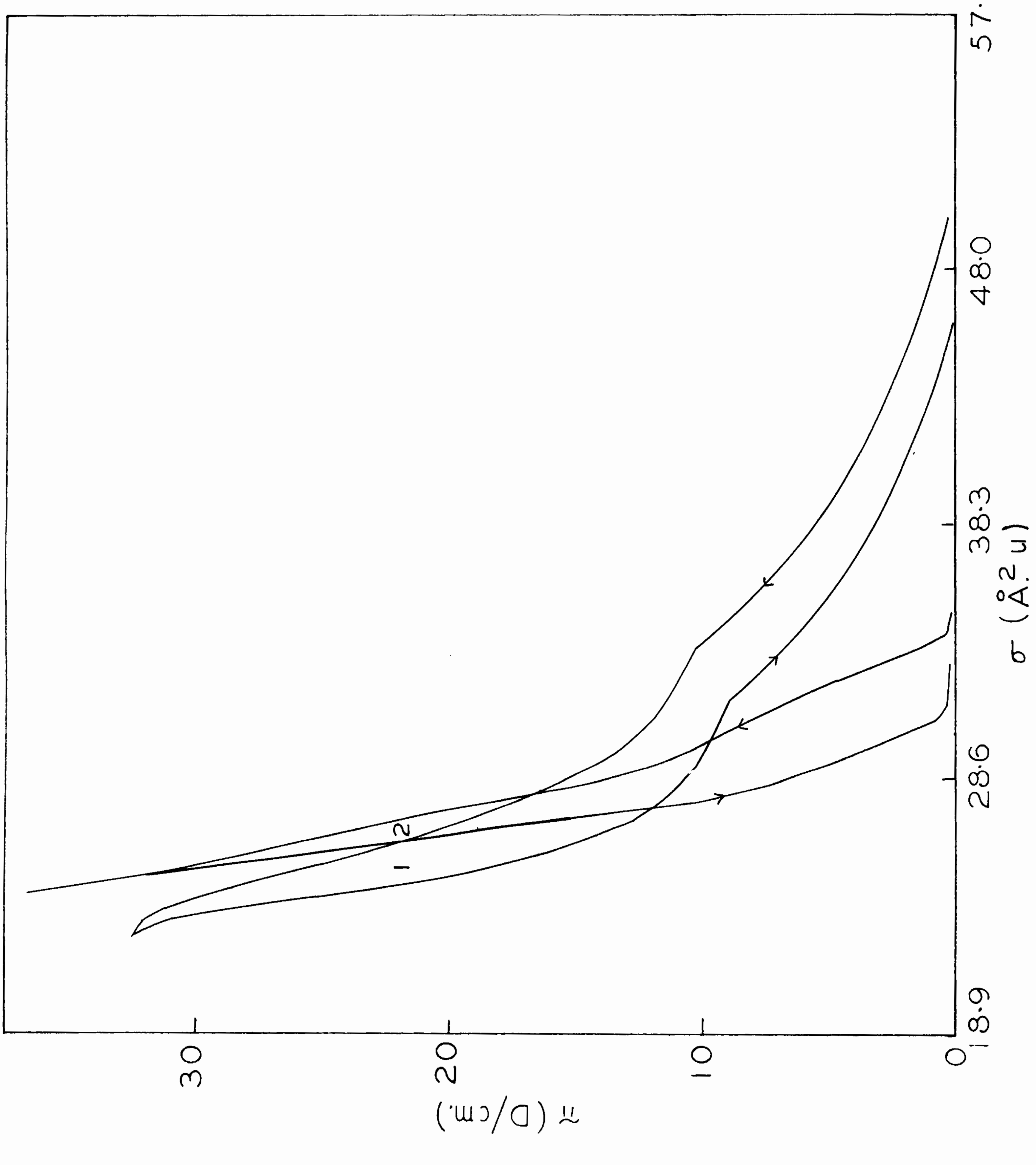

π (D/cm.)
30
20
10
0
18.9
28.6
38.3
48.0
57.7
σ (Å² u)
1
2

Figure 28

Figure 28

π-σ diagram of 3 MSA at a compression rate of 4.5 $Å^2$ / molecule / minute. Initial area 65 $Å^2$ per molecule.

1 obtained at 25°C

2 obtained at 12.1°C

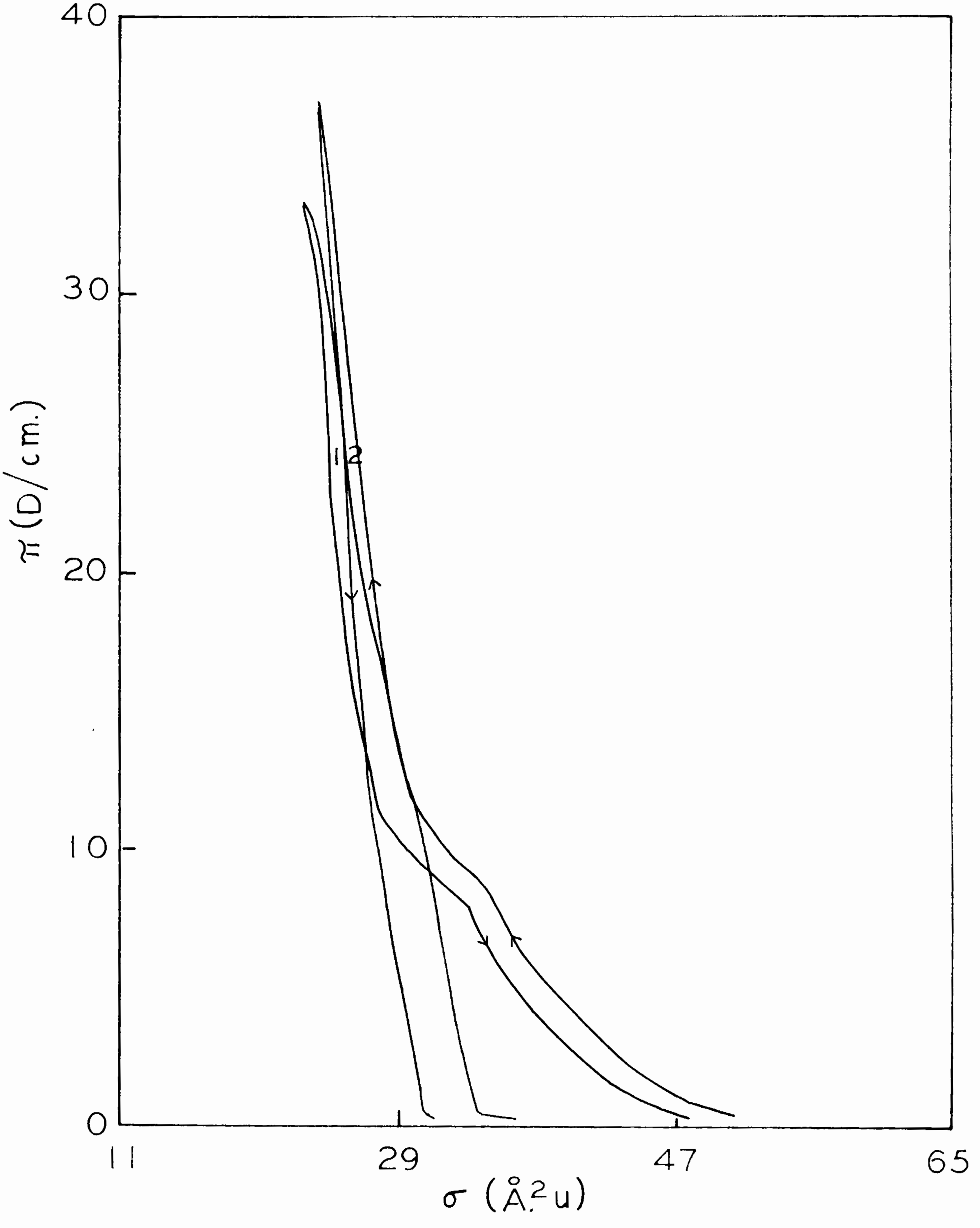
40
30
20
10
0
π (D/cm.)
11
29
47
65
σ (Å.²u)
1
2

Figure 29

Figure 29

π-σ diagram of 3 ESA at a compression rate of 1.848 Å^2 / molecule / minute. Initial area 65 Å^2 per molecule.

1 obtained at 25°C

2 obtained at 12.1°C

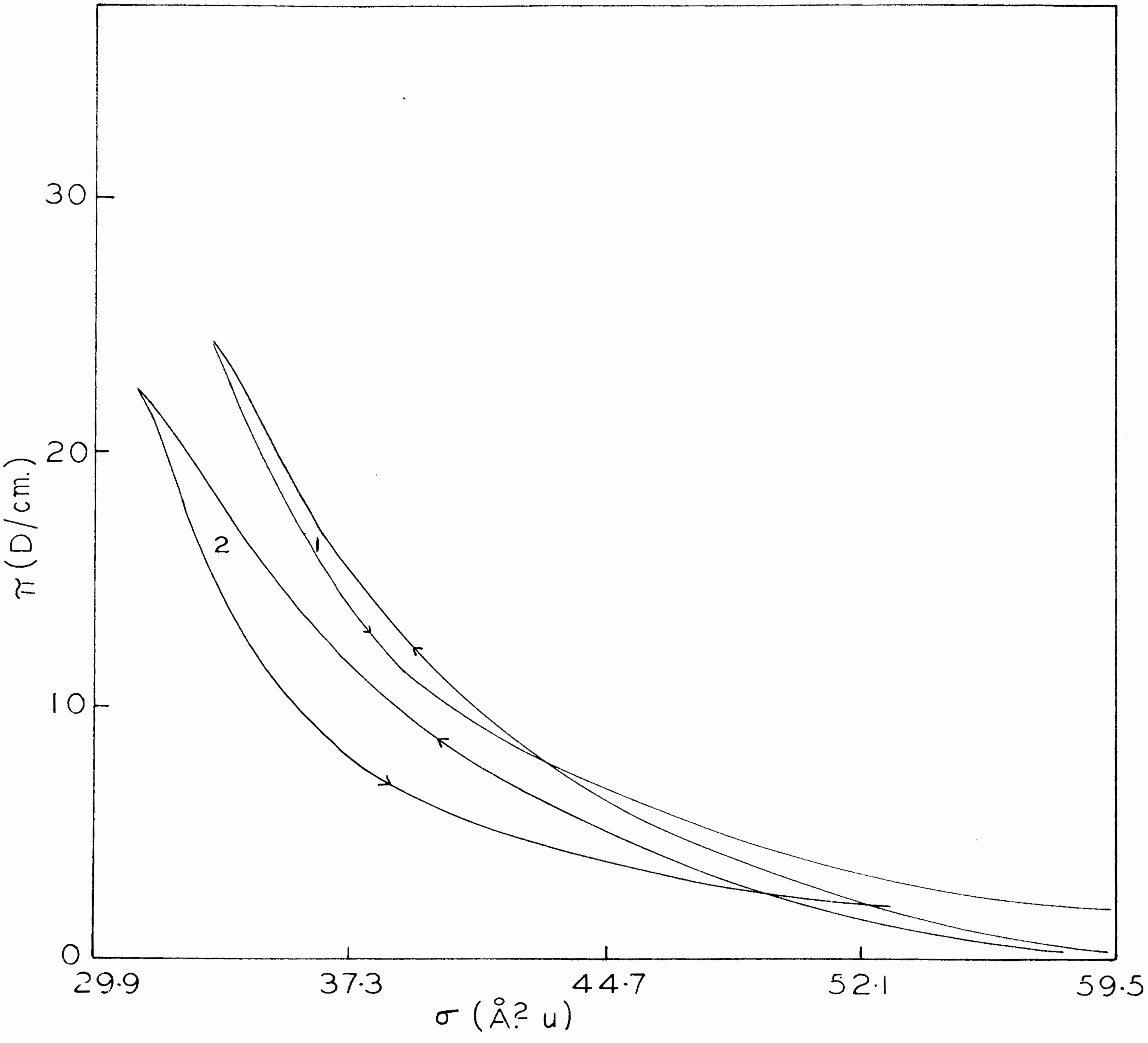
30
20
10
0
π (D/cm.)
29.9
37.3
44.7
52.1
59.5
σ (Å² u)
1
2

Figure 30

Figure 30

$\pi-\sigma$ diagram of 3 ESA at a compression rate of 2.413 Å^2 / molecule / minute. Initial area 65 Å^2 per molecule.

1 obtained at 25°C

2 obtained at 12.1°C

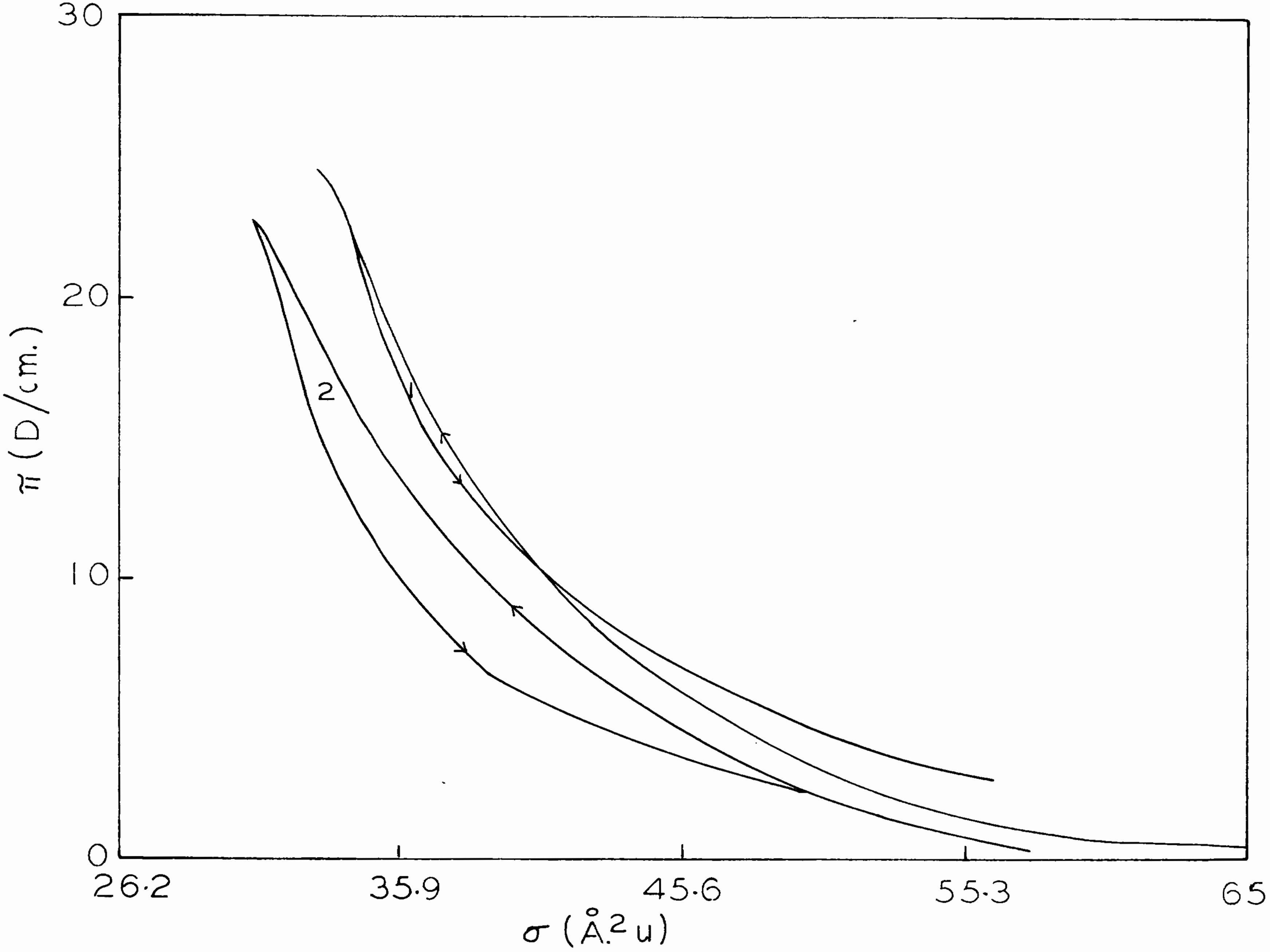
30
20
10
0
π (D/cm.)
26·2
35·9
45·6
55·3
65
σ (Å.²u)
2

Figure 31

Figure 31

π-σ diagram of 3 ESA at a compression rate of 4.5 Å^2 / molecule / minute. Initial area 65 Å^2 per molecule.

1 obtained at 25°C

2 obtained at 12.1°C

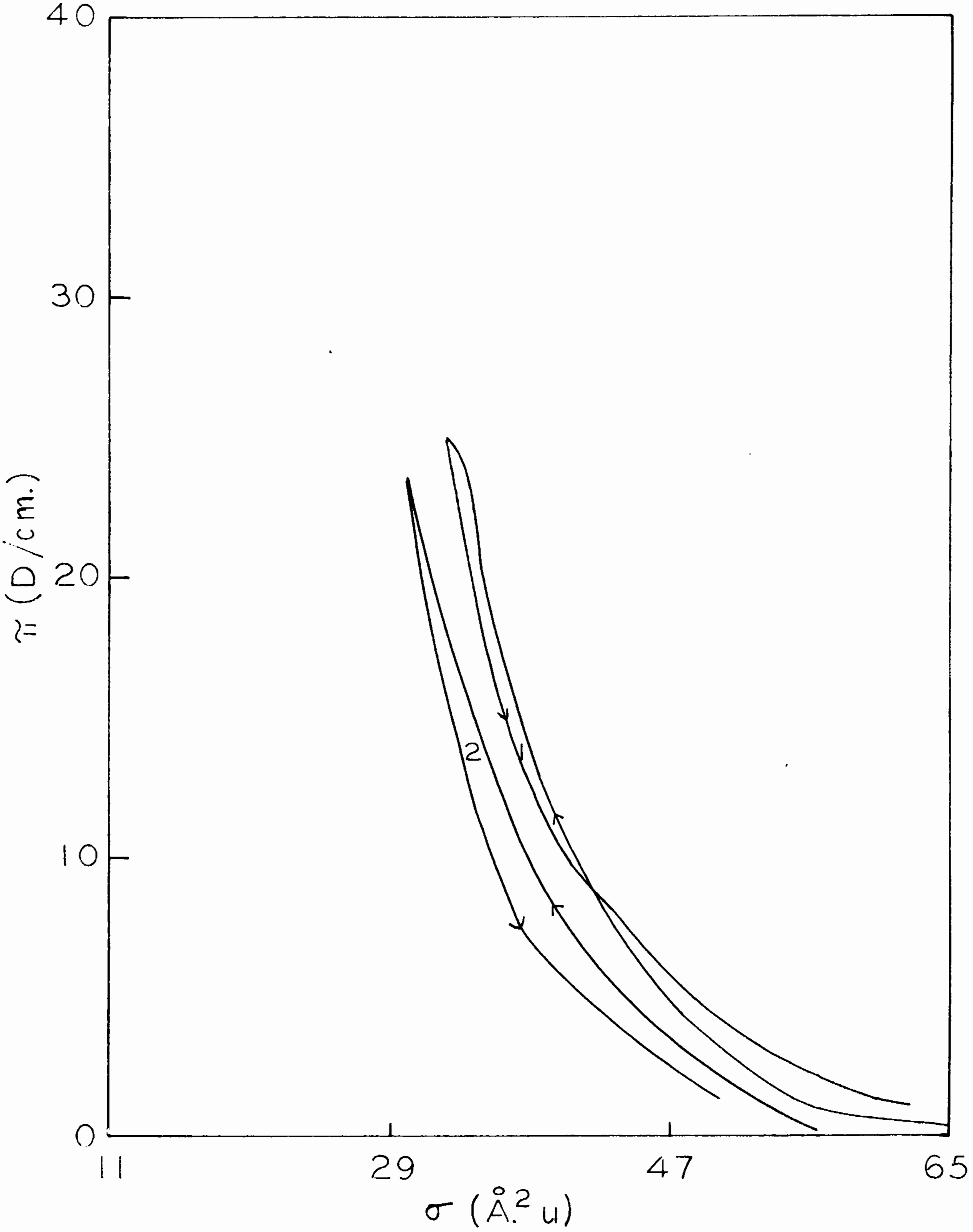
40
30
20
10
0
π (D/cm.)
11
29
47
65
σ (Å.² u)
2

TABLE XLVI

Film characteristics of 3 ESA monolayer

Rate of compression	Temp.	P_1	(-k)
Å^2/mol/min	$^\circ$C	Å^2	cms/dyne
1) 1.848	12.1	57.61	
	25.0	58.32	
2) 2.413	12.1	57.76	
	25.0	60.18	
3) 4.5	12.1	56.90	
	25.0	58.25	0.02869 (L_e) (at 40.8 Å^2, 7.5 d/cm) 0.02387 (L_e) (at 42.1 Å^2, 8.4 d/cm)

(e) <u>10 Phenyl stearic acid (10 PSA):</u>

$CH_3 - (CH_2)_6 - (C_6H_5)\ CH - (CH_2)_9 - COOH$.

The pressure area isotherms for 10 PSA are given in Figures 32 to 34. The compressibility coefficients are presented in Table XLVII.

TABLE XLVII

Film characteristics of 10 PSA monolayer

Rate of compression Å^2/mol/min	Temp. °C	(-k) cms/dyne	Film type
1) 1.848	12.1	0.01403(at 41.2 Å^2, 13 d/cm)	L_e
	25.0	0.02006(at 46.2 Å^2, 10.5 d/cm)	L_e
2) 2.413	12.1	0.01778(at 45.7 Å^2, 9.8 d/cm)	L_e
	25.0	0.01830(at 47.4 Å^2, 10 d/cm)	L_e
3) 4.5	12.1	0.01833(at 47.0 Å^2, 6.3 d/cm)	L_e
	25.0	0.01828(at 49.3 Å^2, 9 d/cm)	L_e

After attainment of the maximum pressure in any of the above experiments with 10 PSA, the surface pressure remained constant with time at constant area per molecule. This is in contrast to the behaviour of the other stearic acid derivatives studied.

Figure 32

Figure 32

π-σ diagram of 10 PSA at a compression rate of 1.848 $Å^2$ / molecule / minute. Initial area of 65 $Å^2$ per molecule.

1 obtained at 25°C

2 obtained at 12.1°C

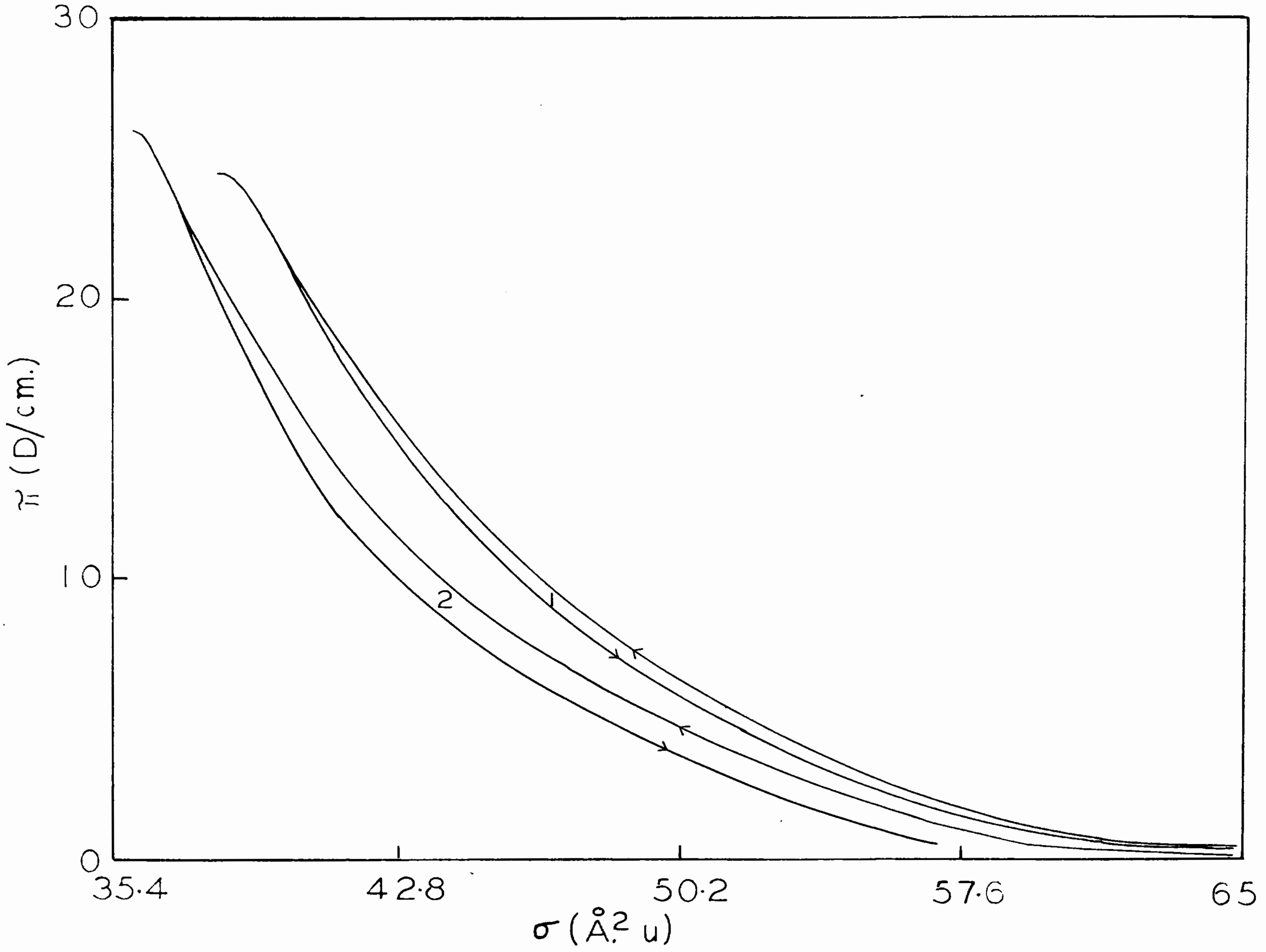
30
20
10
0
π (D/cm.)
35·4
42·8
50·2
57·6
65
σ (Å.² u)
1
2

<u>Figure 33</u>

<u>Figure 33</u>

π-σ diagram of 10 PSA at a compression rate of 2.413 $\mathring{A}^2$ / molecule / minute. Initial area 65 $\mathring{A}^2$ per molecule.

1 obtained at 25°C

2 obtained at 12.1°C

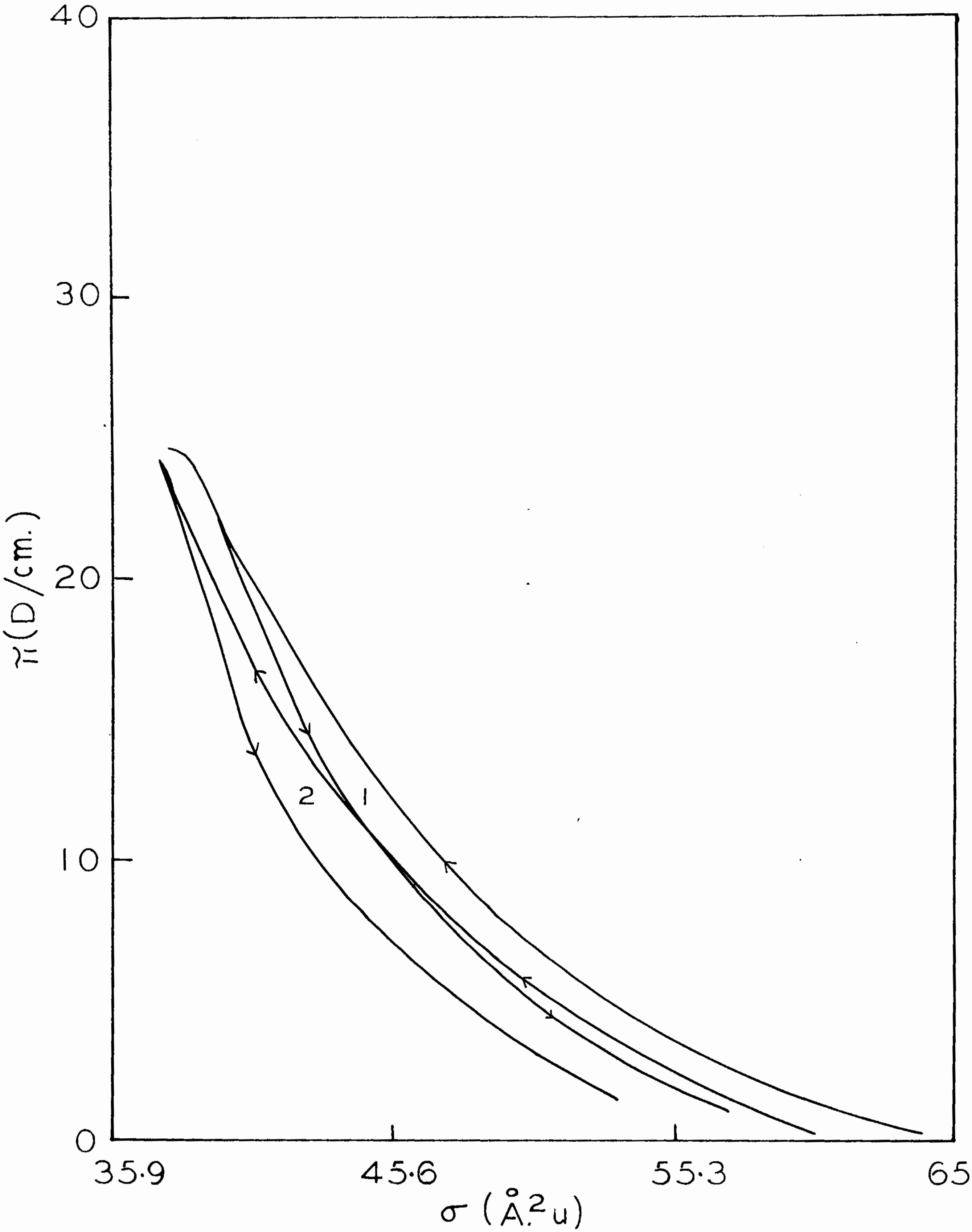
40
30
20
10
0
π (D/cm.)
35·9
45·6
55·3
65
σ (Å.²u)
1
2

Figure 34

Figure 34

$\pi - \sigma$ diagram of 10 PSA at a compression rate of 4.5 $Å^2$ / molecule / minute. Initial area 65 $Å^2$ per molecule.

1 obtained at 25°C

2 obtained at 12.1°C

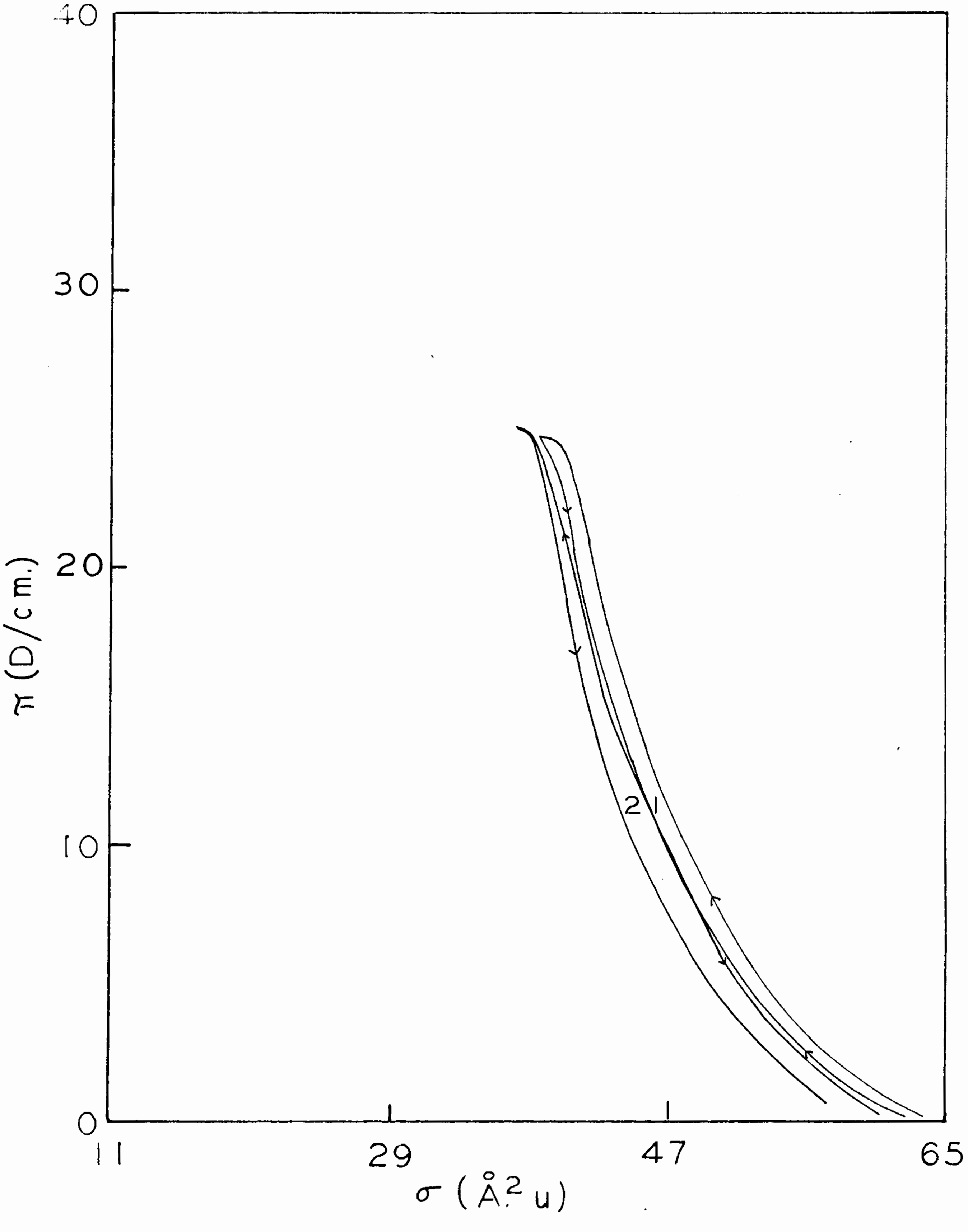
40
30
20
10
0
π (D/cm.)
11
29
47
65
σ (Å.² u)
2
1

(f) 12 Hydroxy stearic acid (12 HSA):

$CH_3 - (CH_2)_4 - CH(OH)\ (CH_2)_{11} - COOH$

Figures 35 to 37 represent π-σ diagrams of 12 HSA under the same experimental conditions. In the isotherms obtained for this acid the most striking characteristic was the appearance of the "maximum" mentioned earlier. Figure 38 is a special plot given to illustrate the appearance of the "maximum" before the equilibrium region is reached. The four individual curves in Figure 38 are taken at 9°C, 12°C, 18°C and 25°C at a compression rate of 7.225 $Å^2$ per molecule per minute in all cases.

The compressibility coefficients for a monolayer of 12 HSA compressed at a rate of 2.413 $Å^2$ per molecule are given in Table XLVIII.

TABLE XLVIII

Film characteristics of 12 HSA monolayer

12.1°C		25°C	
(-k)cms/dyne	Film type	(-k)cms/dyne	Film type
0.00708 (at 21.8 $Å^2$,17.5 d/cm)	L_c	0.00863 (at 23.98 $Å^2$, 12.5 d/cm)	L_c

The compressibility of 12 HSA films in Figure 38 under a rate of compression of 7.225 $Å^2$/mol/min and at 25°C is given in Table XLIX.

Figure 35

Figure 35

$\pi - \sigma$ diagram of 12 HSA at a compression rate of 1.848 Å^2 / molecule / minute. Initial area 65 Å^2 per molecule.

1 obtained at 25°C

2 obtained at 12.1°C

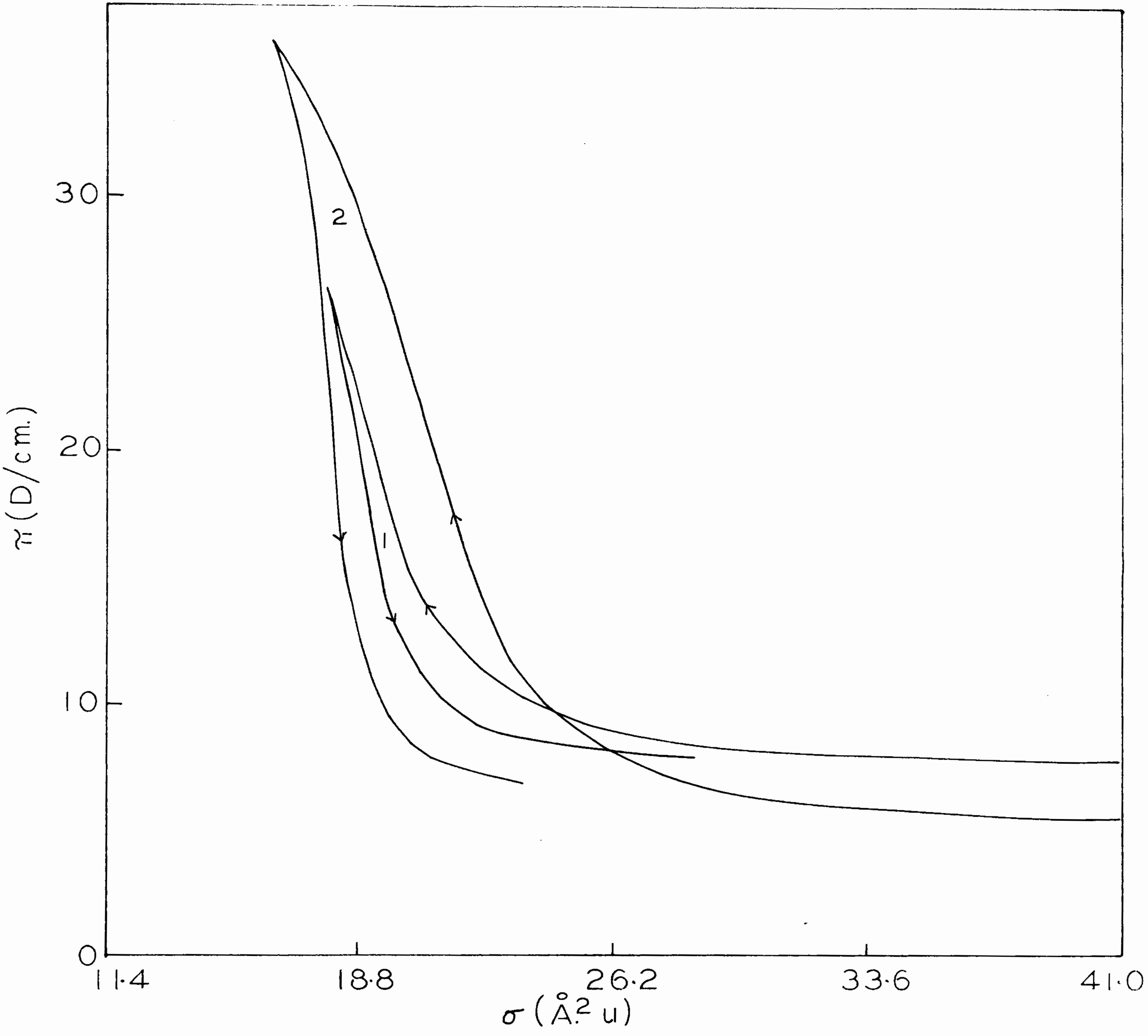

30
20
10
0
π (D/cm.)
11·4
18·8
26·2
33·6
41·0
σ (Å.² u)
2
1

Figure 36

Figure 36

π-σ diagram of 12 HSA at a compression rate of 2.413 $Å^2$ / molecule / minute. Initial area 65 $Å^2$ per molecule.

1 obtained at 25°C
2 obtained at 12.1°C

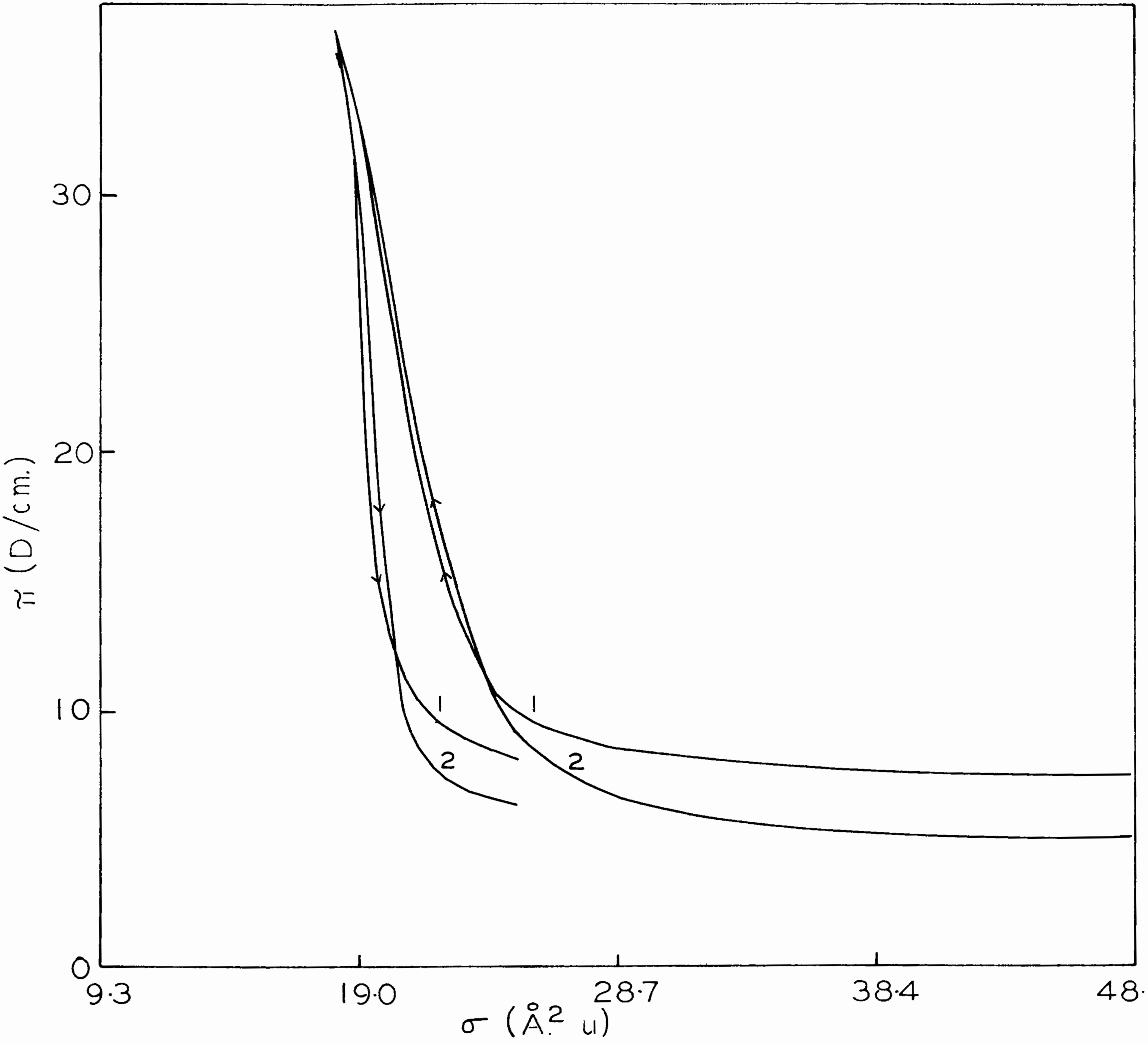
30
20
10
0
π (D/cm.)
9·3
19·0
28·7
38·4
48·1
σ (Å.² u)
1
2
1
2

Figure 37

Figure 37

π-σ diagram of 12 HSA at a compression rate of 4.5 $Å^2$ / molecule / minute. Initial area 65 $Å^2$ per molecule.

1 obtained at 25°C

2 obtained at 12.1°C

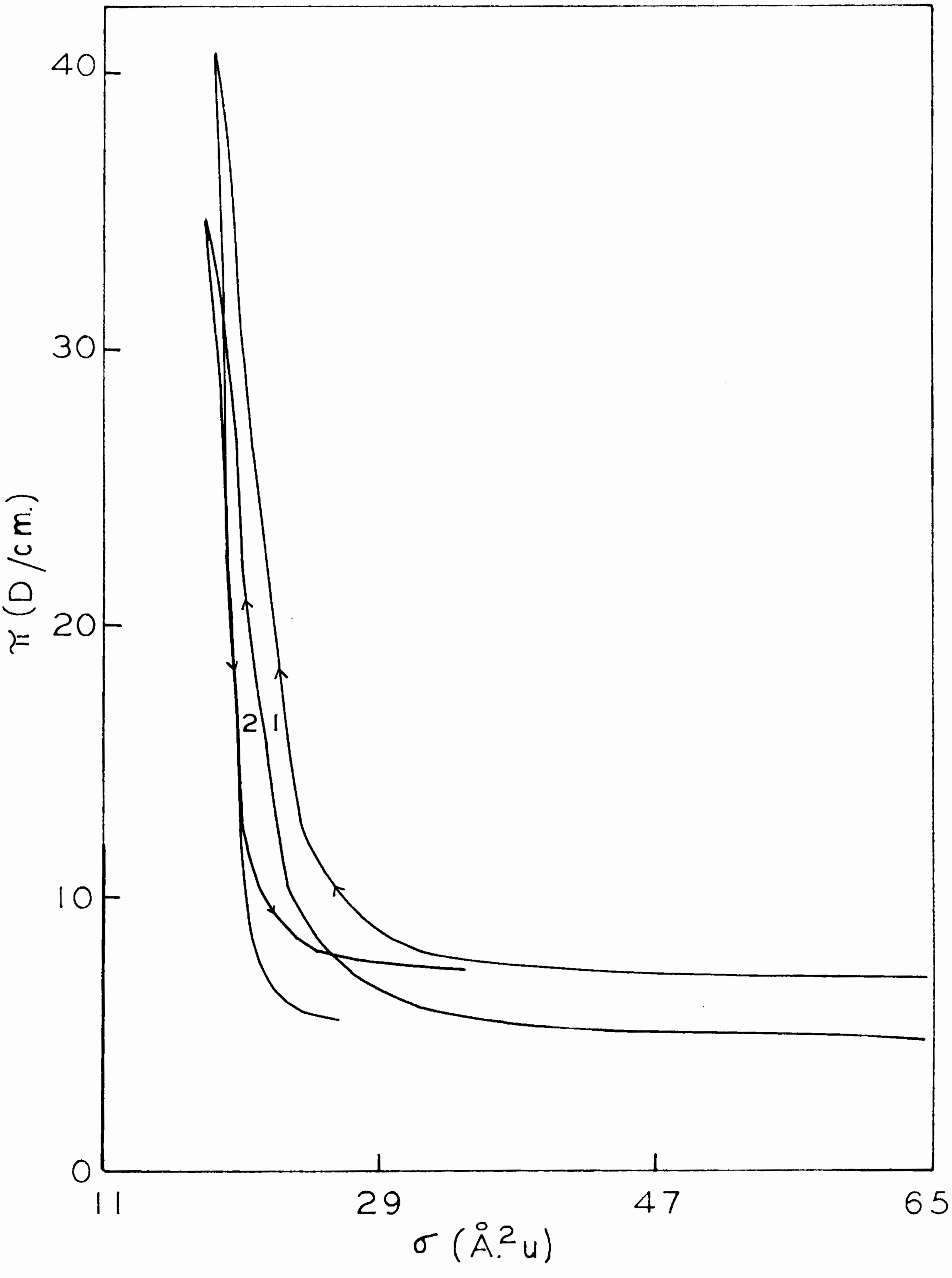

40
30
20
10
0
11
29
47
65
π (D/cm.)
σ (Å.²u)
2
1

Figure 38

Figure 38

π-σ diagram of 12 HSA at a compression rate of 7.225 Å^2 / molecule / minute. Initial area 150 Å^2 per molecule.

1 obtained at 9°C
2 obtained at 12°C
3 obtained at 18°C
4 obtained at 25°C

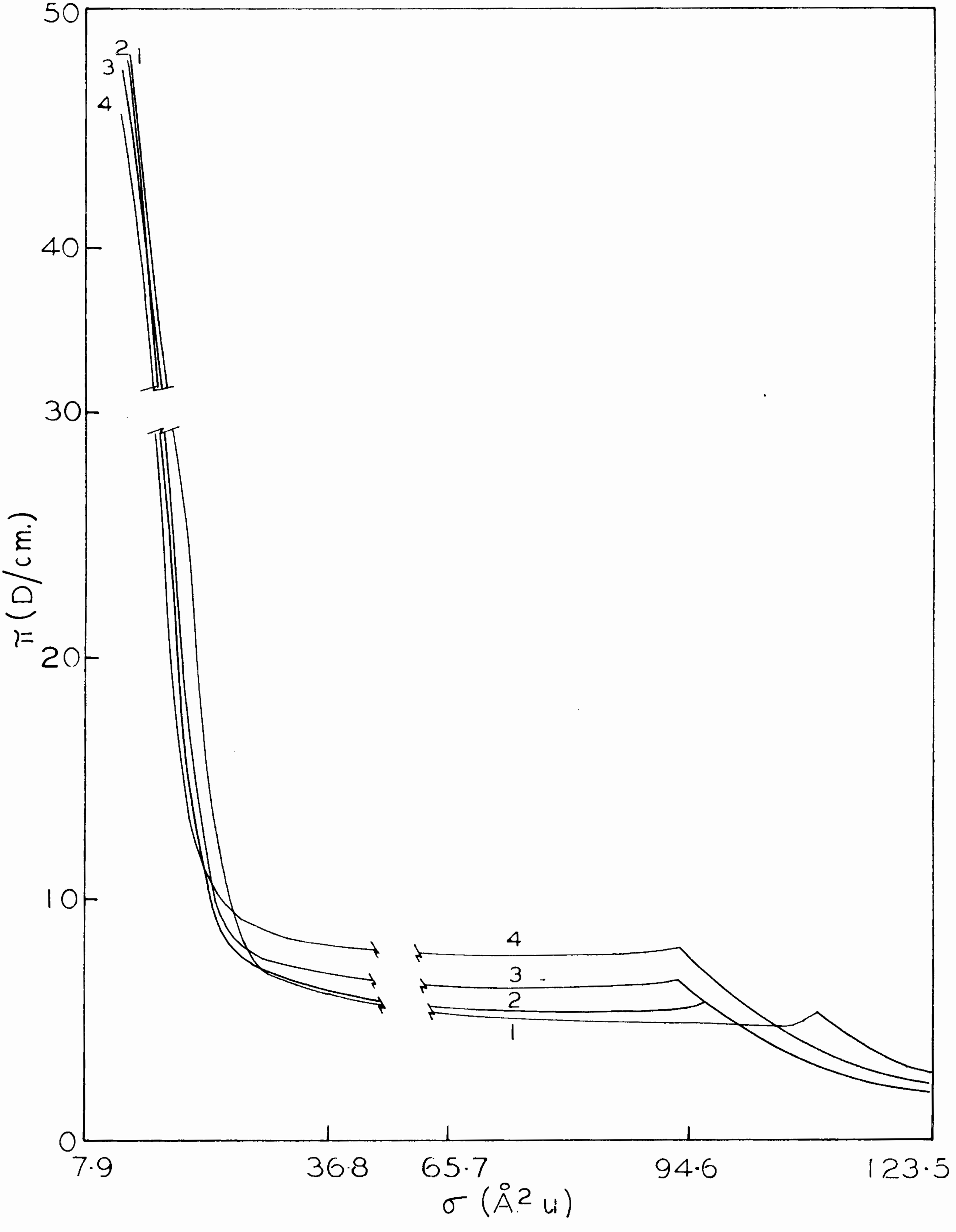
50
40
30
20
10
0
π (D/cm.)
7·9
36·8
65·7
94·6
123·5
σ (Å² u)
1
2
3
4

TABLE XLIX

Compressibility of 12 HSA

	(-k) cms/dyne
1) Low pressure region (before maximum)	0.05299 (at 109.1 Å^2, 3.8 d/cm)
2) Horizontal region	0.4110 (at 31.8 Å^2, 8.5 d/cm)
3) Higher pressure region	0.01009 (at 18.8 Å^2, 27.5 d/cm)

(g) <u>12 Keto stearic acid (12 KSA)</u>:

$CH_3 - (CH_2)_4 -CH(CO) - (CH_2)_{11} - COOH$

π-σ plots of 12 KSA with varying rates of compression at 12.1°C and 25°C are given in Figures 39 to 41. It can be noticed that a marked transition occurs during compression in the film at 12.1°C and at a rate of compression of 4.5 Å^2 per molecule per minute. The compressibility data for this acid is presented in Table L.

In the tables presented under the stearic acid derivatives, film types are abbreviated according to Harkins (12): L_e represents liquid expanded films; L_c represents liquid condensed film; L_s represents super liquid film; L_1 represents liquid intermediate film.

Figure 42 shows the relaxation effects of SA, 10 PSA and 12 HSA monolayers.

Figure 39

<u>Figure 39</u>

π-σ diagram of 12 KSA at a compression rate of 1.848 Å^2 / molecule / minute. Initial area 65 Å^2 per molecule.

1 obtained at 25°C

2 obtained at 12.1°C

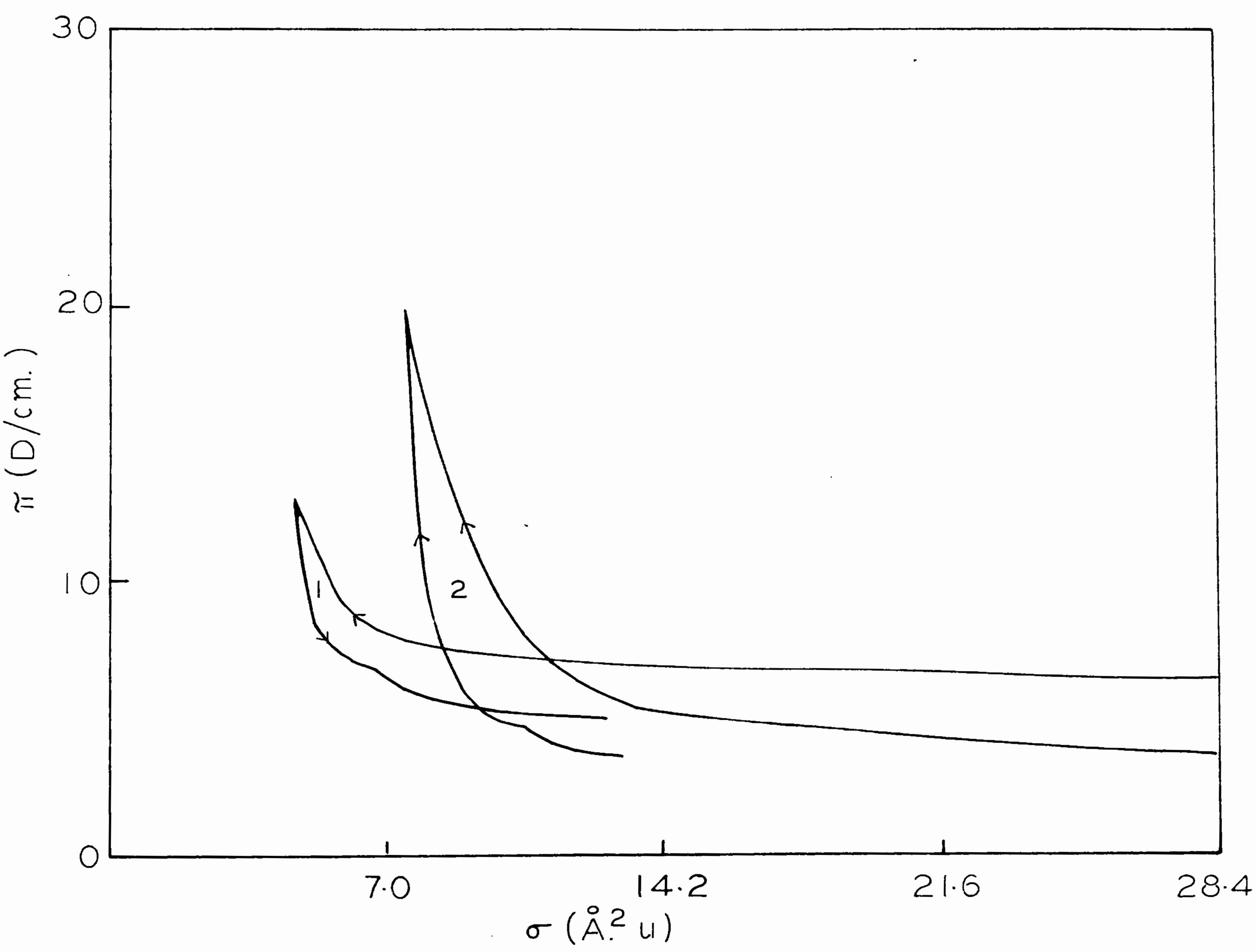
30
20
10
0
π (D/cm.)
7·0
14·2
21·6
28·4
σ (Å.^{2} u)
1
2

Figure 40

Figure 40

π-σ diagram of 12 KSA at a compression rate of 2.413 Å^2/molecule/ minite. Initial area 65 Å^2 per molecule.

1 obtained at 25°C

2 obtained at 12.1°C

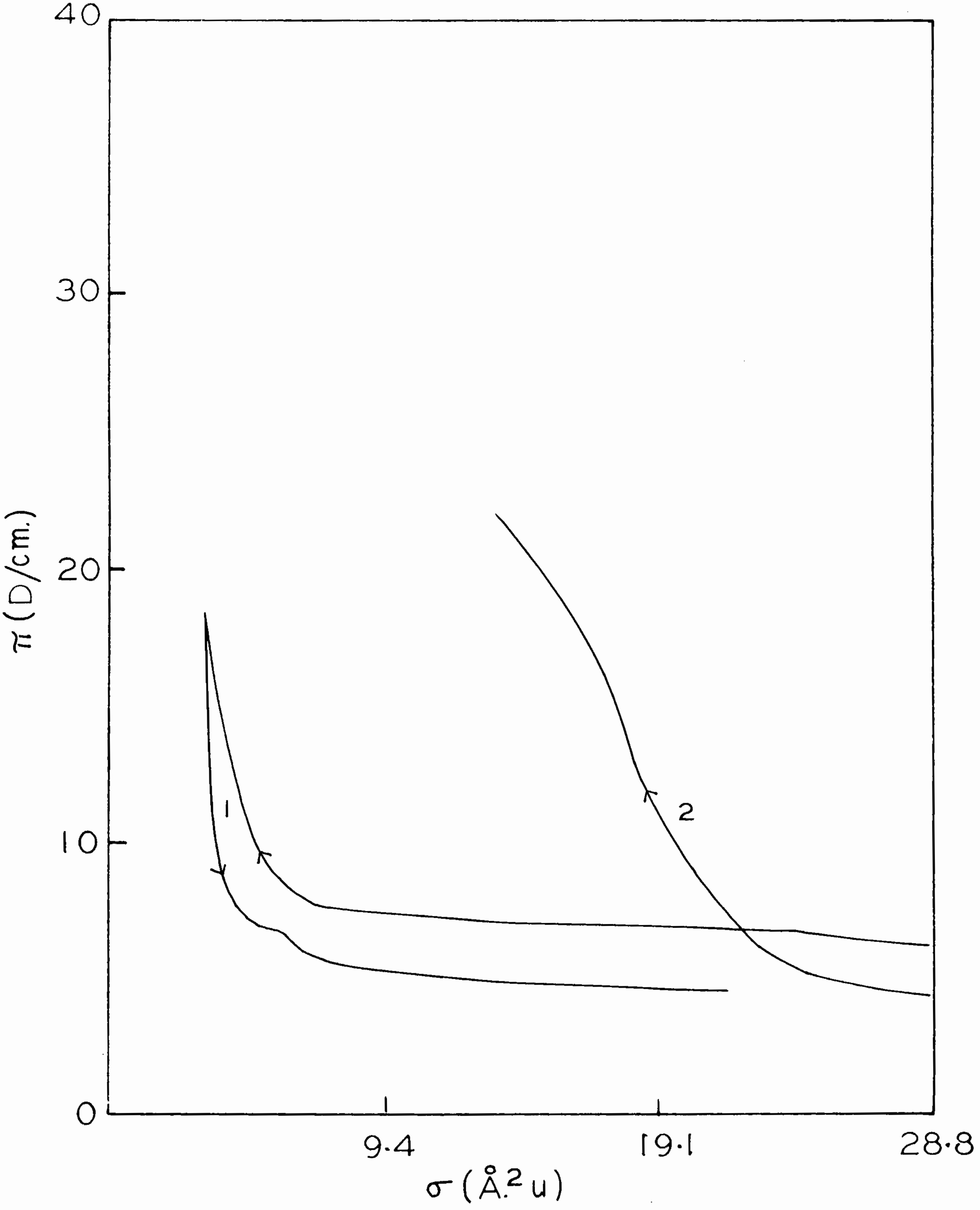
40
30
20
10
0
π (D/cm.)
9·4
19·1
28·8
σ (Å.² u)
1
2

Figure 41

Figure 41

π-σ diagram of 12 KSA at a compression rate of 4.5 $Å^2$ / molecule / minute. Initial area 65 $Å^2$ per molecule.

1 obtained at 25°C

2 obtained at 12.1°C

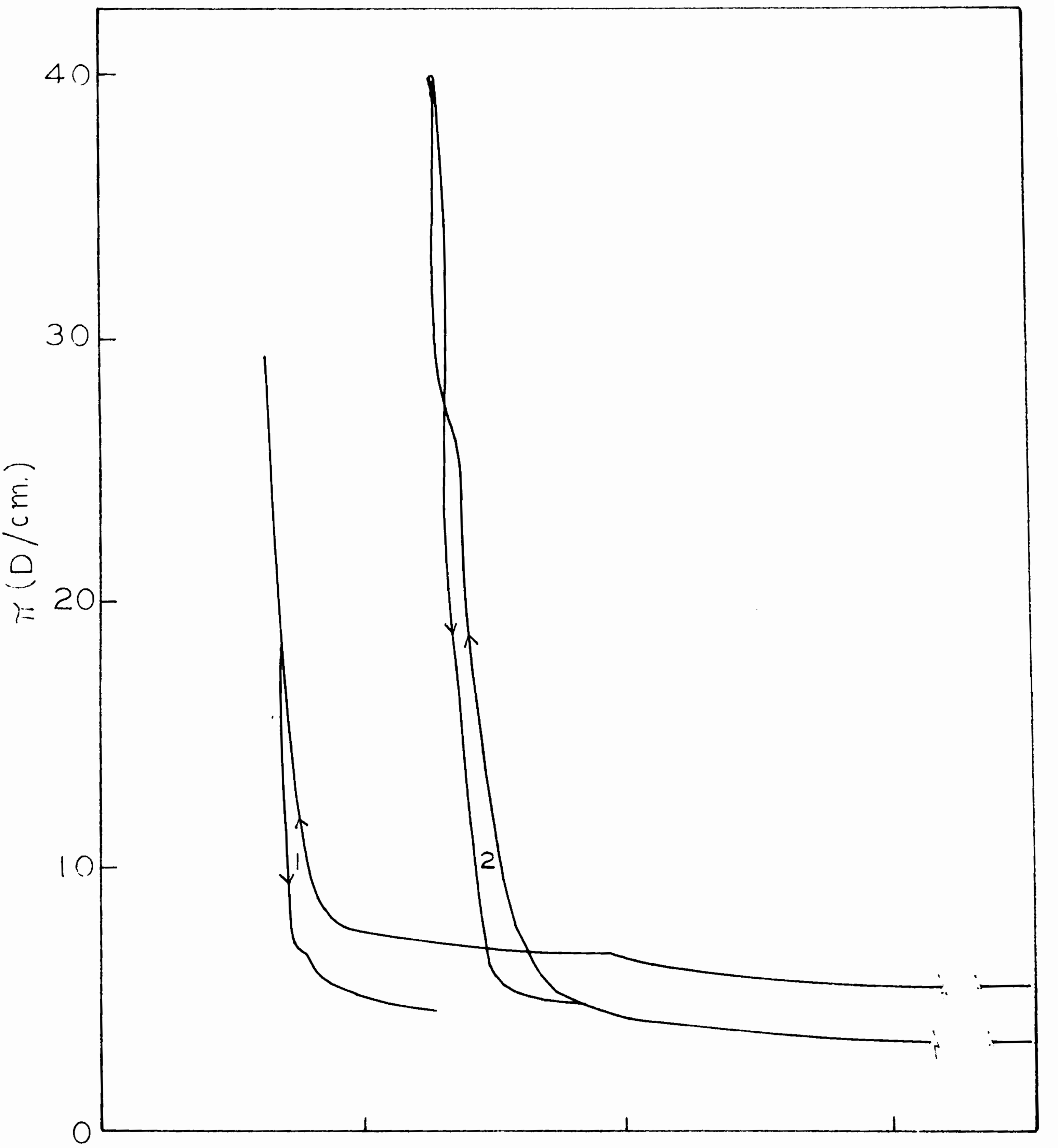
40
30
20
10
0
π (D/cm.)
11
29
47
65
σ (Å² u)
1
2

Figure 42

Figure 42

π-σ diagrams of the Stearic acids showing relaxation effects

1 Stearic acid
2 10 Phenyl stearic acid
3 12 Hydroxy stearic acid

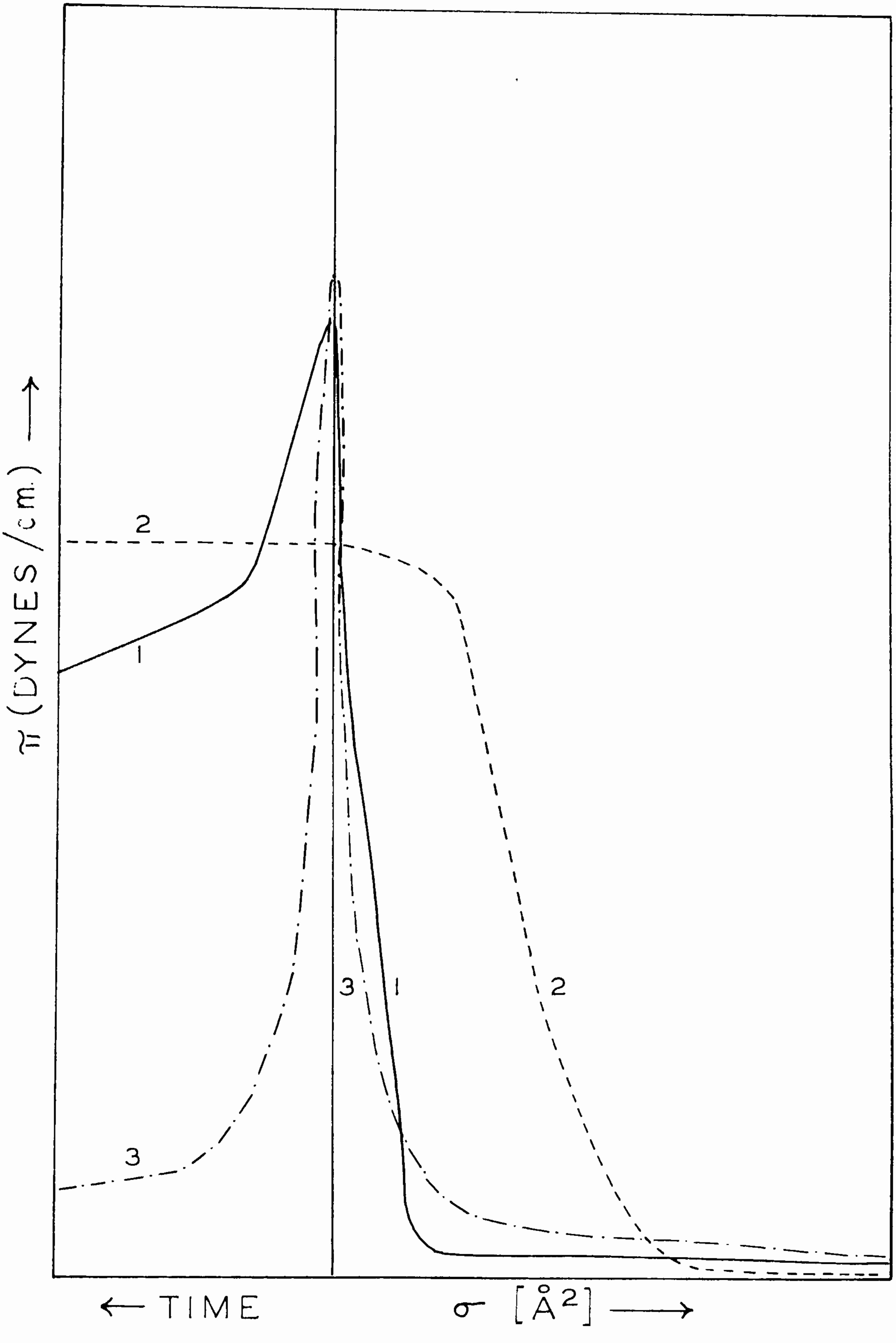
π (DYNES/cm.) ⟶
2
1
3
3
1
2
⟵ TIME
σ [Å²] ⟶

TABLE L

Film characteristics of 12 KSA monolayer

Rate of compression Å^2/mol/min	Temp. °C	(-k) cms/dyne	
1) 1.848	12.1	0.05008 (at 9.4 Å^2, 7.8 d/cm)	(L_e)
	25.0	0.1320 (at 4.9 Å^2, 8.5 d/cm)	(L_1)
2) 2.413	12.1	0.0393 (at 21.1 Å^2, 7.5 d/cm)	(L_e)
	25.0	0.1463 (at 5.4 Å^2, 8.8 d/cm)	(L_1)
3) 4.5	12.1	Before transition 0.01014 (at 20 Å^2, 8 d/cm)	(L_c)
		After transition 0.0038 (at 15.5 Å^2, 30 d/cm)	(solid)
	25.0	0.02411 (at 5.6 Å^2, 15 d/cm)	(L_e)

IV DISCUSSION

(1) Resumè of pertinent information obtained from the studies of the isotopic exchange reaction.

In the present investigations, the study of exchange reactions has been extended to the substrate concentration dependence. The range of substrate concentration employed is between 0.25 N to 2.0 N in KI. These studies have yielded the probable order of the reaction with reference to the substrate concentration. The overall reaction velocity appears to be fairly constant over the range of concentrations and pHs studied. The concentration of the substrate KI was determined by directly weighing the requisite quantity of the salt and dissolving it in the appropriate quantity of water. In view of the limitations of the monolayer technique a more accurate determination of the substrate concentration was deemed unnecessary .

In addition to the study of concentration dependence, some other interesting aspects of the exchange reactions were investigated. Below are given the four sets of studies made in the radioactive work. To aid the discussion the pertinent results are briefly summarised under each set.

(a) The exchange reaction rate constant K^1 has been studied as a function of concentration of the substrate KI solution at two different hydrogen ion concentration. Temperature at which all the experiments were carried out was 25°C ± 0.1. The following information was obtained from this study.

(i) Exchange rate constants increase with substrate concentration ranging from 0.25 N to 2.0 N KI.

(ii) Exchange rate constant at pH = 2 in all cases is higher than that for the corresponding concentration of the substrate KI at pH = 3.

(iii) In the plots to determine the order of the exaction the points were approximately linear except in case of 2 N KI substrate at pH = 3.

(b) The variation of count rate of an active monolayer of AIS during compression was studied, both on 0.01 N HCl and 0.01 N NaOH substrates. The homogeneity of the active films was tested by scanning the monolayer surface with the Geiger tube. These investigations resulted in the following general data.

(i) The plots of the relative counting rate versus the reciprocal of the area were linear between 30 $Å^2$ and 52 $Å^2$. Extrapolation of this plot did not pass through the origin in all cases. This was attributed to the inherent experimental errors of the technique.

(ii) When a monolayer of active AIS on 0.01 N NaOH was compressed the count rate began to decrease after reaching a maximum.

(iii) The first transition point obtained on the curves during compression of a monolayer of AIS was reflected simultaneously on the count rate - time curve. At a constant area per molecule, under high compression, the count rate remained the same while π slowly decreased. Subsequent expansion of a compressed film gave rise to a decrease in the count rate with increasing area per molecule.

(c) Surface potential measurements of both active and inactive monolayers made it possible to draw the following general conclusions.

(i) The surface potential of inactive AIS monolayer at 25°C is higher on 1.0 N KI+0.01 N HCl substrates than on substrates containing 0.01 N HCl alone.

(ii) Surface potentials are all negative except in case of active AIS monolayer at 17.3°C where positive surface potentials were indicated.

(iii) The surface potential of a monolayer of AIS on 1.0 N KI showed a maximum between pH = 2.6 and 3.2.

(v) The transition in the π-σ curves of AIS monolayer on 0.01 N HCl or 1.0 N KI at different temperatures and pHs were reflected by a similar behaviour on the ΔV-σ curves.

(v) Surface potential measurements on a collapsed film made during the study of the exchange in a collapsed AIS monolayer on 1.0 N KI substrates at 25°C, showed fluctuations similar to those obtained in the count rate versus time curves for the exchange reaction.

(2) General discussion on the results of exchange reactions.

The higher value of the exchange constant at lower pH may be due to higher concentration of H^+ ion catalysing the reaction in some unknown way. Alternatively it may result from an increased suppression of the ionization of the AIS acid monolayer at lower pH with concomitant increase in the ease of approach of the substrate I^- ion. Comparing the values obtained for the exchange constant in the present work with those of Robertson (103) for similar concentrations of substrate KI, it can be seen that the exchange constant is higher in the present work. The presence of indifferent salts such as the KCl used in the present concentration dependence investigation has long been known to influence the velocity of chemical reactions in bulk. A "Kinetic salt effect" related to the presence of KCl in the substrate may be an underlying factor for the increased value of the exchange constant in those systems in which KCl was used.

The exchange constant varies approximately linearly with the substrate KI concentration up to 1 N solution. Beyond this concentration, deviations from the linear relation appear. This non-linearity is especially pronounced at higher substrate concentrations and at pH = 3.

An explanation for the nonlinearity of K^1 at higher concentrations may possibly be found in the theory of the double layer as developed by Gouy, Chapman and Stern. The general picture of the double layer as conceived by these workers can be briefly summarized as follows: When two reversible electrodes, polonium and calomel are in contact with a monolayer/substrate system, a potential difference is observed. Gouy (108) and Chapman (109) independently explained the origin of such a potential difference by their well known electrical double layer theories. The double layer was thought to consist of a wall of electrons present in the upper surface phase and an equivalent amount of ionic charge of opposite sign distributed in the solution near the interface. The equations developed for these theories were based on the assumption that the counter ions were dimensionless and that the charged surface was a uniformly charged impenetrable plane (110). Both of these assumptions led to deviations between the theoretical and the experimental picture at high concentrations. The finite dimension of the counter ions became significant at these higher salt concentrations. Stern (111) taking into account the ionic dimensions showed that the capacity of the diffuse layer is strongly dependent on the electrolyte concentration.

On the basis of these theories, Schulman and Hughes (72) and Cassie and Palmer (112) suggested that ΔV the surface potential for ionised films should be given by

$$\Delta V = \frac{12\pi\mu_D}{\sigma} + \psi_s$$

In the above equation ΔV the surface potential is in millivolts; σ is expressed in $\mathring{A}^2$ /molecule; μ_D is the vertical component of the resultant dipole moment expressed in millidebyes; ψ_s is the electrical potential drop (mv) between the charged surface s and the bulk phase. Based on this equation Crisp (113) related ΔV to c the concentration of uni-univalent salt expressed in moles per litre in the expression

$$\frac{\partial \Delta V}{\partial \log c} = 62 \text{ mv.}$$

Davies (114) concluded from this equation that the dipoles in the surface do not attract an appreciable number of counter ions unless the concentration of the salt is very high.

The views of these authors combined with that of Davies and Rideal (115) appears to throw some light on the deviation of K^1 from linearity at high substrate concentrations. At high concentrations an ionic cloud of counter ions of the substrate are formed around each polar group. This ionic cloud can be assumed to cause a screening effect impairing the ready accessibility of substrate I^- ion to the monolayer molecules. If this screening effect were the main operating factor, then the accessibility of I^{131} to substrate iodide ions being lower at higher concentration would lead to a systematic decrease in the value of K^1 as the concentration is increased, the values of K^1 falling below the linear relationship in plots of log a versus log K^1. The experimental observations however, yield values of K^1 at higher concentrations which place K^1 above the general trend of the linear plot. Thus it is very difficult to see why K^1 lies above this line if the screening effect is the main operating factor.

A more plausible explanation for this deviation of K^1 from linearity is provided from Crisp's (113) equation, where the surface potential varies directly as the logarithm of the substrate concentration. Since the surface potential is a function of the vertical component of the dipole moment of the molecule, a change in concentration evidently affects the vertical component. This change in surface potential probably effects the accessibility of the substrate I^- ions in such a way as to increase the rate of reaction and hence K^1 increases.

However a more quantitative and more detailed study of the interdependence of the surface potential on substrate concentration, the reaction velocity on substrate concentration and the surface potential on reaction velocity would have to be undertaken before any truly satisfactory explanation of this behaviour could be made.

Some exchange reactions were followed by the surface potential technique. Exchange reactions studied at 25°C on 1.0 N KI substrate (pH = 2) suggested that the α-iodine was in the water surface and the -COOH was anchored beneath the surface. As the temperature was lowered the surface potential decreased in negativity. This implied a progressive movement of the α-iodine atom with decreasing temperature, out of the water surface to a position above the interface. This would obviously lead to a decrease in exchange rate. As the temperature was raised however the α- iodine atoms would re-enter the surface region to a greater extent and the exchange rate would increase.

In the study of the change in count rate with compression, it can be seen that a linear relationship exists at areas between 32 Å^2 and 50 Å^2 per molecule as shown in Figure 9. Compressions on both acid and alkaline substrates showed similar effects on the surface count rate. The scattered distribution of points in the region of the curve corresponding to very low compression, may be attributed to the presence of a two phase region. This heterogeneous region could have been further investigated if surface potential measurements were made with a movable polonium electrode. Unfortunately the lack of such an electrode limited this investigation and little can be said about this region of the curve. The apparent decrease in relative count rate with compression in the upper region of Figure 9 is probably due to a change in the geometry of the counting arrangment. In two experiments, the Geiger tube was positioned at different places over the surface during compression and the degree of nonlinearity varied for each. The drop in count rate at extremely high compressions on a substrate of 0.01 N NaOH is probably due to a partial solution of the film in the substrate as well as the geometry factor mentioned above.

Surface potential measurements have yielded some useful information when correlated with the corresponding π-σ isotherms . The transition points in the π-σ curves are reflected at similar positions in the ΔV-σ curves. As a film is compressed π begins to rise at a well defined area while

ΔV increases over a range of areas. This behaviour seems to indicate that the π-σ curves do not reflect the progressive changes in orientation as a film is compressed as accurately as does the ΔV-σ curves. The ΔV-σ curves indicate more clearly the region over which the transition begins and is finally completed. The negativity of surface potential of AIS monolayer suggests that the negative end of the total dipole of the molecule in the film is uppermost. These is no doubt that the iodine atom is at the upper end of the polar group and makes a large negative contribution to the resultant moment. Analogous cases have been known the most extreme of which is α-bromo hexa decanoic acid which gives a high negative surface potential (116).

The general shapes of the ΔV-σ curves of AIS monolayer on 1.0 N KI at 25°C for various hydrogen ion concentrations are quite similar. In every curve there is initially a region of gradual increase in the surface potential with compression, then an approximately horizontal region and lastly a region of sharp increase in surface potential at high surface pressure. In all experiments the ΔV-σ curve suggests that as the film is compressed the negative portion of the dipole, the α-iodine, is lifted away from the surface, resulting in a decrease of the negative surface potential.

When the change in surface potential with compression is studied as a function of substrate pH, it is found that on 1.0 N KI solutions at 25°C the ΔV-σ curves pass through a maximum between a pH of 2.6 and 3.2. When a constant area of 50 $\mathring{A}^2$ /molecule is chosen as the reference area, these results parallel closely those of Rabinovitch (104) for the same approximate area. Rabinovitch noted that the exchange rate was a maximum in this pH range. The maximum obtained in the surface potential as a function of pH measurements coincide with the maximum in the exchange velocity as a function of pH. Since the surface potential is a measure of the molecular orientation of the film molecules, it is reasonable to assume that the orientation is most favourable for exchange when the surface potential is close to zero. The variations in reaction velocity with pH as found by Rabinovitch can now be explained in terms of variation of molecular orientation in the surface with pH.

(3) General discussion on the results of π-σ isotherms of the stearic acid derivatives.

This study could be classified into (a) the effect of temperature and rate of compression on the π-σ curves of individual acids (b) hysterèsis and relaxation effect in each case (c) effect of the size of the substituted group along the hydrocarbon chain of stearic acid on π-σ isotherms.

(a) Effect of temperature and rate of compression on the π-σ curves.

The increase in area of the first transition point in case of methyl and ethyl substituted stearic acid was observed at the higher temperature. An increase in temperature resulted in an expansion of the monolayer as can be seen from the numerical values in Tables XLIII to XLVI. The expansion of the films with increasing temperature is obviously connected with the greater thermal agitation of the molecules causing them to occupy greater areas. The first and second transition points in case of stearic acid appear at the same area irrespective of temperatures. This is presumably due to the fact that temperature has no effect since the packing is maximum for both the chains and the heads at the two points of transition. Stearic acid exhibits both L_c phase and L_s phase (almost solid) at 25°C. 2 MSA is a L_e film passing through to L_c beyond the transition point at 25°C. 3 MSA at the point of transition passes from L_e to L_c at 25°C and at 12.1°C, it is a L_c film on both sides of the transition, only passing from a more compressible L_c film to a less compressible one. 3 ESA and 10 PSA are both L_e type of films irrespective of temperature. 12 HSA is a L_c film both at 25°C and 12.1°C. 12 KSA is a L_e type film at lower temperature and L_1 at higher temperatures.

In case of 12 HSA, isotherms for various temperatures exhibited some unusual properties. The equilibrium region shown in Figure 38 appeared at higher surface pressures with increasing temperature. The attainment of the small temperature dependent maximum at temperatures below 25°C was another feature of interest in these isotherms. Varying the rate of compression of films of 12 HSA at temperatures below 25°C did not alter the shape or area of this small maximum at any temperature. The experimental results seem then to indicate that the appearance of this maximum is not time dependent at least in the range of compression rates used in the present study. However use of still higher compression rates may show that this phenomenon actually is time dependent. At the areas per molecule at which this maximum appears the hydroxyl group at the 12 position in the hydrocarbon chain is undoubtedly anchored in the surface. It is tempting to relate the appearance of this maximum to the progressive removal of OH groups from the water surface. The total change in area associated with this small hump in the isotherm and the large area per molecule occupied by the acid after the disappearance of this hump seem to indicate however that the OH group remains in the surface throughout this anamolous region of the isotherm. The maximum then is probably related to a peculiar unkinking of the carbon atoms of the chain probably those beyond the 12 position. If this is true , surface potential measurements would not reflect the appearance of this hump since essentially no change would occur in the vertical component of the dipole moment of the film molecules. Unfortunately the measurement of the surface potential was not possible at the time of this work; so this must remain an open question.

The isotherms of stearic acid at any temperature were essentially the same irrespective of the rate of compression with the transition points P and Q situated at approximately the same area per molecule at all compression rates. Films of 2 MSA and 3 MSA gave isotherms at various compression rates showing the same independence of compression rate as stearic acid. However one rather striking phenomenon associated with the compression rate was found for all the acids studied; the higher the compression rate the higher the final surface pressure attained before collapse.

Films of 12 KSA in contrast to films of the other stearic acid derivatives showed a distinct dependency on compression rate at lower temperatures. At a temperature of 12.1°C a transition region appeared in the isotherm at a compression rate of 4.5 $Å^2$ / mol/ min the highest rate used for this acid, while at the lower compression rates of 1.848 and 2.413 Å^2 per molecule per minute, no such transition region appeared. This is illustrated in Figure 41. From the exceptionally low values of the area per molecule obtained at higher pressures for 12 KSA, it must be recognized that this acid is soluble in the substrates used. The appearance of the transition region at higher compression rates might possibly be related to the rate of solution of 12 KSA and not to the rate of compression.

(b) Hysteresis and relaxation effect.

In all the stearic acid derivatives investigated the films were found to exhibit a pronounced hysteresis (Figures 20 to 41). This could be shown by reversing the direction of travel of the barrier after compression and expanding the film at the same rate at which the film had been previously compressed. The hysteresis effect was generally more pronounced in liquid films. Stearic acid exhibited a hysteresis effect in the L_c region at both 12.1°C and 25°C irrespective of rate of compression. 12 KSA and 12 HSA each of which possessed more than one polar group in the molecules exhibited at lower temperatures hysteresis loops larger than those obtained for stearic acid.

The region of greatest hysteresis occurred in the expanded portion of the π-σ curves where the intermolecular attractions of the film molecules each for the other would be expected to be much smaller than in the more condensed films. The hysteresis effect is probably due more to interaction between the film molecules and substrate water molecules through hydrogen bonds than to interaction between the film molecules themselves. The reproducibility of the hysteresis loops, different for different acids, seems to rule out the possibility that the whole effect arises from an inherent irreversibility of the surface balance itself. The decompression curves for 12 KSA (curve 1, Figures 39 to 41) do not resemble those obtained for the other acids. The effect here may be more a reflection of the apparent solubility of this acid than any true hysteresis effect.

Unimolecular films were compressed at a constant rate of compression until the surface pressure attained a value just below that at which collapse occurred. The movable barrier was then stopped and the surface pressure was recorded as a function of time at constant area. A subsequent decrease in surface pressure with time was interpreted as being the result of a relaxation process active in the film. This process was studied in the various stearic acid derivatives. All these derivatives except 10 PSA showed a pronounced relaxation effect. When relaxation occurred the surface pressure fell in a regular manner with the pressure-time curve reflecting in a very remarkable way the shape of the π-σ compression curve. Breaks in the slope indicating the presence of phase transitions obtained on compression also appeared on the relaxation curve and in many cases the change is slope appeared at a surface pressure very close to the surface pressure of the transition on compression. After the relaxation was allowed to proceed for some time, decompression of the film led to the same π-σ relations obtained originally on the compression curves at higher areas per molecule. The curves for stearic acid and 12 hydroxy stearic acid in which the relaxation process occurred and the curve for 10 phenyl stearic acid in which no relaxation effect was obtained are given in Figure 42.

The relaxation effect may have its origin in the way in which the polar head groups and hydrocarbon chains are arranged in compressed monolayers. However if molecular packing alone is the cause of this relaxation phenomenon one must conclude that the condensed phases of unimolecular films are non-equilibrium states. With sufficiently slow rates of compression the condensed phases would not appear on the isotherm, rather collapse would occur in the expanded films. This interpretation is in part substantiated by the fact that collapse occurred at higher and higher pressures in the condensed film as the rate of compression was increased.

The same experimental facts would however be satisfied by the formation of multilayer islands in regions of the film. The molecules forming the multilayers are effectively removed from the interface and the film simply shows the changes associated with expansion, the effective number of molecules in the monolayer portion of the film is decreasing as multilayer formation progresses. If this explanation is true then the process of collapse in monolayers is open to quantitative or at least semi-quantitative study on the film balance. Surface potential measurements made by scanning the whole surface during the relaxation process should be capable of revealing the formation of progressively more and more multilayer regions. The failure of 10 PSA to show this relaxation effect may be the result of the inability of this acid to form multilayers at the surface pressures attained in this work. The failure of this acid to form the multilayer may in turn be a consequence of the large aromatic substituent hindering the ordered packing of the molecules which may be necessary for multilayer formation.

(c) The effect of the size and chemical nature of the substituent on the π-σ isotherms.

The effect of the size and chemical nature of substituents in the hydrocarbon chain of stearic acid was strikingly illustrated in the present work. A methyl substituent at the 2 or 3 position in the hydrocarbon chain did not essentially change the shape of the isotherm from that obtained for stearic acid itself. The isotherm was simply shifted to larger areas per molecule and thus accounting for the presence of the short side chain. An ethyl substituent in the 3 position however had a much more profound effect on the shape of the isotherm. With this substituent no superliquid phase as obtained at the same temperature with SA, appeared in the isotherm; the film remained in the liquid condensed phase. Evidently a two carbon side chain at the 3 position reduced the approach of the hydrocarbon chains sufficiently to prevent the intermolecular attractive forces from becoming sufficiently large to cause condensation to the superliquid phase at the temperature used. This effect was even more pronounced when an aromatic substituent was present at the 10 position in the hydrocarbon chain. When polar groups such as the hydroxy or keto group were introduced in the chain, however, condensed films were readily obtained on compression at the temperature of the experiments. In the case of 12 HSA the isotherm was shifted to slightly lower areas per molecule than for stearic acid itself. Evidently the presence of the hydroxy group in the hydrocarbon chain results in a general contraction of the film in the condensed phase. This may be related to the possibility of weak hydrogen bond formation between the hydroxy groups in the hydrocarbon chains. Undoubtedly 12 KSA shows a behaviour similar to that of 12 HSA. However the abnormally low areas per molecule obtained with films of this acid can only be explained by assuming partial collapse or partial solution of the acid in the substrate. Similar abnormally low areas per molecule have previously been obtained for diketo stearic acids (117).

V SUGGESTIONS FOR FURTHER WORK

For the studies of substrate concentration dependence in the isotopic exchange reaction, the KI concentrations were only close approximations. This was considered adequate because of the complete lack of knowledge of the surface activity coefficients of both KI and KCl. However a more precise knowledge of the substrate concentration and a method for determining the activity of the KI in the surface region at those high concentrations may do much to clarify the exchange mechanism.

The interesting relation between pH and surface potential found in the present work and the relation between exchange rate constant and pH found by Rabinovitch (104) should be investigated further. Exchange reactions performed at constant surface potential rather than constant surface pressure might prove most interesting, particularly if a relation appears between surface potential and exchange rate.

Relaxation studies in films just below the region of collapse should be extended. A means of scanning the surface with the polonium electrode should be incorporated in the apparatus to assist in this study and in a more detailed study of the phenomenon of collapse itself.

A study of the isotopic iodine exchange reaction in an inert nitrogen atmosphere would remove the complication of air oxidation of the iodide ion in the substrate and the simultaneous change in pH occurring while the exchange is in progress.

The exchange reaction studies should be extended to other positions than the α position in stearic acid. By such an extension the relative reaction rates of isotopic exchange as a function of position in the hydrocarbon chain could be obtained.

The study of isotopic iodine exchange reactions using stearic acid derivatives containing various substituents in the α position with the iodine atom would be an interesting and profitable study. The steric hinderance to exchange of such substituents could be evaluated from an investigation of this type.

The study of the film properties of chain substituted stearic acids should be extended to a systematic investigation of the effect of substituent groups of various kinds on the π-σ and ΔV-σ curves as a function of position in the hydrocarbon tail.

A detailed investigation of the relaxation phenomenon in the chain substituted acids should be initiated to make it possible to interpret the effect in a quantitative manner.

The anomolous "hump" in the π-σ isotherm of 12 HSA should be studied in greater detail. By increasing the sensitivity of the surface balance similar "humps" may be found with other acids.

The reason for the unusually low areas per molecule obtained with 12 KSA should be established. Surface potential measurements might assist in this work in detecting any partial collapse of the film. The use of electrolytes in the substrate might be used to diminish the solubility of the acid and bring the π-σ isotherms of 12 KSA more closely in line with those found for the other stearic acid derivatives.

VI SUMMARY AND CONTRIBUTIONS TO KNOWLEDGE

(1) Exchange reactions between active AIS monolayer and substrate KI were investigated at 25°C for concentrations of KI in the range 0.25 N to 2 N and at pH = 2 and 3. It was observed that the exchange rate increases directly as the concentration of the substrate KI. The order of the reaction with respect to the substrate was approximately 0.5 on the basis of the present study.

(2) Exchange reaction between an active AIS monolayer and 1.0 N substrate KI were investigated at 25°C and 17.3°C with simultaneous measurements of surface potential. The higher exchange rate at 25°C was attributed to the closer proximity to the surface of the I^{131} atom of AIS acid.

The high negative surface potential during a study of collapsed film exchange indicated that the I^{131} in the stearic acid was orientated away from the surface, thereby decreasing the exchange rate.

(3) Surface potential measurements have been made of a monolayer of AIS on 1.0 N KI substrate at 25°C, of varying pH. A maximum was attained in ΔV-pH curves at 50 $\mathring{A}^2$ per molecule between pH = 2.6 and 3.2. This maximum in surface potential parallels that obtained by Rabinovitch (104), for reaction velocity as a function of pH.

(4) π-σ isotherms of a series of stearic acid derivatives were obtained at 12.1°C and 25°C.

(5) These isotherms indicate that there is a tendency for the film to become expanded with the increase in the size of alkyl substituents. Any such substituent tends to increase the area per molecule at zero compression compared to stearic acid.

(6) When more than one polar group is present in the acid e.g. 12 HSA and 12 KSA, the film is highly expanded at high areas per molecule and more condensed at low areas per molecule than are films of stearic acid.

(7) A diffuse transition was noted in the isotherms of 12 HSA characterised by a small maximum in the π-σ plot.

BIBLIOGRAPHY

1. Rayleigh, Lord, Proc. Roy. Soc. 47, 364 (1890)
2. Rayleigh, Lord, Phil. Mag. 30, 386 (1890)
3. Rayleigh, Lord, Ibid 33, 1 (1892)
4. Pockels, A., Nature 43, 437 (1891)
5. Rayleigh, Lord, Phil. Mag. 48, 331 (1899)
6. Devaux, H., Ann. Rep.of Smith. Inst. 261 (1913)
7. Devaux, H., Soc. Franc. Phys. 55, 3 (1914)
8. Devaux, H., Ibid 57,3 (1914)
9. Marcelin, A., Loc. Cit.
10. Langmuir, I., J. Am. Chem. Soc 39, 1849 (1917)
11. Adam, N.K., "Physics and Chemistry of Surfaces" Oxford University Press, 1941
12. Harkins, W.D., "The Physical Chemistry of Surface Films" Reinhold Publishing Corp., New York (1952)
13. Dupre, A., Theorie Mecanique de la Chaleur 369 (1869)
14. Rayleigh, Lord, Scientific Papers 3, 351,397,513,562,572 (1887-92)
15. Langmuir, I., J. Am. Chem. Soc 39, 1864 (1937)
16. Langmuir, I., Cold Spring Har. Symp.(Quant. Biol.) 6, 182 (1938)
17. Harkins, W.D., Davies, C.H., and Clark, G.L., J. Am. Chem. Soc 39, 541 (1917)
18. Harkins, W.D., and Feldman, A., J. Am. Chem. Soc 44,2665 (1922)
19. Harkins, W.D., Coll. Symp. Mono. 6, 31 (1928)

20. Harkins, W.D., Ries, H.E. and Carman, E.F.
J. Am. Chem. Soc. 57, 2224 (1935)

21. Wilhelmy, L. Ann. Phys. 119, 177 (1863)

22. Adam, N.K. Proc. Roy. Soc. (Lon) A101, 452 (1922)

23. Adam, N.K. and Jessop, G. Ibid. A110, 423 (1926)

24. Marcelin, A. Ann. Phys. 4, 461 (1925)

25. Lyons, C.G. and Rideal, E.K.,
Proc. Roy. Soc. (Lon) A124, 333 (1929)

26. Puddington, I.E. J. Coll. Sci. 1, 505 (1941)

27. Harkins, W.D. and Myers, R.J.
J. Chem. Phys. 4, 716 (1936)

28. Harkins, W.D. and Fischer, E.K. Ibid. 1, 852 (1933)

29. Harkins, W.D. and Anderson, T.F.
J. Am. Chem. Soc. 59, 2189 (1937)

30. Bull, H.B. J. Am. Chem. Soc. 67, 4, 8, (1945)

31. Abribat, M. and Pouradier, J. Compt. Rend. 227, 1101 (1948)

32. Matsuura, R. Chem. Abs. 46, 4885 (1952)

33. Gorter, E. and Seeder, W.A. J. Gen. Physiol. 18, 427 (1935)

34. Heynis, J.W.Y. and Maaskant, L.
J. Phys. and Coll. Chem. 54, 1222 (1950)

35. Stenhagen, S. and Stenhagen, E. Nature, 159, 814 (1947)

36. Stenhagen, S. and Stenhagen, E.
Act. Chem. Scand. 3, 1035 (1949)

37. Adam, N.K., Proc. Roy. Soc. (Lon) A99, 336 (1921)

38. Adam, N.K. Proc. Roy. Soc. (Lon) A103, 676 (1923)

39. Adam, N.K. Ibid. A103, 687 (1923)

40. Adam, N.K. and Dyer J.W.W. Ibid. A106, 694 (1924)

41. Muller, A. Ibid. A114, 542 (1927)

42. Muller, A. Ibid. A120, 437 (1928)

43. Adam, N.K. Ibid. A126, 526 (1930)

44. Adam, N.K. Ibid. A126, 366 (1930)

45. Alexander, A.E. Ibid. A179, 470 (1942)

46. Eda, K. and Masuda, Y.
Bull. Chem. Soc. Japan 24, 140 (1951)

47. Rosenheim, O. and Adam, N.K.
Proc. Roy. Soc. (Lon) A126, 25 (1929)

48. Dervichian, D.G. "Surface Chemistry" Butterworth's Publication (Lon) 50 (1949)

49. Muller, A. Nature 129, 436 (1932)

50. Bernal, J.D. Nature 129, 870 (1932)

51. Vold, M.J. J. Coll. Sci. 7, 196-8 (1952)

52. Labrouste, H. Ann. Phys. 14, 164 (1920)

53. Alexander, A.E. Ann. Rep. 41, 5 (1944)

54. Langmuir, I. J. Chem. Phys. 1, 757 (1933)

55. Marsden, J. and Rideal, E.K. J. Chem. Soc. 1163 (1938)

56. Phillips, J.N. and Rideal, E.K.
Proc. Roy. Soc. (Lon) A232, 149 (1955)

57. Hedge, D.G. J. Coll. Sci. 12, 417 (1957)

58. Cary, E.P. and Rideal, E.K.
Proc. Roy. Soc. (Lon) A109, 301 (1925)

59. Harkins, W.D. and Boyd, G.E. J. Phys. Chem. 45, 20 (1941)

60. Adam, N.K.,Berry, W.A. and Turner, H.A.
Proc. Roy. Soc. (Lon) 117, 532 (1928)

61. Langmuir, I. Coll. Symp. Mono. 3, 48 (1925)

62. Langmuir, I. J. Frank. Inst. 143, 218 (1934)

63. Adam, N.K. Proc. Roy. Soc. A155, 684 (1936)

64. Rideal, E.K. "Introduction to Surface Chemistry"
Cambridge Univ. Press,(1926)

65. Harkins, W.D. and Nutting, G.C.
J. Am. Chem. Soc. 61, 1702 (1939)

66. Harkins, W.D.,Young, T.F. and Boyd, G.E.
J. Chem. Phys. 8, 954 (1940)

67. Ehrenfest, P. Proc. Acad. Sci. Amsterdam 36, 115 (1933)

68. Guyot, M.J. Ann. Phys. 10, 506 (1924)

69. Frumkin, A. Z. Phys. Chem. 116, 485 (1925)

70. Schulman, J.H. and Rideal, E.K.
Proc. Roy. Soc. (Lon) A130, 259 (1931)

71. Adam, N.K. and Harding, J.B. Ibid. A138, 411 (1932)

72. Schulman J.H. and Hughes, A.H. Ibid. A138, 430 (1932)

73. Hughes, A.H. J. Chem. Soc. 338, (1933)

74. Marsden, J and Schulman, J.H. Trans. Far. Soc. 34, 748 (1938)

75. Hughes, A.H. and Rideal, E.K.
Proc. Roy. Soc. (Lon) A140, 253 (1933)

76. Gee, G. and Rideal, E.K. Ibid. A153, 116 (1935)

77. Mittelman, R. and Palmer, R.C. Trans. Far. Soc. 38,506 (1942)

78. Pitzer, K.S. J. Chem. Phys. 8, 711 (1940)

79. Eda, K. J. Chem. Soc. Japan. Pure Chem. Sect. 73,260 (1952)

80. Adam, N.K. Proc. Roy. Soc. (Lon) A140, 223 (1933)

81. Fosbinder, R.J. and Rideal, E.K. Ibid. A43, 61(1933)

82. Alexander, A.E. and Rideal, E.K.Ibid. A163, 70 (1937)

83. Alexander, A.E. and Schulman, J.H. Ibid. A161, 115 (1937)

84. Adam, N.K. and Miller, J.F.G. Ibid. A142, 401 (1933)

85. Havinga, E. "Monomolecular layer" Am.Assoc. for the Advancement of Science 203 (1954)

86. Verwey, E.J.W. and Overbeek, J.Th.G. "Theory of the Stability of Lyophobic Colloids" (1948)

87. Kogl, F. and Havinga, E. Rec. Trav. Chim. 59, 601 (1940)

88. Davies, J.T. Trans. Far. Soc. 45, 448 (1949)

89. McKay, H.A.C. Nature 139, 283 (1937)

90. McKay, H.A.C. J. Am. Chem. Soc. 65, 702 (1943)

91. Purlee, L., Kahn, M. and Riebsomer, J.L. Ibid. 76, 3796 (1954)

92. Van Der Straaten, H. and Aten, Jr. A.H.W.Ibid. 76, 3798 (1954)

93. Zeltman, A.H. and Kahn, M. Ibid. 76, 1554 (1954)

94. Behrens, H. and Maddock, A.G. J. Chem. Phys. 22, 1139 (1954)

95. Kahn, M. and Freedman, A.J. J. Am. Chem. Soc. 76,929 (1954)

96. Hammet, L.P. "Physical Organic Chemistry" Mc Graw Hill Book Co. Inc. N.Y. 312 (1951)

97. Friedlander, G. and Kennedy, J.W. "Introduction to Radiochemistry" John Wiley and Sons Inc. N.Y. 285 (1949)

98. Hughes, E.D. et al J. Chem. Soc. 1525 (1935)

99. Hughes, E.D. et al Ibid. 1173 (1936)

100. Cowdrey, W.A. et. al. J. Chem. Soc. 1252 (1937)

101. Cowdrey, W.A. et.al. Ibid. 209 (1938)

102. Robertson, R.F., Winkler, C.A. and Mason, S.G.
Can. J. Chem. 34, 316 (1956)

103. Robertson, R.F. "Kinetics of Iodine Exchange in Monolayers"
Ph.D. Thesis, McGill Univ. (1955)

104. Rabinovitch, W. "Chemical Reactivity in Monolayers"
Ph.D. Thesis, McGill Univ. (1956)

105. Dervichian, D.G. J.Physique 6, 221 (1935)

106. Mauer, F.A. Rev. Sci. Ins. 25, 598 (1954)

107. Dervichian, D.G. J. Chem. Phys. 7, 931 (1939)

108. Gouy, G. Ann. Phys. 9, 7 (1917)

109. Chapman, D.L. Phil. Mag. 6, 25 (1913)

110. Hoskin, N.E. Trans. Far. Soc. 49, 1471 (1953)

111. Stern, O Z. Electrochem. 30, 508 (1924)

112. Cassie, A.B.D. and Palmer, R.C. Trans. Far. Soc. 37,156 (1941)

113. Crisp, D.J. "Surface Chemistry" Butterworth's Publication
95 (1949)

114. Davies, J.T. Proc. Roy. Soc. (Lon) A208, 204 (1951)

115. Davies, J.T. and Rideal, E.K. J. Coll. Sci. Suppl. 1, 1 (1954)

116. Frumkin, A. J. Chem.Phys. 4, 624 (1936)

117. Schneider, V.L., Holman, R.T. & Burr, G.O.
J. Phys. and Coll. Chem. 53, 1016, (1949)